

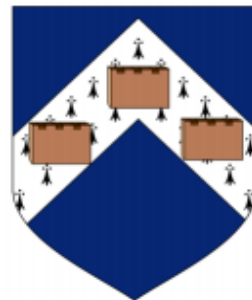
Form and Function of the Craniomandibular Complex in Subterranean Rodents

Andrew Fergus McIntosh

Submitted in partial fulfilment of the requirements for the degree
of Doctor of Philosophy in Medical Sciences



University of Hull



University of York



March 2016

Abstract

Rodents are the most speciose mammalian order and are represented in arboreal, semi-aquatic, subterranean and terrestrial niches. To flourish in such environments, rodents must exhibit morphological traits that can reflect functions that are needed to survive. This thesis focuses on the functional morphology of digging subterranean rodents and in particular, African mole-rats (Bathyergidae). Species dependent, subterranean rodents dig using a number of different methods. This thesis concentrates on the morphological differences in the craniomandibular complex in scratch digging and chisel-tooth digging subterranean rodents. Scratch digging rodents use only their claws to remove softer soil whilst their chisel-tooth digging counterparts use their incisors in concert with their powerful masticatory muscles to remove harder soils.

Chapter two looks at morphological traits associated with bite force and gape in African mole-rats (Bathyergidae). The study shows that chisel-tooth digging rodents have morphological traits that are associated with a larger bite force at wider gapes, which is probably achieved by having a temporalis with a greater mechanical advantage.

Chapter three examines a selection of chisel-tooth digging, scratch digging and terrestrial rodents. It shows that the upper incisors of chisel-tooth digging rodents have a larger radius of curvature. Also, it shows that chisel-tooth digging rodent cranial shape converges in morphospace and covaries with the upper incisors, although these results were not significant when phylogeny was accounted for.

Chapter four shows that, using finite element analysis, the cranium of a chisel-tooth digging mole-rat can create larger bite forces at wider gapes, compared to a scratch digging mole-rat. Using a novel method of combining geometric morphometrics with finite element analysis, this study also shows that the cranium of the chisel-tooth digging rodent deforms less, making it more efficient at performing chisel-tooth digging tasks.

Overall, this thesis shows that the craniomandibular form of subterranean rodents can be strongly influenced by function. The digging method used by a subterranean rodent is therefore important to how they have evolved.

Table of Contents

Abstract.....	1
Table of Contents.....	2
List of Figures.....	6
List of Tables.....	12
Acknowledgements.....	14
Author’s Declaration.....	15
Chapter 1: Introduction and literature review.....	16
1.1 The masticatory system.....	16
1.2 Morphological integration.....	19
1.3 Rodentia.....	22
1.4 Subterranean rodents	25
1.4.1 Digging in subterranean rodents	27
1.5 Intergeneric relationships of the Bathyergidae	28
1.6 Geographical distribution of the Bathyergidae	30
1.7 Ecology and Sociality.....	32
1.8 Aims	34
1.8.1 Chapter 2	34
1.8.2 Chapter 3	34
1.8.3 Chapter 4	35
1.9 Methods	35

1.9.1	3-D biomechanical models.....	35
1.9.2	Geometric morphometrics.....	36
1.9.3	Phylogenetic comparative methods	38
1.9.4	Finite element analysis.....	39

Chapter 2: Functional implications of the craniomandibular complex in African mole-rats (Rodentia: Bathyergidae).....43

2.1	Introduction	43
2.1.1	Morphological predictions related to bite force.....	45
2.1.2	Morphological predictions related to gape	46
2.1.3	Biomechanics of a chisel-tooth digger.....	46
2.2	Materials and Methods	48
2.3	Results	54
2.3.1	Morphological predictors of bite force (including upper incisor procumbency).....	54
2.3.2	Morphological predictors of gape.....	58
2.3.3	Allometric relationship of morphological traits.....	61
2.3.4	Biomechanical implications of morphological traits	66
2.4	Discussion.....	70
2.4.1	Bite force	70
2.4.2	The curious case of the naked mole-rat	72
2.4.3	Incisor procumbency in chisel-tooth digging rodents.....	75
2.4.4	Gape	75
2.4.5	Conclusions	79

Chapter 3: The effect of digging on craniodental morphology in rodents	80
3.1 Introduction	80
3.2 Materials and Methods	84
3.2.1 Rodent sample	84
3.2.2 Assessing incisor morphology	86
3.2.3 Assessing cranial morphology	88
3.2.4 Assessing covariation between incisor and cranial morphology .	
92	
3.3 Results	93
3.3.1 Incisor morphology	93
3.3.2 Cranial morphology	97
3.3.3 Covariation of incisor and cranial morphology	99
3.4 Discussion.....	100
3.4.1 Incisor morphology	100
3.4.2 Cranial morphology	102
3.4.3 Covariation of incisor and cranial morphology	103
3.4.4 Conclusion.....	104
 Chapter 4: Digging biomechanics of the cranial form in African mole-rats (Family: Bathyergidae)	 105
4.1 Introduction	105
4.2 Materials and Methods	108
4.2.1 Sample and model construction	108
4.2.2 Material properties	108
4.2.3 Constraints.....	109

4.2.4	Modelling muscle loads and changes in gape.....	109
4.2.5	Comparison of performance indicators between finite element models	111
4.2.6	Geometric morphometric analysis of cranial deformations...	112
4.3	Results	116
4.3.1	Models scaled to force:area ratio	116
4.3.2	Models scaled to bite force	121
4.4	Discussion.....	125
4.4.1	Models scaled to force:area ratio	125
4.4.2	Models scaled to bite force	127
4.4.3	Conclusion.....	128
Chapter 5: Discussion of thesis.....		130
References		136
Appendix A (for chapter 2).....		154
Appendix B (McIntosh and Cox, 2016).....		154

List of Figures

- Figure 1.1. European rabbit, *Oryctolagus cuniculus* (left) and Fringe-lipped bat, *Trachops cirrhosis* (right). Representation of the differences in two main masticatory muscles (temporalis and masseter) of an herbivore (left) and an omnivore (right). Models not to scale. Figure modified from Watson et al. (2014) and Santana (2014). 17
- Figure 1.2 Left lateral view of 3D reconstructions of the skull, mandible and masticatory muscles of (A) Hystricomorph, (B) Myomorph and (C) Scuiromorph. Abbreviations: adm, anterior deep masseter; iozm, infraorbital part of zygomaticomandibularis; lt, lateral temporalis; mt, medial temporalis; pdm, posterior deep masseter; sm, superficial masseter; t, temporalis. All scale bars: 5 mm. Taken from Cox and Jeffery, 2011. 21
- Figure 1.3 Skull of the Eocene protrogomorph *Ischyrotomus*, with the jaw musculature restored. Abbreviations: M. LAT.-Masseter lateralis, dashed portions lying beneath Masseter superficialis; M. PROF.-dashed lines indicating the course of the Masseter profundus; M. SUP.-Masseter superficialis; PT. E.-dashed line indicating course of Pterygoideus externus; TEMP.-Temporalis. Muscle nomenclature differs from Figure 1.2 due to the complex nature of the masseter layers and dissection techniques of researchers. This thesis therefore follows the nomenclature of Cox and Jeffery (2011). Taken from Wood, 1965..... 23
- Figure 1.4 Mandibular types (A) scuirognathous jaw and (B) hystricognathous jaw in ventral view. Dashed line represents the incisor plane. The angular process is coloured in red. Taken from Hautier et al, 2011. 24
- Figure 1.5 Phylogenetic tree of the Rodentia order. Taken from Blanga-Kanfi et al., 2009..... 26
- Figure 1.6 Comparative cranial morphology of a scratch digger (above) and a chisel-tooth digger (below). Modified from Stein (2000). 28
- Figure 1.7. Phylogenetic tree of extant genera of the Bathyergidae. Units-million years ago. Modified from Seney et al., 2009..... 29
- Figure 1.8. A basic example of a 3rd class lever system. 36
- Figure 1.9. Taken from O'Meara (2012). The figure shows a tree, the tree's variance-covariance matrix, and the vector of means (which, under Brownian motion, would equal the root state). Highlighted are the branches leading to covariance between taxa A and B (red) and the branches leading to variance in D (blue). 39

Figure 1.10 Relationship between stress and strain in skeletal bone. Taken from Rayfield (2007).	41
Figure 2.1 Phylogeny of bathyergid mole-rat genera in this analysis. Chisel-tooth digging (blue), scratch digging (red). Adapted from Seney et al (2009).	48
Figure 2.2 Morphological predictors of bite force (A-C) and gape (D) shown on skull and mandible of <i>Heliophobius argenteocinereus</i> . A. Dorsal view of skull. B. Right lateral view of skull (zygomatic arch removed). C. Ventral view of skull. D. Medial view of left hemimandible. Abbreviations: BL, basilar length; CL, condyle length; CH, condyle height; CW, cranial width; HH, head height; JL, jaw length; OP, occlusal plane; RL, rostral length; α , incisor procumbency angle. Dashed line represents occlusal plane on mandible. Further details of measurements given in Table 2.2 and 2.3.	50
Figure 2.3 Calculation of muscle moment arm (MMA) of temporalis and jaw moment arm (JMA) to evaluate mechanical advantage of temporalis. Abbreviations: BFV, bite force vector; JMA, jaw moment arm; MFV, muscle force vector; MMA, muscle moment arm; OP, occlusal plane.	53
Figure 2.4 Box plot showing head height (relative to cranial length) in chisel-tooth digging (blue) and scratch digging (red) bathyergid genera. Black lines within boxes represent median values. Boundaries of boxes represent 25th and 75th quartiles. Whiskers extend to 1.5 times the interquartile range and white dots represent outliers that fall outside this range.	55
Figure 2.5 Box plot showing cranial width (relative to cranial length) in chisel-tooth digging (blue) and scratch digging (red) bathyergid genera. Black lines within boxes represent median values. Boundaries of boxes represent 25th and 75th quartiles. Whiskers extend to 1.5 times the interquartile range and white dots represent outliers that fall outside this range.	56
Figure 2.6 Box plot showing upper incisor procumbency in chisel-tooth digging (blue) and scratch digging (red) bathyergid genera. Black lines within boxes represent median values. Boundaries of boxes represent 25th and 75th quartiles. Whiskers extend to 1.5 times the interquartile range and white dots represent outliers that fall outside this range.	57
Figure 2.7 Box plot showing rostral length (relative to cranial length) in chisel-tooth digging (blue) and scratch digging (red) bathyergid genera. Black lines within boxes represent median values. Boundaries of boxes represent 25th and 75th	

quartiles. Whiskers extend to 1.5 times the interquartile range and white dots represent outliers that fall outside this range.	58
Figure 2.8 Box plot showing jaw length (relative to cranial length) in chisel-tooth digging (blue) and scratch digging (red) bathyergid genera. Black lines within boxes represent median values.....	59
Figure 2.9 Box plot showing condyle length (relative to cranial length) in chisel-tooth digging (blue) and scratch digging (red) bathyergid genera. Black lines within boxes represent median values. Boundaries of boxes represent 25th and 75th quartiles. Whiskers extend to 1.5 times the interquartile range and white dots represent outliers that fall outside this range.	60
Figure 2.10 Box plot showing condyle height (relative to cranial length) in chisel-tooth digging (blue) and scratch digging (red) bathyergid genera. Black lines within boxes represent median values. Boundaries of boxes represent 25th and 75th quartiles. Whiskers extend to 1.5 times the interquartile range and white dots represent outliers that fall outside this range.	61
Figure 2.11 Box plot showing allometric residuals of head height from equation in Table 2.4 in chisel-tooth digging (blue) and scratch digging (red) bathyergid genera. Black lines within boxes represent median values. Boundaries of boxes represent 25th and 75th quartiles. Whiskers extend to 1.5 times the interquartile range and white dots represent outliers that fall outside this range.....	63
Figure 2.12 Box plot showing allometric residuals of cranial width from equation in Table 2.4 in chisel-tooth digging (blue) and scratch digging (red) bathyergid genera. Black lines within boxes represent median values. Boundaries of boxes represent 25th and 75th quartiles. Whiskers extend to 1.5 times the interquartile range and white dots represent outliers that fall outside this range.....	63
Figure 2.13 Box plot showing allometric residuals of rostral length from equation in Table 2.4 in chisel-tooth digging (blue) and scratch digging (red) bathyergid genera. Black lines within boxes represent median values. Boundaries of boxes represent 25th and 75th quartiles. Whiskers extend to 1.5 times the interquartile range and white dots represent outliers that fall outside this range.....	64
Figure 2.14 Box plot showing allometric residuals of jaw length from equation in Table 2.4 in chisel-tooth digging (blue) and scratch digging (red) bathyergid genera. Black lines within boxes represent median values. Boundaries of boxes represent 25th and 75th quartiles. Whiskers extend to 1.5 times the interquartile range and white dots represent outliers that fall outside this range.....	64

Figure 2.15 Box plot showing allometric residuals of condyle length from equation in Table 2.4 in chisel-tooth digging (blue) and scratch digging (red) bathyergid genera. Black lines within boxes represent median values. Boundaries of boxes represent 25th and 75th quartiles. Whiskers extend to 1.5 times the interquartile range and white dots represent outliers that fall outside this range.....	65
Figure 2.16 Box plot showing allometric residuals of condyle height from equation in Table 2.4 in chisel-tooth digging (blue) and scratch digging (red) bathyergid genera. Black lines within boxes represent median values. Boundaries of boxes represent 25th and 75th quartiles. Whiskers extend to 1.5 times the interquartile range and white dots represent outliers that fall outside this range.....	65
Figure 2.17 Mechanical advantage of the temporalis at gapes between 0° and 100° in chisel-tooth digging (blue) and scratch digging (red) bathyergid genera. Species means are represented.....	67
Figure 2.18 Mechanical advantage of the superficial masseter at gapes between 0° and 100° in chisel-tooth digging (blue) and scratch digging (red) bathyergid genera. Species means are represented.....	68
Figure 2.19 Mechanical advantage of the deep masseter at gapes between 0° and 100° in chisel-tooth digging (blue) and scratch digging (red) bathyergid genera. Species means are represented.	69
Figure 2.20 Lateral view of the mandibles of <i>Heliophobius argenteocinereus</i> (above) and <i>Bathyergus suillus</i> (below). Arrows indicate the coronoid process.....	78
Figure 3.1 Mid-sagittal slice of CT scan in two subterranean rodents: chisel-tooth digging <i>Georychus capensis</i> (above) and scratch digging <i>Bathyergus suillus</i> (below). Notice the posterior displacement of the incisor root in <i>Georychus capensis</i> compared with <i>Bathyergus suillus</i> . Figure scaled to cranial length of <i>Georychus capensis</i>	82
Figure 3.2 Phylogeny of sample used in this study. Modified from Fabre et al. (2012).	83
Figure 3.3 Measurement of measuring radius of curvature. The length of the incisor (L) is measured using the base of the triangle (a). Red points represent the 3 the points placed on to surface of the incisor.	86
Figure 3.4 Landmark configuration represented on <i>Fukomys mechowii</i> . A, dorsal view. B, ventral view. C, lateral view. List of landmarks and anatomical descriptions in Table 3.2.	90

Figure 3.5. OLS model fitted through origin showing the relationship between upper incisor length and upper incisor radius of curvature. Chisel-tooth digging genera are in blue. Non-tooth digging genera are in red.	93
Figure 3.6. Phylogenetic ANCOVA representing the relationship between cranial length, upper incisor radius of curvature and digging method. Chisel-tooth digging genera are in blue. Non-tooth digging genera are in red. Genus numbers are given in Table 3.1. Solid line represents PGLS of chisel-tooth digging and dashed line represents PGLS of non-tooth digging.....	94
Figure 3.7. PGLS representing the relationship between cranial length and upper incisor second moment of area. Chisel-tooth digging genera are in blue. Non-tooth digging genera are in red. Genus numbers are given in Table 3.1. Line represents PGLS through all data.	95
Figure 3.8 Phylogeny of data with accompanying SMA residual values from PGLS of cranial length and upper incisor SMA. Chisel-tooth digging genera residuals are in blue. Non-tooth digging genera residuals are in red.	96
Figure 3.9 Principal components analysis with surface warps representing shape variation across PC1 and PC2 axes. Chisel-tooth digging genera are in blue. Non-tooth digging genera are in red. Genus numbers are given in Table 3.1.	97
Figure 3.10 Phylogenetic principal components analysis with surface warps representing non-phylogenetic shape variation across PC1 and PC2 axes. Chisel-tooth digging genera are in blue. Non-tooth digging genera are in red. Genus numbers are given in Table 3.1	98
Figure 3.11 Partial least squares analysis with cranial surface warps representing cranial shape and incisor covariation across PLS 1(accounts for 93.7% covariance). Chisel-tooth digging genera are in blue. Non-tooth digging genera are in red. Genus numbers are given in Table 3.1.....	99
Figure 3.12 Phylogenetic partial least squares analysis representing cranial shape and incisor covariation across PLS 1). Chisel-tooth digging genera are in blue. Non-tooth digging genera are in red. Genus numbers are given in Table 3.1.	99
Figure 4.1. Muscle arrangements and muscle vectors of the masticatory muscles represented in both FE models. A, <i>Bathyergus model in lateral view</i> . B, <i>Bathyergus model in ventral view</i> . C, <i>Fukomys model in lateral view</i> . D, <i>Fukomys model in ventral view</i> . Colours of muscle vectors: temporalis, red; superficial masseter, cyan; deep masseter, royal blue; IOZM, green; anterior ZM, purple; posterior ZM, yellow; lateral pterygoid, brown; medial pterygoid, orange.....	115

Figure 4.2. Von Mises stress contour maps across models scaled to force:area in lateral view. Left column is <i>Fukomys</i> model, right column is <i>Bathyergus</i> model at differing gape angles.	116
Figure 4.3. Von Mises stress contour maps across models scaled to force:area in dorsal view. Left column is <i>Fukomys</i> model, right column is <i>Bathyergus</i> model at differing gape angles.	117
Figure 4.4. PCA plot representing the differences of deformations between the two models scaled to force:area ratio. Mean unloaded model represented as a black cross. Blue points represent <i>Fukomys</i> models and red points represent <i>Bathyergus</i> models. Models at occlusion (circles), at 30° gape (triangles), 60° gape (squares) and 90° gape (diamonds).	119
Figure 4.5. Transformation grids and surface warps associated with PCA plot (Figure 4.4) representing the differences of deformation between the two models scaled to force:area ratio. Arrows represent the change in size and shape between unloaded mean model and target. A, unloaded mean model; B, size and shape change from unloaded model to <i>Fukomys</i> model in occlusion; C, size and shape change from unloaded model to <i>Bathyergus</i> model in occlusion; D, size and shape change from unloaded model to <i>Fukomys</i> model at 90° gape; E, size and shape change from unloaded model to <i>Bathyergus</i> model at 90° gape.	120
Figure 4.6. Von Mises stress contour maps across models of increasing gape scaled to a bite force of 40N in lateral view.	121
Figure 4.7. Von Mises stress contour maps across models of increasing gape scaled to a bite force of 40N in dorsal view.	122
Figure 4.8. PCA plot representing the differences of deformations between the two models scaled to bite force of 40N. Mean unloaded model represented as a black cross. Blue points represent <i>Fukomys</i> models and red points represent <i>Bathyergus</i> models. Models at occlusion (circles), at 30° gape (triangles), 60° gape (squares) and 90° gape (diamond).	124
Figure 4.9 Transformation grids and surface warps associated with the PCA plot (Figure 4.8) representing differences of deformation between the two models scaled to bite force. Arrows represent the change in size and shape between mean unloaded model and target. A, mean unloaded model; B, size and shape change from unloaded model to <i>Fukomys</i> model at 90° gape; C, size and shape change from unloaded model to <i>Bathyergus</i> model at 60° gape.	124

List of Tables

Table 2.1 List of Bathyergidae specimens used in this study. Note not all specimens could be used in each test due to damage (see appendix Table 7.1).....	49
Table 2.2 Morphological predictors on the cranium to be measured. All linear measurements were size adjusted by dividing by basilar length. Measurements shown in Figures 2.2A-C.	51
Table 2.3 Morphological predictors on the mandible to be measured. All linear measurements were size adjusted by dividing by basilar length. Measurements shown in Figure 2.2D.....	51
Table 2.4 Allometric equations ($y=axb$; reduced major axis regression) to assess influence of size (x =basilar length) on morphological variables.....	62
Table 3.1 List of genera analysed including specimen number, diet and mode of digging. Abbreviations for dietary categories: O, omnivore; GH, generalist herbivore; SH, specialist herbivore. Dietary categories follow method of Samuels (2009). Subterranean rodent genera are in bold.....	85
Table 3.2. 29 cranial landmarks and a description of their anatomical positions.....	91
Table 4.1. Median von Mises stress, bite force output and mechanical efficiency across both models at increasing gape.	118
Table 4.2. Median von Mises stress of both models scaled to bite force of 40N.	123
Table A.1 Number of individual specimens included in each T-test analysis.....	154

Dedication

To my parents, who I can never fully repay for the opportunities they have given me.
Also to my siblings, who have always set the bar high.

Acknowledgements

Firstly, I would like to thank my supervisor Dr Phil Cox. I am immeasurably grateful to him for affording me this chance. His speediness and attention to detail have greatly improved the quality of this thesis. The guidance he provided throughout the entire project not only took the research in the right direction, but also gave me the confidence to see it through to the end. After three and a half years, I now consider him not only a brilliant supervisor, but also a friend.

To the many people I have met through CAHS. Many thanks must go to Dr Laura Fitton, whose advice and friendship has contributed greatly to my time at the centre; she has the patience of a saint. I would also like to thank the members of my Thesis Advisory Panel: Dr Sam Cobb, Prof. John Currey and Prof Jonathan Bennett. All of them made sure that the project stayed in the right direction and was finished on time. To Prof Paul O'Higgins, who helped me with all my geometric morphometric and finite element problems and to Dr Nick Milne, who helped me through the problems with curvature quantification and other fun things. For all my friends in the PhD office who made it a pleasure to come to work. To Karen Swan, who made sure my sugar levels were at a level that was necessary to write a thesis. To Ricardo Godinho, whose wealth of knowledge made sure many interesting debates were had. To Philip Morris, a professional tea maker who always made sure my mug was full. To all the past PhD students who all contributed to the project: Jason Dunn, Hester Baverstock, Vivi Toro Ibacache and Miguel Pröa. I would also like to thank past masters students Amber Collings and Thomas Puschel for their friendship, antics and knowledge.

Outside of the centre, I would like to thank all the friends I have met through my time at York. Alex Stokes, Daniel Agahi, Robin Karfoot, Anuja Chatterjee, Charles McSwiggan and Dil-veer Kang who all made living in York one hazy fun adventure.

Finally, to Leslie Pryor, who has been with me throughout the entire write up period. Her love, kindness and generosity were a major factor in helping me finish this project.

Author's Declaration

I confirm that this work is original and that if any passage(s) or diagram(s) have been copied from academic papers, books, the internet or any other sources these are clearly identified by the use of quotation marks and the reference(s) is fully cited. I certify that, other than where indicated, this is my own work and does not breach the regulations of HYMS, the University of Hull or the University of York regarding plagiarism or academic conduct in examinations. I have read the HYMS Code of Practice on Academic Misconduct, and state that this piece of work is my own and does not contain any unacknowledged work from any other sources.

Chapter 1: Introduction and literature review

1.1 The masticatory system

Extant species have survived to this day due to their ability and their ancestors' ability to adapt to an environment and reproduce. This requires many biological systems within the species to be highly integrated and function successfully. One such system is the masticatory apparatus. This has been extensively studied in evolutionary biology due to its obvious importance in food consumption, a fundamental task for evolutionary success (e.g. Maynard Smith and Savage, 1959; Turnbull, 1970; Crompton and Parker, 1978; Weijs, 1980; Wheelwright, 1985; Herring, 1993; Binder and Van Valkenburgh, 2000; Dumont and Herrel, 2003; Taylor and Vinyard, 2004; Eng et al., 2009; Santana, 2015). Food resources vary greatly between and within ecological niches and as such a species needs to adapt its abilities to exploit these resources. These adaptations have helped create the diversity seen in mammalian morphology (Schluter, 2000).

Although all mammals masticate, there is great diversity of the components within the mammalian masticatory system (Herring, 2007). The mammalian masticatory system is made up of a cranium and a mandible. The system is thought of as a 3rd class lever (see below), where the mandible pivots about the cranium at the TMJ (temporomandibular joint; Figure 1.1). The output force is at the point of contact of food at the teeth and the input force is the work of the muscles. In general, all mammals have three key masticatory muscle complexes: temporalis; masseter; pterygoid. These muscles are attached to the craniomandibular system and each muscle's function is species dependent. In terms of size, each individual muscle mass is normally examined relative to the mass of the whole specimen's masticatory musculature (Turnbull, 1970). This method highlights the muscles which dominate the masticatory apparatus of individual species. For example, animals with a carnivorous or omnivorous diet tend to have a dominating temporalis muscle. This muscle's dominance is common in animals that have a hinge-like TMJ which involves the mandible rotating about the cranium. Animals with an herbivorous diet tend to have a dominating masseter and pterygoid complex, and involve anteroposterior movement of the TMJ. Figure 1.1 highlights the differences in the muscular arrangement of an omnivorous animal (the fringe-lipped bat, *Trachops cirrhosis*) and an herbivorous animal (the European rabbit, *Oryctolagus cuniculus*). This figure shows that the omnivorous fringe-lipped bat has a much larger temporalis compared to its masseter; whereas the herbivorous rabbit has a much larger

masseter compared to its temporalis. Both these muscle complexes close the mandible. However, the temporalis muscle pulls backwards, and is important in animals that require a large, high velocity bite (an important characteristic for carnivores). The masseter tends to pull forward and is more important in animals that require a highly controlled movement of the mandible for chewing (an important characteristic for herbivores). Turnbull (1970) categorised mammals into groups based on the masticatory muscles. His three specialised groups included carnivore shearing, ungulate grinding and rodent gnawing. Carnivore shearing involves opposing teeth shearing past one another in a scissor like action at high force. Ungulate grinding involves mandibular movements that allow the cheek teeth to grind in occlusion and rodent gnawing allows an anteroposterior movement of the mandible to exclusively occlude either the incisors or the cheek teeth. As such all three specialised groups have differing proportions of temporalis, masseter and pterygoid depending on the specialised movement of the mandible (e.g. Figure 1.1).

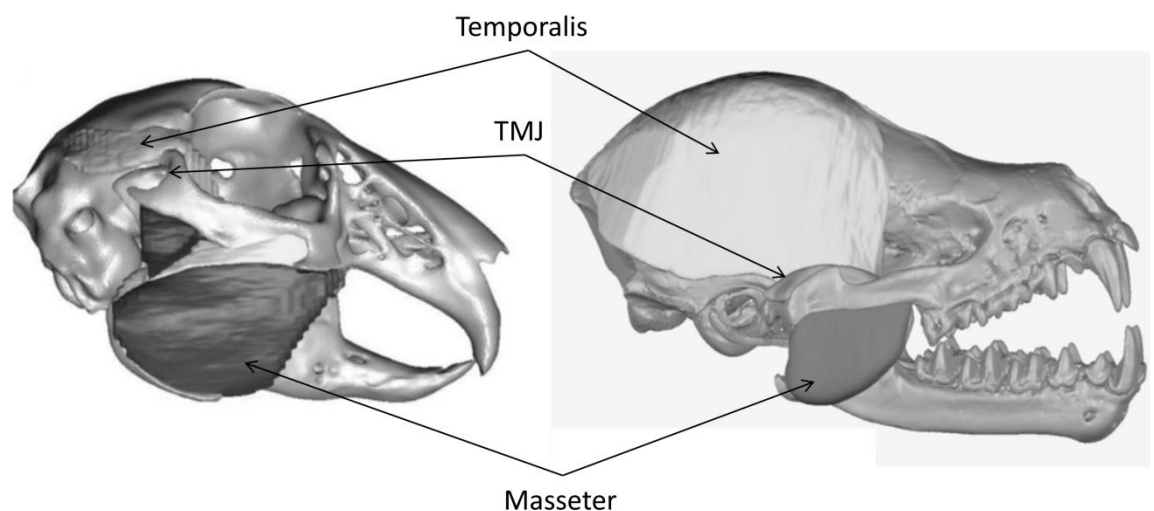


Figure 1.1. European rabbit, *Oryctolagus cuniculus* (left) and Fringe-lipped bat, *Trachops cirrhosis* (right). Representation of the differences in two main masticatory muscles (temporalis and masseter) of an herbivore (left) and an omnivore (right). Models not to scale. Figure modified from Watson et al. (2014) and Santana (2014).

In order to successfully consume and digest food items, animals must be able to fit the food in their mouths and break it down for manageable digestion. As such, maximum bite force and gape are two limiting factors in food consumption. Bite force has been shown to correlate strongly with food hardness in different vertebrate diets (e.g. Kiltie, 1982; Herrel et al., 1996, 2001, 2002; Williams et al., 2009; Santana et al., 2010), whereas gape can limit the size of food ingested by the animal (e.g. Gans, 1961; Herring and Herring, 1974; Herring, 1975; Emerson and Radinsky, 1980; Smith, 1984).

Bite force and gape capabilities are reflected by craniomandibular and muscular morphology. For example, animals known to produce a relatively larger bite force have increased head heights, wider skulls, and smaller fibre lengths, larger physiological cross sectional areas and higher mechanical advantages of the jaw muscles (Maynard Smith and Savage, 1959; Dumont and Herrel, 2003; Turnbull, 1970; Van Daele et al., 2009; Taylor and Vinyard, 2004; Taylor et al., 2009; Taylor and Vinyard, 2009; Santana et al., 2010; McIntosh and Cox, 2016; Chapter 2). Animals known to produce a wider gape have longer jaws, lower condyle heights, anteroposteriorly longer condyles, longer muscle fibre length (Herring and Herring, 1974; Gans and de Vree, 1987; Vinyard and Payseur, 2008; Taylor et al., 2009; Perry and Wall, 2008; Terhune et al., 2015). Interestingly, musculoskeletal features that facilitate a large bite force can also have a negative impact on the performance of gape, and vice versa. For example, longer muscle fibres, running parallel to the force generating muscle axis, improve muscle stretching and excursion, enabling the jaw to open wider (Herring and Herring, 1974; Williams and Goldspink, 1978). However, shorter fibres with a greater pennation angle (angle from force-generation axis) allow more fibres to be packed into a smaller space [larger physiological cross sectional area (PCSA)] and produce a larger bite force (Gans, 1982; Powell et al., 1984; van Eijden et al., 1997). In addition longer jaw lengths, although beneficial to gape capabilities, decrease the mechanical advantage of the masticatory muscles, especially during incisor biting (e.g. Maynard Smith and Savage, 1959; Turnbull, 1970; Dechow and Carlson, 1990; Weijs, 1980; Herrel et al., 2008).

Due to this mechanical trade-off between bite force and gape, most craniomandibular morphologies are adapted to produce a large bite force at narrow gape, or a small bite force at wide gape. However, food hardness has been shown to increase with food item size (e.g. Aguirre et al., 2003) and therefore some animals will require a large bite force at a wide gape. Turnbull (1970) found that animals requiring these types of masticatory actions have a dominating temporalis muscle, whereas animals that produce a large bite force at a narrow gape have a dominating masseter muscle. This is due to the superficial masseter's role in restricting gape (Herring and Herring, 1974). An animal that requires a large gape will therefore require a masseter with longer fibres (therefore reducing its bite force capacity). In order to improve its bite force, the temporalis muscle has to 'pick up the slack' left by the reduction in bite force capability of the masseter. Indeed, Taylor and Vinyard (2009) showed that tufted capuchins, which are renowned for their

tough diet, compared with other types of capuchin, had significantly larger temporalis PCSAs, without reducing the length of the muscle fibres. This muscle arrangement therefore allowed the tufted capuchins to bite down harder on their food items without compromising their gape capabilities as seen in other types of capuchin.

Carnivores are the quintessential example of using the large bite force and wide gape method of mastication (Emerson and Radinsky, 1980), as carnivorous prey can often exceed the size of the predator (Andersson et al., 2011). Carnivores represent many phylogenetically distant taxa, with a diverse range of ecologies (Nowak, 1999). Despite this diversity, morphological convergence of the masticatory system has occurred in many carnivorous lineages (for review see Van Valkenburgh, 2007). Indeed, convergence of carnivorous cranial shape on feeding ecology has been found in marsupial and placental mammals (Wroe and Milne, 2007; Goswami et al., 2011). These types of morphological convergences seen in certain clades were probably driven by biomechanical adaptations due to the need to respond to similar environments. For example, bone cracking has evolved separately three times within the Carnivora (Werdelin and Solounias, 1991; Wang et al., 1999). Bone cracking requires large bite force in order to break and digest bones. In order to achieve this bite force, bone crackers have reduced their snout length, which improves the mechanical advantage of the masticatory muscles. The skulls of bone crackers also feature a high sagittal crest, which allows for an expansion of the attachment site of the temporalis (Werdelin, 1989). Indeed, an FEA study on bone cracking skulls showed how the temporalis (compared with the masseter) drives the increase of bite force in these carnivores (Tseng and Wang, 2010), potentially showing how important the temporalis muscle is in constraining the shape of the cranium of mammals which require a large bite force.

1.2 Morphological integration

The craniomandibular complex, along with its associated musculature, makes up the components that form aspects of the mammalian masticatory system. As I have discussed above, the selection pressure on aspects of performance such as bite force and gape are high, as morphologies often converge when optimising these performance metrics. However, as well as contributing to the masticatory system, the cranium also

contains the brain and major sensory organs. This means that any evolutionary shift in morphology towards a more efficient masticatory system requires that any changes are not detrimental to the function of other organs stored in the cranium. This leads to the evolution of a functionally integrated mammalian cranium.

Morphological integration is the relationship among parts within an anatomical structure and how these parts covary (Olson and Miller, 1958). These parts can be of a genetic or phenotypic nature and must work and evolve together in order to create a successfully functioning unit. Studies of morphological integration can take place at a variety of different levels (e.g. developmental or evolutionary), depending on the origin and variation of the sample in question (Klingenberg, 2013). For example, quantifying how integration takes place ontogenetically requires a sample of the same species at different developmental stages. Studying the ontogenetic integration of the masticatory system in a species can quantify the direction of development of the system, and how these directions differ inter-specifically, showing the constraints and variabilities placed on the evolution of the mammalian masticatory system (e.g. Mitteroecker et al., 2004; Wilson and Sánchez-Villagra, 2010; Sebastião and Marroig, 2013).

When asking questions about functional adaptations and optimisations in the craniomandibular complex, it is important to understand how these changes affect other structures within the complex. The ability to quantify how two structures covary can potentially show how certain anatomical parts can constrain the shape of the overall structure. For example, all rodents contain a pair of continually growing incisors within the bony alveoli of the cranium. The angle of the upper incisor protruding from the rostrum varies a great deal within rodents. Rodents that have incisors that project far forward from the rostrum also have roots that extend behind the cheek teeth (Landry, 1957a; see Chapter 3). As the mammalian cranium is a very complex structure with many specialised, coordinated components (Cheverud, 1996), changes such as the incisors being rooted behind the cheek teeth and into parts of the orbit will almost certainly have repercussions for the other components of the highly integrated cranium. The effect of cranial and incisor morphological integration within the rodent masticatory system has not been studied before and is a central theme in this thesis (Chapter 3). Interestingly, rodent developmental pathways associated with teeth and skeletal tissues are thought to be independent (van Genderen et al., 1994; Kratochwil et al., 1996; Neubüser et al., 1997; James et al., 2002, for review see McCollum and Sharpe, 2001). Therefore, if cranial and incisor morphology is shown to be integrated in

rodents, it is an example of phenotypic accommodation, due to the two separate parts being controlled by different genetic stimuli (West-Eberhard, 2003; Badyaev, 2009).

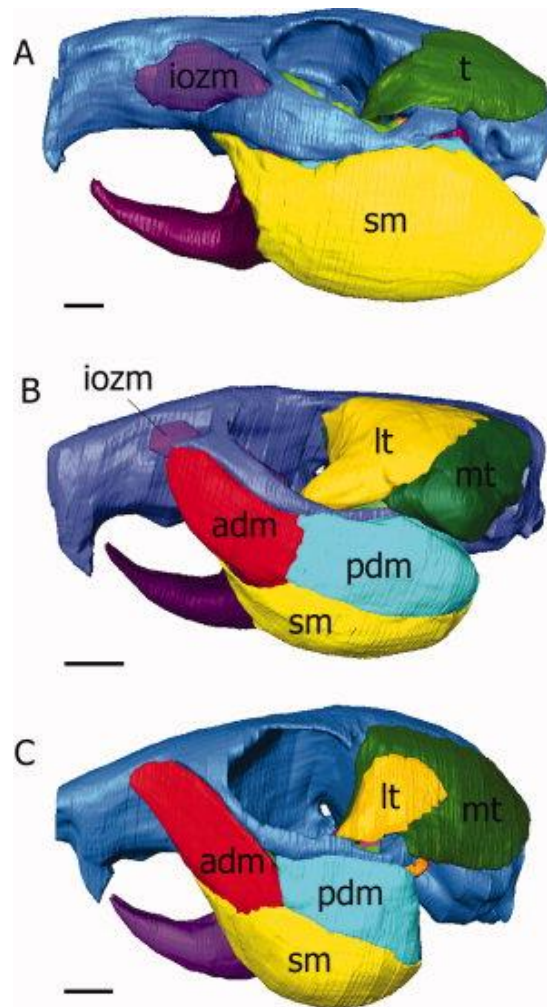


Figure 1.2 Left lateral view of 3D reconstructions of the skull, mandible and masticatory muscles of (A) Hystricomorph, (B) Myomorph and (C) Scuriomorph. Abbreviations: adm, anterior deep masseter; iozm, infraorbital part of zygomaticomandibularis; lt, lateral temporalis; mt, medial temporalis; pdm, posterior deep masseter; sm, superficial masseter; t, temporalis. All scale bars: 5 mm. Taken from Cox and Jeffery, 2011.

1.3 Rodentia

The order Rodentia (from the latin *rodere*, “to gnaw”) is the most diverse order of mammals and currently contains 2227 species and counting (Wilson and Reeder, 2005). The first clade of rodents appears in the Eocene, evolving from Paleocene animals with primitive masticatory musculature arrangements already adapted for gnawing (Nevo, 1979). All extant rodents gnaw with large, ever-growing incisors with no enamel on the lingual side. The rodent must gnaw with their incisors regularly in order to maintain a normal length, or malocclusion due to incisor overgrowth may occur (Herzberg and Schour, 1941). Due to dentine being exposed on the lingual side of the incisor, the softer dentine is worn away at a faster rate compared to the harder enamel, leaving the rodent with a chisel-like tip, useful for biting food materials, defence, and in some cases for burrow construction (see below). Rodents have two upper incisors and two lower incisors and predominantly use their lower incisors to gnaw, a trait unique to rodents (Druzinsky, 2015). The incisors curve backwards into the skull/mandible and are rooted above/behind the molars. Rodents do not have canines and instead have a diastema that divides the exposed incisors and molars. This unusual dental arrangement is not unique to rodents and has independently evolved in a number of mammalian species, such as the aye-aye and wombat. This dental arrangement evolving independently in such phylogenetically distant species is an interesting example of evolutionary convergence but more work needs to be done to show the biomechanical implications of such dental arrangements in these diverse mammals.

Rodent classifications in the past often used the unique masticatory system to define the order and as such grouped rodents based on the morphology of their masticatory muscles, into suborders Sciuromorpha (squirrel-like rodents), Hystricomorpha (porcupine-like rodents) and Myomorpha (mouse-like rodents) (Brandt, 1855; Simpson, 1945). Each of these arrangements of the musculature represents an expansion of the masseter onto the rostrum (see Figure 1.2). In Sciuromorpha, part of the masseter has expanded anterodorsally onto the root of the zygomatic arch and rostrum. This type of muscular arrangement is seen in the Sciuridae (squirrels), Castoridae (beavers) and Geomyoidea (pocket gophers, kangaroo rats and kangaroo mice). In Hystricomorpha, a deeper part of the masseter has expanded into the orbit and through an enlarged infraorbital foramen to attach on the snout. This arrangement is seen in the

Anomaluridae (scaly-tailed squirrels), Ctenodactylidae (gundis), Caviomorpha (South American rodents), Dipodidae (jerboas, jumping mice and birch mice), Pedetidae (springhare), Phiomorpha (African mole-rats, cane rats and the dassie rat). The Myomorpha arrangement combines the features of sciuriforms and hystricomorphs with the whole origin of the masseter expanding onto the rostrum (see Figure 1.2 for representation of each morphotype). This arrangement is seen in the Muroidea (mice and rats) and Gliridae (dormice).

The three rodent morphotypes have arisen convergently many times in the evolution of rodents and therefore are not monophyletic groups (Blanga-Kanfi et al., 2009; Churakov et al., 2010; Fabre et al., 2012). Also, some of the rodent groups, such as the Bathyergidae (see below) do not fully fit into any of the three morphotypes. However, Brandt's classification persists in the literature to describe the muscle arrangements of the masticatory system due to the seminal paper by Wood (1965). In his paper he also describes the primitive rodent condition "protrogomorph" seen in pre-Oligocene fossil rodents and the extant mountain beaver *Apodontia rufa* (see Figure 1.3). This condition is unlike the three groups described by Brandt (1855) (Figure 1.2), as protrogomorphous rodents lack the expansion of the masseter onto the rostrum.

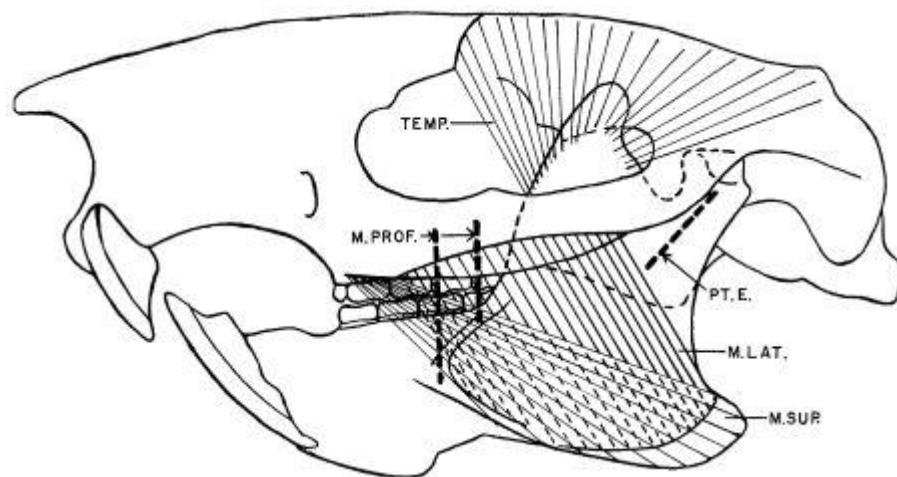


Figure 1.3 Skull of the Eocene protrogomorph *Ischyrotomus*, with the jaw musculature restored. Abbreviations: M. LAT.-Masseter lateralis, dashed portions lying beneath Masseter superficialis; M. PROF.-dashed lines indicating the course of the Masseter profundus; M. SUP.-Masseter superficialis; PT. E.-dashed line indicating course of Pterygoideus externus; TEMP.-Temporalis. Muscle nomenclature differs from Figure 1.2 due to the complex nature of the masseter layers and dissection techniques of researchers. This thesis therefore follows the nomenclature of Cox and Jeffery (2011). Taken from Wood, 1965.

An alternative classification for the order was proposed by Tullberg (1899). This classification divided the rodents into two suborders, Hystricognathi and Sciuromorphi, based on the angular process of the mandible (Figure 1.4). The hystricognathous jaw shows the angular process lateral to the plane of the alveolus of the incisors. In contrast, the sciuromorphous jaws are characterised by an angular process originating in the same plane that includes the alveolus of the incisors. Tullberg's classification has been slightly more resilient in the literature compared to Brandt's due to phylogenetic techniques showing the Hystricognathi as a monophyletic group (Fabre et al., 2012), but the Sciuromorphi are almost certainly a paraphyletic group. However, Hautier et al. (2011, 2015) showed using sophisticated shape analysis that some Hystricognathi species have jaws more similar to those described as Sciuromorphi. Therefore, due to the complex nature of rodent diversity and morphological convergences, rodent classification studies must be revisited in the context of phylogeny, morphology and palaeontology (Hautier et al., 2015).

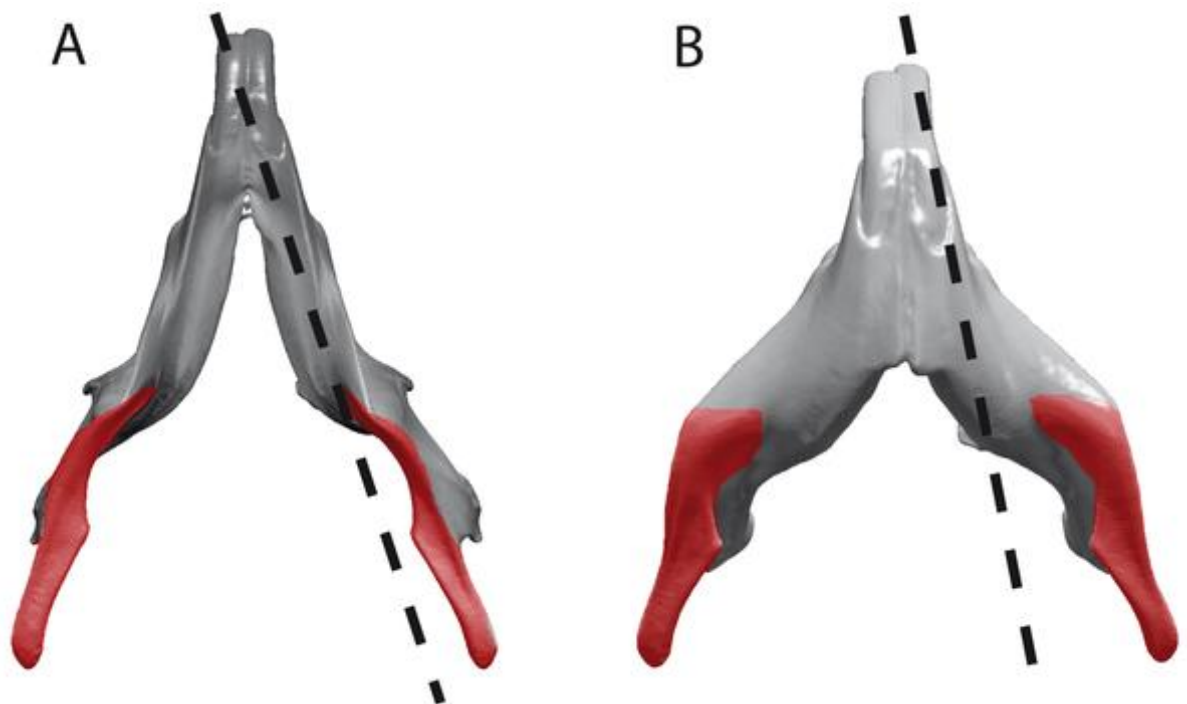


Figure 1.4 Mandibular types (A) sciuromorphous jaw and (B) hystricognathous jaw in ventral view. Dashed line represents the incisor plane. The angular process is coloured in red. Taken from Hautier et al, 2011.

1.4 Subterranean rodents

Of the 2227 extant rodent species, approximately 250 spend their lives underground, in all continents except for Australia and Antarctica (Begall et al., 2007). Subterranean rodents are represented in six families of rodent: Bathyergidae; Cricetidae; Ctenomyidae; Geomyidae; Octodontidae and Spalacidae, with rodents evolving a subterranean lifestyle in multiple separate lineages within the rodent phylogeny. Subterranean rodents spend the majority of their lives in self constructed burrows in the ground. Burrowing adaptations in rodents occurred early in rodent evolution, around the Eocene-Oligocene radiation (e.g. in Bathyergidae) and evolved independently in the Miocene-Pliocene radiation (e.g. in Geomyidae and Spalacidae). However, mammals adapting to underground conditions probably occurred much earlier. A basal member of the mammalian lineage (*Fruitafossor windscheffi*) from the late Jurassic was described with morphological characteristics associated with burrowing animals (Luo and Wible, 2005). This provides evidence that fossoriality accompanied mammalian evolution at the very earliest radiations. Evolutionary parallelisms in multiple lineages of rodent towards fossoriality probably occurred due to the many benefits that an underground lifestyle can provide. Primarily, the subterranean ecotope is simple and relatively stable compared to the above-ground environment. For example, less than a few centimetres below ground, temperatures fluctuate a lot less than above ground (above ground temperatures can fluctuate as much as 20°C, whereas below ground temperature fluctuations are close to zero (Kenagy, 1973) and by about 30cm nearly all daily temperature fluctuations disappear (Reichman et al., 1985). This insulation protects subterranean mammals from extreme temperatures and weather conditions that animals above ground are faced with. This type of protection also keeps out predators such as birds and most terrestrial carnivores, although some small carnivores such as ferrets, weasels and snakes do go into burrows after rodents (Hoogland, 1981; Reichman and Smith, 1990). This ecological simplicity led to many morphological convergences in subterranean rodents, with none more obvious than adaptations to burrow construction (Nevo, 1979).

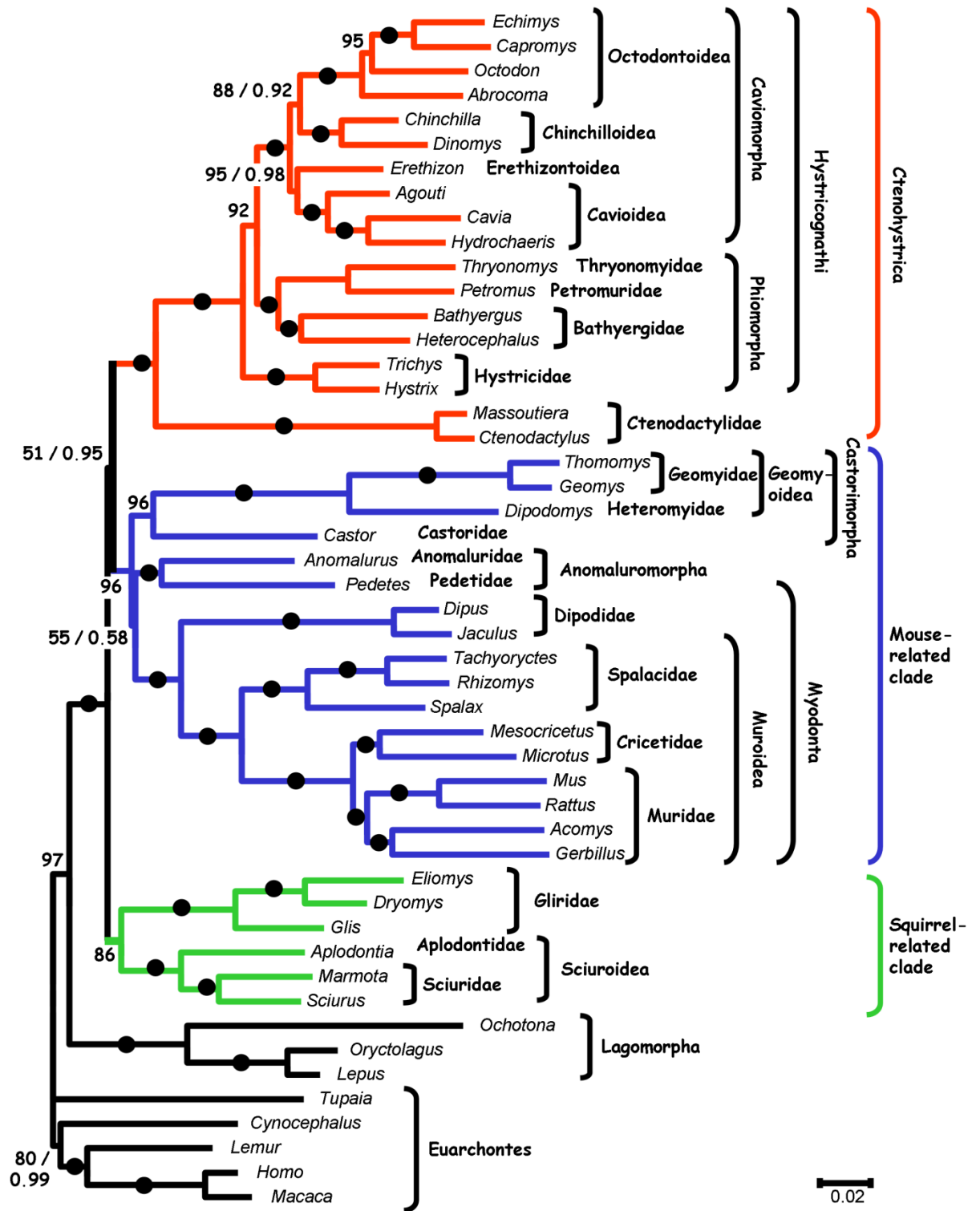


Figure 1.5 Phylogenetic tree of the Rodentia order. For each node the ML bootstrap percentage (BP) and the Bayesian posterior probabilities (PP) are given at the right and left of the slash, respectively Taken from Blanga-Kanfi et al., 2009.

1.4.1 Digging in subterranean rodents

As said above, the mammalian craniomandibular complex has been extensively studied in the context of food acquisition (e.g. Dumont and Herrel, 2003; Vinyard et al., 2008; Hiiemae and Kay, 1972; Attard et al., 2011). However, the mammalian craniomandibular complex is a functionally dual structure which is used in feeding, defence, mating rituals and in the case of some subterranean rodents, digging. These aspects of the craniomandibular complex are poorly studied despite having an important influence on evolutionary success. This thesis aims to look at the influence of digging on the craniomandibular complex in subterranean rodents [with an emphasis on the bathyergids (see below)] and to compare these morphological differences to other rodents with similar digging methods. Morphological and functional convergence in subterranean rodents is most clearly seen in the morphology associated with digging (Nevo, 1979; Nevo and Reig, 1990). However, it has also been shown that changes in soil types do not represent a selective pressure on the digging apparatus of cururos (*Spalacopus cyanus*) (Bacigalupe et al., 2002). In subterranean rodents, there are two main types of digging methods: scratch digging and chisel-tooth digging (Hildebrand, 1985; Figure 1.6). There is a third specialised digging method called head-lifting, which uses the incisors and the spade shape head of the rodent in combination to create a “drill and shovel” movement. This digging method is used by some members of the Spalacidae. However, there are no specimens present in any of the samples in this thesis that use this method to dig and will therefore not be discussed further.

Scratch digging rodents use their forelimbs in an alternating manner of flexion and extension, where the soil is primarily broken down and loosened by the claws. This mode of digging is used predominately by Geomyids, including *Geomys*, *Ctenomys* and *Bathyergus* also operate using this mode of digging (Landry, 1957; Ognev, 1962; Lessa and Thaeler, 1989; Gambaryan and Gasc, 1993; Camin et al., 1995).

Chisel-tooth digging rodents use their procumbent incisors, along with powerful head and jaw muscles, to break down and remove soil. This mode of digging has been observed in all the members of the Bathyergidae, with the exception of *Bathyergus*. It has also been observed in certain members of the Spalacidae family, including some species in the genera *Cannomys*, *Rhizomys* and *Tachyoryctes* (Holliger, 1916; Landry, 1957a; Jarvis and Sale, 1971; Lessa and Thaeler, 1989; van der Merwe and Botha, 1998; Becerra et al., 2012).

It has been suggested that the type of digging adopted also causes restrictions to the type of habitat that can be selected. For instance, scratch diggers (see below) are often restricted to sandy soils, whereas chisel-tooth diggers can exploit a wider range of harder soils (Lessa and Thaler, 1989).

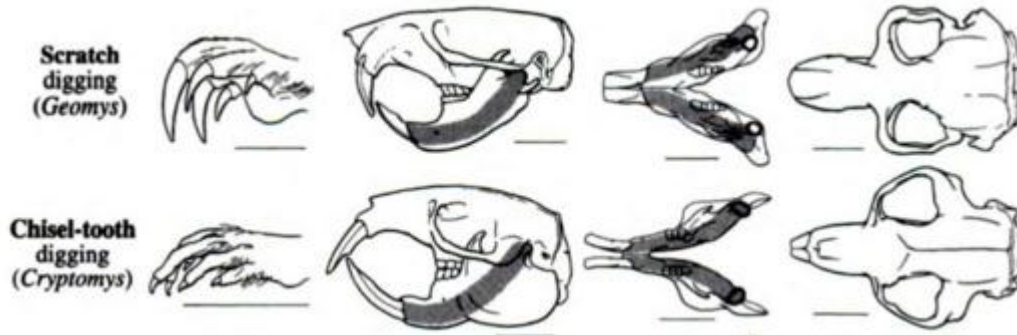


Figure 1.6 Comparative cranial morphology of a scratch digger (above) and a chisel-tooth digger (below). Modified from Stein (2000).

1.5 Intergeneric relationships of the Bathyergidae

All members of the Bathyergidae family are chisel-tooth diggers, with the exception of *Bathyergus* which is a scratch digger. As can be seen from Figure 1.7, *Heterocephalus* is the basal genus in the family, whereas *Bathyergus* is nested deep within the crown. This means it is most parsimonious to assume that the common ancestor was a chisel tooth digger. As *Bathyergus* uses the scratch digging method, this makes the Bathyergidae a particularly good cohort for studying morphological changes associated with digging in rodents.

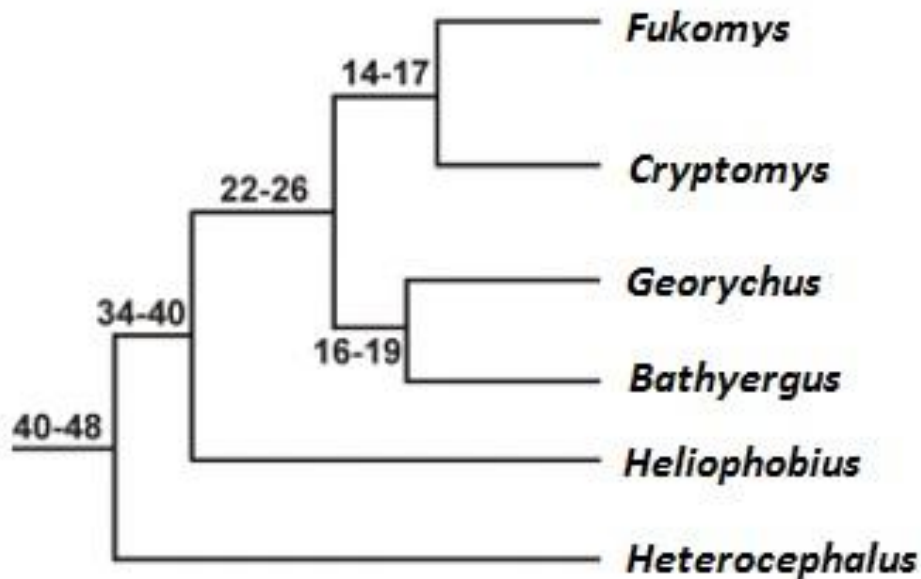


Figure 1.7. Phylogenetic tree of extant genera of the Bathyergidae. Units-million years ago. Modified from Seney et al., 2009.

African mole-rats (family: Bathyergidae) are a unique group of subterranean rodents due to their particular masticatory muscle arrangement. In the past, it was deemed difficult to place the bathyergids into Brandt's groupings due to the lack of expansion of the masseter onto the rostrum. Despite this ambiguity, they seemed closest to the hystricomorphs due to characteristics in their reproductive system (Faulkes et al., 1990) and molecular phylogeny (Nedbal et al., 1994). However, the configuration of the masseter muscle complex in the Bathyergidae resembles that of the protrogomorph condition (Figure 1.3), which leads to the idea that the Bathyergidae have, in an evolutionary sense, reversed their muscular arrangement compared to the other rodents (Landry, 1957b; Maier and Schrenk, 1987; Cox and Faulkes, 2014). As mentioned above, because the Hystricognathi has persisted within the literature because there is strong support that the hystricognaths are a monophyletic group (Fabre et al., 2012) and so all members of the group have a shared common ancestor. Phylogenetic analyses (Faulkes et al., 2004; Ingram et al., 2004; Kock et al., 2006; Blanga-Kanfi et al., 2009) and morphological analysis (Gomes Rodrigues et al., *in press*) have placed the family within this suborder. The hystricognath group can then be split into the Old World infraorder Phiomorpha, of which the Bathyergidae is a member, and the New World caviomorphs. Bathyergids' closest relatives are the rock rats (Petromuridae) and the cane rats (Thryonomyidae) (Blanga-Kanfi et al., 2009) (see Figure 1.5).

The Bathyergidae consists of 6 extant genera, the largest number within subterranean rodents: *Heterocephalus*; *Heliophobius*; *Georchycus*; *Bathyergus*; *Cryptomys* and *Fukomys* (Figure 1.7). The basal genus of this family is the eusocial naked mole-rat *Heterocephalus glaber* (Allard and Honeycutt, 1992). At the next dichotomy, *Heliophobius* is the 2nd most basal member, forming a sister lineage to the rest of the family. *Georchycus* and *Bathyergus* group into a monophyletic clade (Faulkes et al., 2004). The relationship between *Cryptomys* and *Fukomys* is still poorly resolved, and as a result these were considered part of the same genus until very recently. Morphological synapomorphies between the other genera allow them to be grouped without any ambiguity. However, *Cryptomys* and *Fukomys* cannot be separated on morphological and traditional morphometric data. It is however recognised that *Cryptomys* and *Fukomys* are indeed two separate genera, based on nuclear and mitochondrial analyses (Nevo et al., 1987; Janecek et al., 1992; Filippucci et al., 1997; Faulkes et al., 1997, 2004; Walton et al., 2000; Ingram et al., 2004; Kock et al., 2006; Deuve et al., 2008).

1.6 Geographical distribution of the Bathyergidae

The Bathyergidae have a diverse distribution throughout sub-Saharan Africa, living in a wide range of habitats of different altitudes, soil types, vegetation and rainfall patterns. The social genera of mole-rat i.e. *Heterocephalus*, *Cryptomys* and *Fukomys* are smaller than their solitary counterparts and are found in more xeric conditions. It is believed that the social genera are particularly successful and have a wider distribution than solitary genera (Jarvis and Bennett, 1990).

The genus *Bathyergus* is composed of 2 species, the Cape dune mole-rat (*Bathyergus suillus*) and the Namaqua dune mole-rat (*Bathyergus janetta*). Both are solitary and are endemic to the south and south west of Africa. The Cape dune mole-rat is associated with sand dunes and in areas of high rainfall; it is also the largest of all Bathyergidae, weighing up to 2500g. They also exhibit sexual dimorphism, with males being significantly larger than females (Davies and Jarvis, 1986). The Namaqua dune mole-rat differs in its choice of habitat, as it resides in more xeric conditions (South Africa has some of the lowest rainfall in Africa). This is of particular interest to the study of evolution of sociality, as sociality is thought to be linked to conditions of decreasing moisture (Bennett and Faulkes, 2000).

The more social genera, *Cryptomys* and *Heterocephalus*, which are generally smaller than the other Bathyergids, rarely exceed 600g (Wallace and Bennett, 1998).

Heterocephalus glaber or the naked mole rat is found in the arid regions of East Africa, with very low rainfall (as little as 400mm per year). The species is generally found in hard soil areas and its members are the smallest of the Bathyergidae, with a mean body mass of 34g (Sherman et al., 1991). Until recently, *Cryptomys* were the most speciose of the Bathyergidae family. However, the majority of the species were moved to the genus *Fukomys* following phylogenetic analyses (Kock et al., 2006). The only species well represented in this genus is unsurprisingly named, the common mole-rat (*Cryptomys hottentotus*), which has a wide distribution. They are spread throughout most of Southern Africa and so ironically are rather uncommon in the Bathyergidae family, as they can be found in both mesic and xeric conditions.

The genus *Fukomys* is the most recently named African mole-rat (Kock et al., 2006). Their relationship with *Cryptomys* has been a difficult one to differentiate. On a sub-familial level, groupings of the Bathyergidae are not corroborated by molecular evidence (Walton et al., 2000). Morphological analyses (supported by molecular analysis) show discrete groups of *Heterocephalus*, *Bathyergus*, *Georchus* and *Heliophobius*. However, *Cryptomys* and *Fukomys* cannot be distinguished easily morphologically, which is why for a long time the two groups were placed in one genus (*Cryptomys*). Having said this, recent geometric morphometric data has shown subtle differences between the two (Van Daele et al., 2004). When the group was analysed on a molecular level (Ingram et al., 2004), it was clear that the genus needed to be divided into two, culminating in Kock et al. (2006) announcing a new genus, *Fukomys*. While the *Cryptomys* genus is exclusively in southern Africa, the *Fukomys* genus is widely spread throughout the continent, resulting in a genus with increased diversity of chromosomal form compared to other African mole-rats (Van Daele et al., 2007a). This initial spread of *Fukomys* has left extant, but separated, populations in central Africa, especially in areas such as Democratic Republic of Congo, Angola and Zambia (*F. mechowii*/ giant mole-rat). A new species of mole-rat has only recently been described by Van Daele et al. (2013), Caroline's mole-rat, *F. vandewoestijneae*. This new species has been placed without doubt in the sister clade of the giant mole-rat, *F. mechowii* using earlier chromosomal and DNA sequence studies (Van Daele et al., 2004, 2007b) and has been shown to have a distinct cranial morphology from its closest relative using morphometric analyses (Van Daele et al., 2013). It was located on the Zambezi-Congo

River watershed and there is currently no indication that there is any overlap with the giant mole-rat. Other species from the genus *Fukomys* have been described in loci as far west as Ghana (*F. zechi*), Nigeria (*F. foxi*) and Nigeria/Sudan/Uganda (*F. ochraceocinereus*) (Van Daele et al., 2007b). The varied biogeography of the genus may explain the increased variation of karyotype number ($2n=40-78$) when compared with the other members of the Bathyergidae family (*Heterocephalus*- $2n=60$, *Heliophobius*- $2n=60-62$, *Bathyergus*- $2n=56$, *Georychus*- $2n=54$, *Cryptomys*- $2n=54$). They are also rather unusual amongst Bathyergidae as they consist of solitary, social and eusocial species and therefore are a suitable model for studying the evolution of sociality among mammals, an interesting topic that has not yet been fully resolved. (Burda et al., 2000).

The Cape mole-rat, *Georychus capensis*, resides in the south-western and southern parts of the Cape of Good Hope Province in South Africa (Nowak, 1999). These areas have average rainfalls of over 500mm per annum and therefore it can be said that the Cape mole-rat is exclusively found in mesic conditions. It is a solitary rodent and has an average body size of 180g for both sexes (Sherman et al., 1991)

Finally, the silvery mole-rat, *Heliophobius argenteocinereus* has a large geographical distribution covering 18 latitudinal degrees, from Eastern Africa south of the Equator. This geographical distribution may explain its karyotypic variation ($2n=60-62$). These areas are characterised by a high annual rainfall, which on average exceeds 900mm (Bennett and Faulkes, 2000). Body size of the silvery mole-rat is on average around 180g for both sexes (Jarvis and Bennett, 1991).

1.7 Ecology and Sociality

Mole-rats are herbivorous, and primarily eat geophytes, which are perennial plants with a high nutritional value. They consist of an underground storage organ, such as a bulb, tuber, corm or rhizome. The parts of the plant that live above ground deteriorate during adverse weather conditions, but the buds of the plant are perpetually available throughout the entire year. Mole-rat genera *Georychus* and *Bathyergus* also consume above ground vegetation from grasses and forbs (Davies and Jarvis, 1986; Robb et al., 2012) in particular, the Cape dune mole-rat (*B. suillus*) consumes 50% of its diet in

above ground vegetation. Geophytes are unavailable to most animal species due to the protection measures that the plants implement to defend themselves. Some geophytes are known to be toxic and contain cardiac glycosides (Watt and Breyer-Brandwijk, 1962), whereas others maintain physical barriers such as thick tunics and spinous coverings (Lovegrove and Jarvis, 1986). These defences do not constrain the mole-rats from consumption of geophytes, as they seem to be immune to toxins and their chisel-like incisors can penetrate the protective coverings of the geophytes (Bennett and Faulkes, 2000). This therefore means there is little competition from non-mole-rat species, and is probably one of the main reasons for the family's large geographical spread.

Although mole-rats are predominately herbivorous, there is evidence that they occasionally ingest invertebrates which are commonly found in mole-rat burrows (Jarvis, 1991; Burda and Kawalika, 1993). However, the gut (Jarvis and Bennett, 1991) and the dentition (Roberts, 1951) of all mole-rats are adapted to a high-fibre herbivorous diet and so omnivory within the family is probably a rare occurrence.

Ecology and sociality has been shown to be linked within the mole-rat family. The amount of energy available in an area, i.e. the abundance of geophytes, affects the body size, and regional differences have been found in the naked mole-rat (Jarvis, 1981), the common mole-rat (Bennett and Faulkes, 2000) and the silvery mole-rat (Barciova et al., 2009). It has been hypothesised that smaller, social mole-rats can exploit regions with less energy, i.e. the small eusocial naked mole-rat, compared to the larger, solitary Cape dune mole-rats. A number of authors have proposed that the distribution, size and digestibility of the geophytes, as well as the variation of rainfall, relates to the sociality amongst the Bathyergidae, i.e. the larger, more sociable colonies are associated with a decreasing geophyte density and rainfall (Jarvis et al., 1994; Faulkes et al., 1997). Seasonal variations within habitats have also been studied in the silvery mole-rat, *Heliophobius argenteocinereus* (Zelova et al., 2011). This work concluded that daily energy expenditure in this species increased 1.4 times after the first heavy rainfall of the wet season, which is probably due to the increased burrowing activities. This adaptation to their environment could explain the large geographical distribution of a solitary species (the silvery mole-rat), along with its ability to remove harder soil more efficiently using a chisel-tooth method of digging (Lessa, 1990). This is in contrast to the solitary scratch diggers in the genus *Bathyergus*, which are geographically

constrained in southern South Africa, and are associated with loose coastal sands and an abundance of resources (Bennett and Faulkes, 2000).

1.8 Aims

The aim of this thesis is to elucidate digging function from the skulls of subterranean rodents using a number of sophisticated techniques such as traditional/ geometric morphometrics, finite element analysis and other 3D biomechanical models. The results of this thesis are contained in chapters 2, 3 and 4 and each chapter's aims are as follows:

1.8.1 Chapter 2

This chapter uses the subterranean rodent family, Bathyergidae as an example to show how morphology reflects function. As discussed above, bathyergids consist of five genera of chisel-tooth diggers and one genus of scratch digger. Their very similar environment and diet make them a good example to investigate how differing digging functions reflect morphology associated with digging. The chapter first describes biomechanical requirements of morphology to produce a high bite force and wide gape, two characteristics essential for a successful chisel-tooth digger. Linear measurements and 3D biomechanical models are then used to compare the differences in morphology of chisel-tooth and scratch digging rodents to show if there are functional implications in morphology.

1.8.2 Chapter 3

As discussed above, chisel-tooth digging has arisen independently in multiple lineages of subterranean rodent. Previous studies have already shown that the cranial shapes of chisel-tooth digging rodents converge in morphospace (Samuels and Van Valkenburgh, 2009, Gomes Rodrigues et al., *in press*). On top of this, it has been observed that chisel-tooth digging rodents have upper incisor roots that are displaced posteriorly in comparison to scratch digging rodents (Landry, 1957a). Using a diverse sample of subterranean and terrestrial rodents, this chapter aims to quantify rodent cranial shape using geometric morphometrics and phylogenetic comparative methods (see below) to confirm the morphological convergence of chisel-tooth digging cranial shape. The incisor morphology is quantified using radius of curvature and second moment of area (see chapter 3) to show if chisel-tooth digging rodents possess upper incisors that are

significantly different from other rodent upper incisors. Finally, using partial least squares (see below), this study assesses the covariation between cranial shape and incisor morphology in my rodent sample to show how/if these structures constrain craniodental form in rodents.

1.8.3 Chapter 4

This chapter aims to investigate the performance of the subterranean rodent cranium in relation to digging to show if the previously found chisel-tooth digging cranial shape is beneficial or detrimental to its ability to produce a high bite force and wide gape. This will be achieved using a novel approach combining finite element analysis and geometric morphometrics (see below). One chisel-tooth digger and one scratch digger from the Bathyergidae family will be compared to show differences in digging performance metrics.

1.9 Methods

In order to achieve these aims, the following methods have been used in this thesis:-

1.9.1 3-D biomechanical models

In chapter 2, the mechanical advantages of three key masticatory muscles (deep masseter, superficial masseter and temporalis) is measured. Mechanical advantage is the measurement of efficiency of each muscle if it was modelled as a static third class lever/moment arm (e.g. Maynard Smith and Savage, 1959; Adams and Rohlf, 2000; Metzger and Herrel, 2005; McIntosh and Cox, 2016; Chapter 2).

In a third class static lever system, an input force is applied between a pivot/fulcrum and a load (Figure 1.8). In masticatory biomechanics, the force is the input from the masticatory muscle e.g. temporalis, the pivot is the temporomandibular joint (TMJ), and the load is the bite point. In order for the system to be able to deal with a certain load it either increases the size of the force, or decreases the distance of the load from the pivot. Therefore in masticatory biomechanics, a system is said to have increased mechanical advantage if the muscle input is larger, or the bite point is closer to the TMJ i.e. has a short jaw.

It is hypothesised that if a muscular system has a higher mechanical advantage, then it can convert a higher amount of its input energy into a higher bite force.

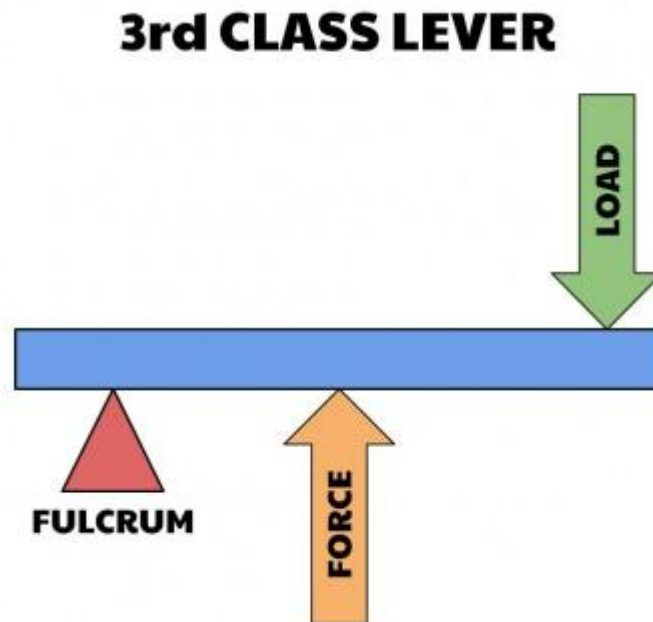


Figure 1.8. A basic example of a 3rd class lever system.

1.9.2 Geometric morphometrics

Geometric morphometrics (GMM) is a statistical method to quantify shape (for review see O'Higgins, 2000). It is a vast improvement on traditional morphometrics such as linear distances, angles and ratios due to the well understood and well behaved statistical shape space of Kendall (Kendall, 1984) and the ability of the methods to allow visualisation of results at all stages of analysis. It is based on representing biological form as homologous points in a Cartesian coordinate system. These homologous points are known as landmarks and are normally placed in anatomical positions of a specimen that are equivalent in all specimens in a given sample. Such examples of anatomical positions normally include cranial foramina, sutures and bony processes. Increasing the amount of landmarks on a specimen improves the accuracy of the shape 'captured' in the analysis. As there are only a finite number of anatomical landmarks on biological specimens, other landmarks must be used in order to capture a more accurate shape. Examples of non-anatomical landmarks include maxima and minima of curves, median between two points etc. Landmarks have been categorised

into types and it is thought that using anatomical landmarks is most accurate when trying to capture equivalency (Bookstein, 1991; Dryden and Mardia, 1998; but see Oxnard and O'Higgins, 2009).

In my study, landmarks are taken from microCT scans that are represented as surfaces in commercial visualisation software. The landmarks are therefore in 3D and represented in the same global Cartesian coordinate system. In this description, a whole set of landmarks on each specimen will be called a configuration. In order to quantify the variation of shape within a sample, a generalized Procrustes superimposition is carried out on the coordinates (Rohlf and Slice, 1990). This procedure translates all landmark configurations to a common coordinate system, usually a centroid of the average configuration. Each configuration is then scaled to unit centroid size, which is the square root of the sum of squared distances of each landmark from the centroid of the given configuration. Each configuration is then rotated in an iterative process in a manner which eventually minimises each squared inter-landmark distance. This process of translating, scaling and rotating removes all non-shape aspects of each configuration and represents the sample in Kendall's shape space (Kendall, 1984). Each configuration therefore has new coordinates called Procrustes shape coordinates, which represent the variation of shape within the sample (although see chapter 4 for an example of using GMM to evaluate size and shape of an object).

Due to its multivariate nature, in order to visualise the shape variations on a graph, a principal components analysis must be carried out. This analysis rotates the multivariate data (without compromising the variation of shape in the sample) in order to represent the maximum proportion of total variance in the successive PCs in the sample as possible. Further statistical tests can then be carried out using principal component scores (representing single specimens) to assess the significance of the shape variation within a sample e.g, multivariate analysis of variance (MANOVA).

The covariation between two or more *a priori* structures can also be assessed from multivariate/shape data using partial least squares (PLS) (Rohlf and Corti, 2000; Bookstein et al., 2003). This process decomposes a non-diagonal matrix of the partitioned variance-covariance matrix of the two structures into a pair of axes that quantifies the covariation between them. This process is known as singular value decomposition (Eckart and Young, 1936). PLS is preferred over regression methods due

to not having to assign direction to either variable (or structure) i.e. independent or dependent.

1.9.3 *Phylogenetic comparative methods*

The central limit theorem states that the mean and variance of a large number of independent random points will have a normal distribution i.e. a bell-shaped curve. All parametric statistical tests e.g. ANOVA, require input data to conform to the central limit theorem. However, biological data cannot be described as independent random points, as contemporary species have evolved from common ancestors and therefore are not strictly independent (Felsenstein, 1985). This fundamental violation of a tests assumption may lead to a higher rate of type I or II errors. It is therefore necessary to account for or remove this phylogenetic correlation within biological data. In evolutionary biology, independent contrasts (Felsenstein, 1985) and phylogenetic regression (Grafen, 1989) are the two most popular methods for removing (independent contrasts) or accounting for (phylogenetic regression) phylogenetic correlation.

Independent contrasts work under the idea that the evolutionary difference of a trait between a pair of sister taxa (adjacent species on a tree) is independent from any phylogenetic inertia that the raw biological data are subjected to and are thus not violating any statistical assumptions. These independent contrast points can therefore be used in any standard statistical tests. Independent contrasts work under the assumption that traits are evolving under a Brownian motion model of evolution (Felsenstein, 1985). Brownian motion assumes that the evolutionary change is undirected, has a mean of zero and variance is proportional to time. In a phylogeny, time is represented as the branch length. The difference between two sister taxa on a phylogeny is therefore assumed to be a proportion of variance from the original raw data point.

The other popular method, which accounts for phylogenetic correlation, is the phylogenetic regression (Grafen, 1989). Normal linear regression goes by the equation of a straight line ($Y = \beta X + \epsilon$) where Y is the dependent variable (trait), X is the independent variable, β is a vector containing parameters (including intercept) of the univariate or multivariate linear regression model (Rencher and Schaalje, 2008) and ϵ is a vector containing the residual error in the model. Under an Ordinary Least Squares (OLS) regression model, ϵ is a covariance matrix given by the residual variance (multiplied by an identity matrix). Residual variance is the variance in the dependent

variable that is not explained by the regressors. However, in a phylogenetic case, the regression model has to account for phylogenetic correlations. An evolutionary covariance matrix is included in the β and ε vectors (see Figure 1.9) which accounts for the phylogenetic relationships. Including this evolutionary matrix in a linear model is a special case of Generalised Least Squares (GLS) called Phylogenetic Generalised Least Squares (PGLS) (Martins and Hansen, 1997). This is the method that is used in this thesis to account for phylogeny, and will be modelled using Brownian motion.

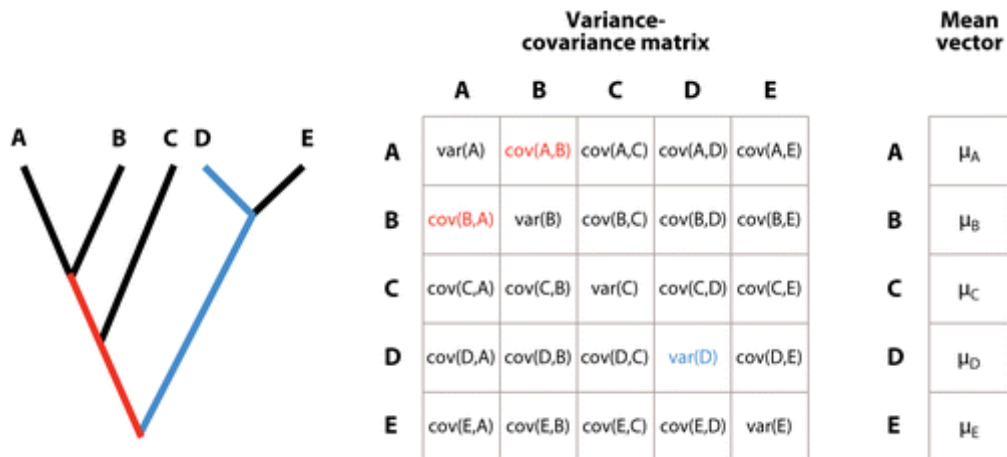


Figure 1.9 Taken from O'Meara (2012). The figure shows a tree, the tree's variance-covariance matrix, and the vector of means (which, under Brownian motion, would equal the root state). Highlighted are the branches that contribute to covariance between taxa A and B (red) and the branches leading to variance in D (blue).

1.9.4 Finite element analysis

Chapter 4 uses a technique originally developed for engineers called finite element analysis (FEA). In a commercial sense, it is used to study the stresses and strains in products designed by engineers to assess the structural integrity of an object such as a bridge or plane. These designs can then be altered to improve the object's safety factors, and so reducing the probability that the object will fail under a given load.

Engineers first incorporated FEA into their repertoire when computer power became large enough to solve the analytically intensive FE equations, especially in the aerospace industry (Levy, 1953). FEA was then adopted by the field of biomechanics, principally for research into orthopaedic medicine (Huiskes & Chao 1983). It wasn't until 2001 before the first study using FEA in functional morphology appeared, looking at the cranial design of a theropod dinosaur (Rayfield et al., 2001). Since this inaugural study, a plethora of publications using FEA to study the form of many extant and

extinct vertebrate skeletons has appeared in the literature. The majority of these studies have focused on the stress, strain and deformations of the vertebrate skull in response to forces applied by the masticatory muscles. Studies have included extant primates (e.g. Fitton et al., 2012), rodents (e.g. Cox et al., 2012), bats (e.g. Dumont et al., 2005), crocodiles (e.g. McHenry et al., 2006), pigs (e.g. Bright & Gröning, 2011) and humans (e.g. Toro-Ibacache et al., 2016). Other studies have concentrated on the form of extinct vertebrate crania such as dinosaurs (e.g. Button et al., 2014), hominins (e.g. Smith et al., 2015) and rodents (Cox et al., 2015). Although most of these studies involve the crania, some have also included FEA of the mandible in animals such as crocodiles (e.g. Porro et al., 2013), humans (e.g. Gröning et al. 2011) and ostriches (e.g. Rayfield 2011).

FEA has been popular due to the non-invasiveness of the technique. Before FEA studies became popular in biology, stresses and strains in biological structures were measured using strain gauges, which had to be bound to the surface with loads placed on the skull (e.g. Hylander et al., 1987; Herring and Teng, 2000). Unlike design engineers, morphologists test nature's designs, with most studies not changing the shape of the object for optimisation purposes, but testing the shape under different loading conditions that potentially could occur in nature (Rayfield, 2007).

Stress is the measure of an applied load (e.g. muscle) at a given orientation on a surface (e.g. coronoid process) and equals force per unit area. When an object is under a load, it will deform. How much an object changes from its original form is known as strain. The direction and magnitude of stress and strain depend not only on the applied load, but also on the material properties of the surface the load is being applied to. For example, a material can be isotropic, which means the material is directionally independent when a load is applied. Most FE studies model bone as isotropic, but this might not always be the case (e.g. Geraldes and Phillips, 2014). A material can also be anisotropic, and is directionally dependent, and so may only deform in a certain direction. Material properties of an object are represented by Young's modulus (elasticity), Poisson's ratio (change in width after a give change in length), shear properties (shear modulus) and density. In FEA, these properties are all assigned to a structure in order to estimate how it performs under a given load (see Figure 1.10).

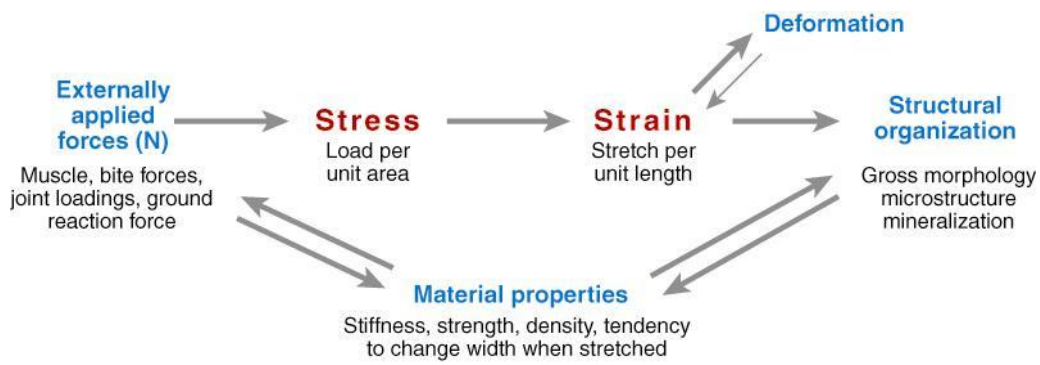


Figure 1.10 Relationship between stress and strain in skeletal bone. Taken from Rayfield (2007).

In order to model how a specific biological form responds to its function, boundary conditions must be present. For instance, when modelling masticatory performance of the skull, the skull is normally constrained at the TMJ (normally in all directions). The bite point must also be constrained, but normally only in the axis of the orientation of bite forces at the tooth. Other boundary conditions include the sizes of muscle attachments and muscle force values, which can normally be estimated using physiological cross-sectional areas. In order to test how gape affects the performance of FE models, a rotation matrix can be used to rotate the direction of muscle vectors around the TMJ, something that will be examined in this thesis. Specific methods of creating FE models can be found in Chapter 4.

Fundamentally, FEA is attempting to model biological reality. It is therefore important to know how accurate these models are in mirroring what is actually occurring. As FEA moves from its infancy to a well-established technique in the field of vertebrate morphology, it has gone through rigorous testing in the form of sensitivity and validation studies. Importantly, a model in any form can only be as accurate as the input it receives. Parameters such as material properties, constraints and loads are often unknown or can only be roughly estimated in biological models. Therefore, model outputs must be cautiously interpreted. Indeed, some studies have shown that FEA model outputs (e.g. strain values) do not match *in vivo* measurements in absolute terms (Strait et al., 2005; Bright and Rayfield, 2011; Porro et al., 2013). These studies do show however that the relative values between FE model outputs and *in vivo* measurements match (e.g. areas of high and low strain in FE models are also areas of high and low strain measured *in vivo*).

As one of the main aims in this thesis is to test how gape affects the performance of two different cranial morphologies using two unvalidated FE models, it is justified to compare the performance of each model relative to differing input values (e.g. different muscle vector orientations).

Chapter 2: Functional implications of the craniomandibular complex in African mole-rats (Rodentia: Bathyergidae)

This chapter is a modified version of the publication: MCINTOSH, A. F. & COX, P. G. 2016. Functional implications of craniomandibular morphology in African mole-rats (Rodentia: Bathyergidae). *Biological Journal of the Linnean Society*, 117, 447-462. DOI: 10.1111/bij.12691

2.1 Introduction

Anatomical adaptations for digging in subterranean rodents have been well documented (Nevo, 1979); such modifications could be the result of numerous different evolutionary strategies. Lessa and Thaler (1989) proposed two alternative evolutionary strategies for digging in two genera of pocket gopher: an increase in incisor procumbency to facilitate chisel-tooth digging versus an enlargement of the forearms to enable scratch digging. Scratch digging primarily involves soil removal via enlarged forelimbs, and is used by numerous fossorial mammals, including many rodents (e.g. Hildebrand, 1985; Reichman and Smith, 1990; Nevo, 1999). Chisel-tooth digging, which involves the use of incisors powered by head and jaw muscles to remove compact soil, evolved to allow subterranean species to exploit harder soils (Lessa and Thaler, 1989) and is associated with many skull modifications such as more procumbent incisors, wider crania, enlarged zygomatic arches, longer rostra and larger temporal fossae (Landry, 1957a; Agrawal, 1967; Lessa, 1990; Samuels and Van Valkenburgh, 2009; Gomes Rodrigues et al., *in press*).

Incisor procumbency, the angle of the incisor protruding from the rostrum or mandible, is a well-studied adaptation associated with chisel-tooth digging (Lessa, 1990). Stein (2000) notes that, although chisel-tooth digging is accomplished primarily by the lower incisors, with the upper incisors being used to anchor the skull to the soil (Jarvis and Sale, 1971), it is the upper incisors that show greater variability in their procumbency. An example of this exists in the rodent family Bathyergidae (the African mole-rats or blesmols), in which the chisel-tooth diggers *Cryptomys* and *Georychus* have been shown to have significantly greater upper incisor procumbency compared with the

scratch digger *Bathyergus*. Lower incisor procumbency however was not significantly different between the three genera (Van der Merwe and Botha, 1998). This association between upper incisor procumbency and chisel-tooth digging is said to allow a more favourable angle of attack for anchoring the head of the rodent to the burrow wall when compared to more recurved upper incisors (Lessa, 1990; Vassallo, 1998; Korth and Rybczynski, 2003). Upper incisor procumbency is influenced by the degree of curvature of the incisor and the position of the incisor in the rostrum (Landry, 1957a; Akersten, 1981). Within the Bathyergidae, the root of the incisor of chisel-tooth diggers extends behind the molar tooth row, a trait unique amongst rodents (Ellerman, 1940). This is in contrast to the scratch digging *Bathyergus*, whose upper incisor is rooted above the first molar. It has been suggested by Van der Merwe and Botha (1998) that the posterior displacement of the upper incisor root in chisel-tooth digging rodents promotes increased procumbency.

It has already been shown in previous studies that chisel-tooth digging rodents converge in overall cranial shape (Samuels and Van Valkenburgh, 2009). However, does this cranial morphology actually represent an adaptation for chisel-tooth digging? Previous research has shown that certain morphological characteristics are associated with high bite force (e.g. Dumont and Herrel, 2003; Freeman and Lemen, 2008; Van Daele et al, 2009) and wide gape (e.g. Herring, 1972; Herring and Herring 1974; Vinyard et al, 2003; Terhune et al, 2015); two characteristics essential for optimal chisel-tooth digging.

Bite force and gape are limiting factors for animals in the context of their feeding and behavioural ecology. For instance, the force at which an animal can bite will limit the range of hardness of food items that the animal can consume, with previous studies showing a correlation between bite force, food mechanical properties and diet (e.g. Kiltie, 1982; Binder and Van Valkenburgh, 2000). In contrast, gape limits the size of food that an animal can ingest (e.g. Gans, 1961; Herring and Herring 1974; Pough and Groves, 1983; Wheelwright, 1985). Although bite force and gape have been widely studied in the context of dietary inferences (Herrel et al, 2001; Dumont and Herrel, 2003; Vinyard et al, 2003; Taylor and Vinyard 2004; Williams, 2009; Santana et al, 2010), very little research has focused on behaviour such as fossorial activity (Van Daele et al, 2009). Furthermore, despite several studies on morphological predictors of bite force and gape, few have combined morphological predictors with biomechanical modelling to show how morphological traits affect the biomechanics of the system.

The main aims of this study were to highlight key morphological traits in the craniomandibular complex that would improve the performance of bite force and/or gape in a particular family of subterranean rodents, the African mole-rats (Bathyergidae). Bathyergids are especially interesting when investigating the morphological correlates of digging because chisel-tooth digging is seen in five of the six genera of bathyergids (*Cryptomys*, *Fukomys*, *Georchus*, *Heliophobius* and *Heterocephalus*), whereas *Bathyergus* is the only genus to use the scratch digging method (Nowak, 1999; Stein, 2000). Furthermore, recent phylogenies (Figure 2.1; Faulkes et al, 2004; Seney et al, 2009; Patterson and Upham, 2014) agree that the scratch digging genus *Bathyergus* is nested deep within the crown of Bathyergidae, indicating that chisel-tooth digging is ancestral for the family and has been lost in *Bathyergus*. Despite this, previous research has shown that the cranium of *Bathyergus* is morphologically different from the chisel-tooth digging bathyergids, having more in common with other, more distantly related scratch digging rodents (Samuels and Van Valkenburgh, 2009). Thus, the skull of *Bathyergus* has changed, either by adaptation to a different selection pressure, or by genetic drift owing to the release of the constraint of chisel-tooth digging.

The objective of this study is to ascertain whether the cranial morphology of chisel-tooth digging bathyergids better facilitates high bite force and wide gape than does the cranial morphology of the scratch digging *Bathyergus*. I hypothesise that the change in morphology of *Bathyergus*, whether mediated by selection or drift, will have decreased its tooth digging abilities, which will be manifest in reduced bite force and gape. Based on previous work there are a number of predictions that can be made:

2.1.1 *Morphological predictions related to bite force*

An increase in bite force has been found to be strongly correlated with an increase in head height in *Fukomys* mole-rats (Van Daele et al, 2009) and bats (Dumont and Herrel, 2003). I therefore hypothesise that chisel-tooth diggers will have relatively increased head heights compared to scratch diggers.

Chisel-tooth diggers tend to have broader zygomatic arches and larger temporal fossae to accommodate larger, more powerful masticatory muscles (e.g. Hildebrand, 1985; Stein, 2000; Samuels and Van Valkenburgh, 2009) and so it is hypothesised that chisel-tooth diggers will have relatively wider crania compared to scratch diggers.

An increase in upper incisor procumbency has been shown to be associated with chisel-tooth digging in a number of subterranean rodents (Landry, 1957a; Lessa, 1990; Vassallo, 1998; Samuels and Van Valkenburgh, 2009). This increase in procumbency has also been associated with an increase in rostral length (Lessa and Patton, 1989; Mora et al, 2003). It was therefore hypothesised that chisel-tooth digging rodents will have increased upper incisor procumbency and a longer rostrum compared to scratch diggers.

2.1.2 *Morphological predictions related to gape*

Gape has been shown to be strongly predicted by jaw length in animals whose masticatory biomechanics have been extensively studied, such as snakes (e.g. Hampton and Moon, 2013). Vinyard and Payseur (2008) also found a significant correlation between maximum gape and jaw length in classical inbred strains of house mice. In addition, the cranium and mandible in rodents strongly covary (Hautier et al, 2012). As it has been hypothesised that rostral length increases in chisel-tooth digging rodents, if this covariation occurs in subterranean rodents, then it is also expected that there will be an increase in jaw length combined with that of rostral length in chisel-tooth digging rodents. Thus, it is hypothesised that chisel-tooth diggers will have a relatively longer jaw compared to scratch diggers.

Elongated antero-posterior lengths of articulating joint surfaces are known to increase joint mobility (Ruff, 1988; Hamrick, 1996). An increased antero-posterior length of the condyle articular surface has also been linked to increased gape in primates (Vinyard et al, 2003) and house mice (Vinyard and Payseur, 2008). Gape also increases theoretically in mammals with reduced condyle heights (height of condyle above the molar tooth row) as this reduces stretch in masticatory muscles during gape (Herring and Herring, 1974). Hence, I hypothesise that chisel-tooth digging mole-rats will have lower condyles with longer articulating surfaces than the scratch digging genus *Bathyergus*.

2.1.3 *Biomechanics of a chisel-tooth digger*

The performance of the masticatory apparatus is traditionally assessed by modelling the jaw as a static third class lever and calculating mechanical advantage (MA) of each masticatory muscle (Maynard Smith and Savage, 1959). MA is the ratio of the muscle moment arm to the jaw moment arm and is affected if either moment arm is changed within the system. The jaw moment arm is the distance from the pivot (in mammalian

masticatory biomechanics this is equivalent to the temporomandibular joint [TMJ]) to the bite force vector, and the muscle moment arm is the perpendicular distance from the TMJ to the muscle force vector. Movement of the bite point towards the TMJ (assuming constant muscle attachments) will result in a higher MA, as the jaw moment arm has been reduced. This biomechanical definition explains why there is a trade-off between gape and bite force. An increase in jaw length is associated with larger gape (e.g. Hampton and Moon, 2013) but will also increase the jaw moment arm, reducing the MA of the masticatory muscle, and therefore reducing bite force. It is clear that craniomandibular adaptations that facilitate an increase in gape therefore decrease bite force capabilities, and vice versa. Due to this trade-off, animals that need both large gapes and large bite forces, e.g. carnivores, may show unique morphological adaptations. Animals that must produce high bite forces at large gapes normally have larger temporalis muscles compared to animals that produce larger bite forces with smaller gapes, in which case the masseter dominates (Turnbull, 1970). As specimens with soft tissues were not available for this study, it was assumed that the relative sizes of the masticatory muscles were similar between specimens. However, using bony proxies it is possible to estimate the mechanical advantage and performance of a select number of masticatory muscles. It was therefore hypothesised that in chisel-tooth digging subterranean rodents, the temporalis muscle would have a higher mechanical advantage compared to that of scratch digging subterranean rodents to enable the production of a high bite force at large gape. It was also hypothesised that MA of temporalis would be maintained at larger gapes in chisel-tooth diggers compared to scratch diggers.

As all bathyergid mole-rats have a similar diet of geophytes (Bennett and Faulkes, 2000), any morphological adaptations towards the ability to produce a large bite force and gape found in chisel-tooth diggers are likely to be driven by extensive burrowing in compact soil. Previous studies on mastication in pocket gophers (Geomyidae) suggested that cranial shape in pocket gophers was primarily an adaptation towards fossoriality and secondarily reflected masticatory function (Wilkins and Woods, 1983; Wilkins, 1988); it is hypothesised that the morphology of bathyergids has adapted in a similar manner.

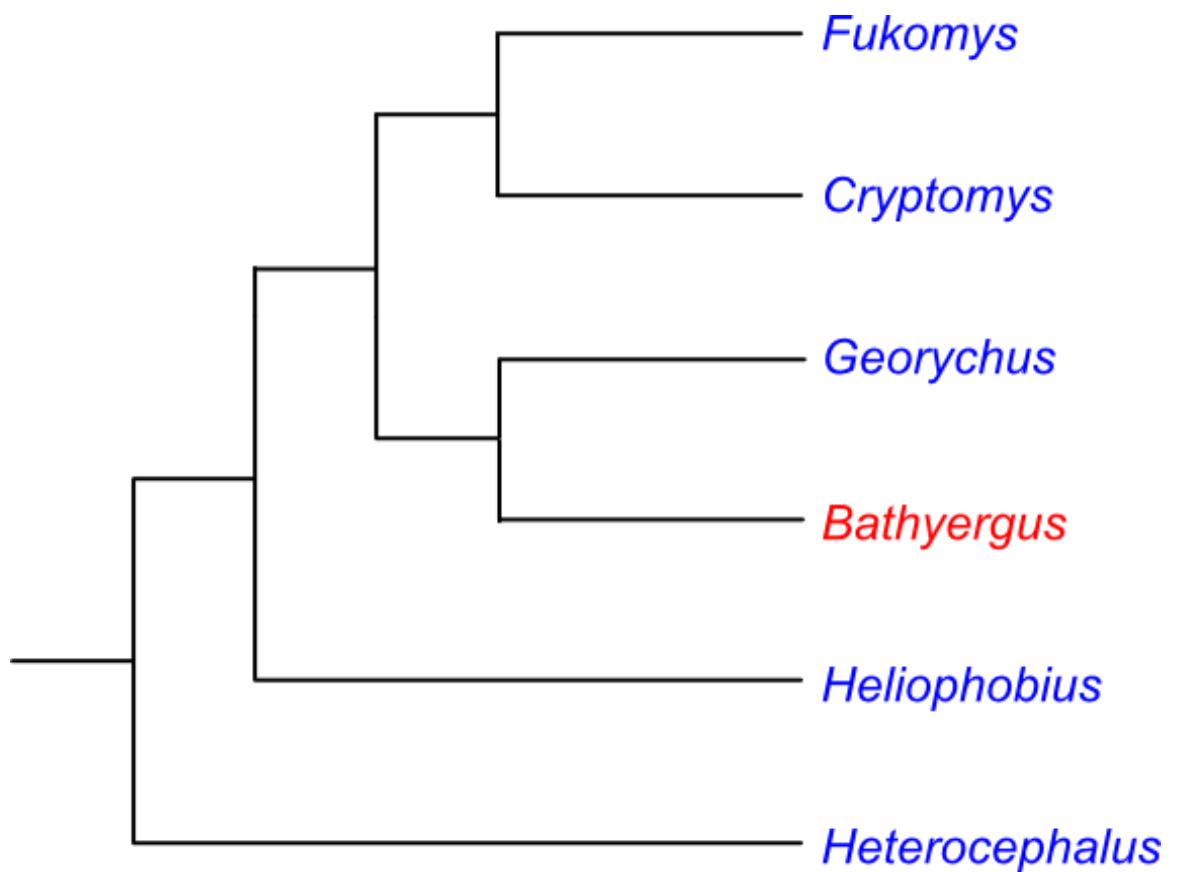


Figure 2.1 Phylogeny of bathyergid mole-rat genera in this analysis. Chisel-tooth digging (blue), scratch digging (red). Adapted from Seney et al (2009).

2.2 Materials and Methods

A sample of 47 crania and mandibles from the subterranean rodent family Bathyergidae, representing adult mole-rats of both sexes, were used in this analysis. The sample comprised five species of chisel-tooth digging rodents (*Cryptomys hottentotus*, *Fukomys mechowii*, *Georychus capensis*, *Heliophobius argenteocinereus* and *Heterocephalus glaber*) and one species of scratch digging rodent (*Bathyergus suillus*), representing all six extant genera of bathyergid mole-rats (Table 2.1).

Table 2.1 List of Bathyergidae specimens used in this study. Note not all specimens could be used in each test due to damage (see appendix Table A.1).

Species	Digging Method	Quantity
<i>Bathyergus suillus</i>	Scratch	11
<i>Cryptomys hottentotus</i>	Chisel-tooth	6
<i>Fukomys micklei</i>	Chisel-tooth	10
<i>Georychus capensis</i>	Chisel-tooth	5
<i>Heliophobius argenteocinereus</i>	Chisel-tooth	10
<i>Heterocephalus glaber</i>	Chisel-tooth	5

The specimens were scanned on an X-Tek Metris microCT scanner at the University of Hull (Medical and Biological Engineering Research Group), and the resulting scans had isometric voxels ranging between 0.01-0.07 mm. MicroCT scans were automatically reconstructed in Avizo 8.0 (FEI, Hillsboro, OR) using a predefined grey scale to render a 3D volume of each specimen. From the reconstructions, 3D landmark co-ordinates were recorded to enable the calculation of six linear measurements – three from the cranium (cranial width, head height and rostral length) and three from the mandible (jaw length, condyle length and condyle height). In addition, the procumbency angle of the upper incisor was measured based on the method outlined in Landry (1957a). All measurements taken are detailed in Table 2.2, Table 2.3 and Figure 2.2. Linear measurements were scaled relative to basilar length (the midline distance along the cranial base from the anterior extremity of the premaxillae to the margin of the foramen magnum). Each linear measurement was also regressed against basilar length to show the effects of allometric scaling. Due to the error contained in the variables and the ambiguity of dependence between variables, a reduced major axis model was fitted. Both variables were logged in order to fit the standard allometric equation, $y=ax^b$. The equations, R^2 and P values for each measured variable are given in Table 2.4. For significant allometric correlations, residuals were calculated from the equations in Table 2.4. For visualisation purposes the isometric and allometrically corrected residual data were displayed as box plots, with each genus shown separately. However, owing to small sample sizes of *Cryptomys*, *Georychus* and *Heterocephalus*, for statistical testing the specimens were grouped by digging method. Between ten and 11 specimens of the

scratch digging *Bathyergus*, and between 25 and 36 specimens of chisel-tooth digging mole-rats were included in each analysis. Following Ruxton (2006), the unequal variance *t*-test (Welch's *t*-test) was used to test for significant differences between the scratch digging and chisel-tooth digging groups, except where there was evidence of non-normality in the data, in which case the non-parametric Mann-Whitney *U* test was employed. The normality of the data in each group was tested using the Shapiro-Wilk test. All statistical tests were performed using PAST (Hammer et al, 2001). To check that the over-represented chisel-tooth genera (*Fukomys* and *Heliophobius*) were not unduly influencing the results, the tests were rerun using just five randomly-selected specimens of each; however, the results were unchanged.

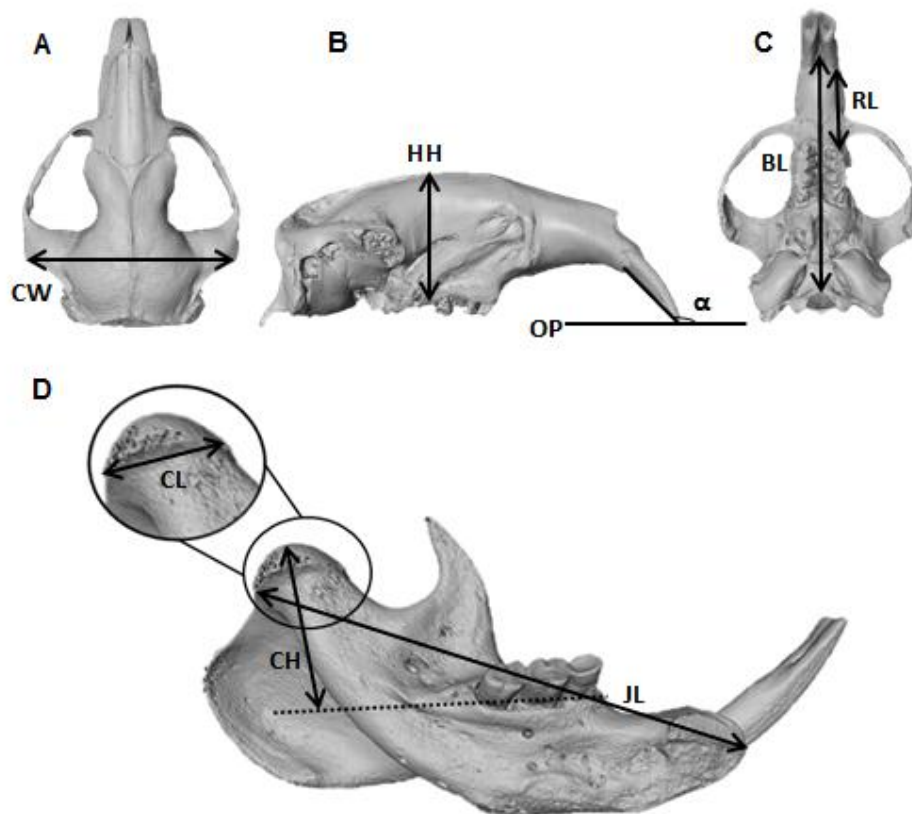


Figure 2.2 Morphological predictors of bite force (A-C) and gape (D) shown on skull and mandible of *Heliophobius argenteocinereus*. A. Dorsal view of skull. B. Right lateral view of skull (zygomatic arch removed). C. Ventral view of skull. D. Medial view of left hemimandible. Abbreviations: BL, basilar length; CL, condyle length; CH, condyle height; CW, cranial width; HH, head height; JL, jaw length; OP, occlusal plane; RL, rostral length; α , incisor procumbency angle. Dashed line represents occlusal plane on mandible. Further details of measurements given in Table 2.2 and 2.3.

Table 2.2 Morphological predictors on the cranium to be measured. All linear measurements were size adjusted by dividing by basilar length. Measurements shown in Figures 2.2A-C.

Cranial measurement	Definition	Prediction
Head height (HH)	Distance from bregma to posterior margin of the palatine in the midsagittal plane	Bite force increases with increased HH
Cranial width (CW)	Distance between left and right posterior zygomatic arches	Bite force increases with increased CW to accommodate enlarged masticatory muscles
Rostral length (RL)	Distance from upper incisor tip to posterior point of tooth row	Bite force increases with decreasing rostral length due to decreasing of out lever length
Upper incisor procumbency (α)	Angle of Thomas (see Landry, 1957a)	Chisel-tooth diggers have reportedly increased upper incisor procumbency angles

Table 2.3 Morphological predictors on the mandible to be measured. All linear measurements were size adjusted by dividing by basilar length. Measurements shown in Figure 2.2D.

Mandible measurements	Definition	Prediction
Jaw length (JL)	Distance from incisor alveolus to the posterior surface of the mandibular condyle	Gape increases with increased jaw length
Condyle length (CL)	Anteroposterior length of condylar articular surface	Gape increases with elongated condyles as greater rotation is facilitated
Condyle height (CH)	Height of the condyle above the molar tooth row (perpendicular to occlusal plane)	Gape increases with lower condyle heights as muscle stretch is reduced

In addition to the cranial and mandibular measurements outlined above, the performance of three major masticatory muscles (superficial masseter, deep masseter

and temporalis) was measured in each specimen for a comparison between chisel-tooth digging and scratch digging systems. These muscles were selected as together they make up over 80% of the masticatory muscles in mole-rats (Bekele, 1983; Cox and Faulkes, 2014). Performance was measured by calculating the MA of each muscle using moment arms (Figure 2.3; example using temporalis muscle). Muscle moment arms (MMA) were calculated for the selected muscles, along with the jaw moment arm (JMA) for each specimen. Mechanical advantage was calculated as the ratio between these two variables.

The cranium and mandible of each specimen were re-orientated with respect to one another in Avizo 8.0 to simulate incisal occlusion (see Figure 2.3). Incisal occlusion was defined by the tips of the upper and lower incisor being in contact, and each mandibular condyle being in contact with the articular surfaces of the corresponding glenoid fossa. Following this, a bite force vector (BFV) was defined as a line going directly through the incisor bite point (point of contact between incisors), orthogonal to the occlusal plane of the hemi-mandible. JMA was calculated as the perpendicular distance from the fulcrum (condyle tip) to the BFV (see Figure 2.3). The incisor was the only bite point chosen in this study as chisel-tooth digging is carried out exclusively by the incisors.

The angle between the jaw moment arm and the line from the fulcrum to the bite point (angle θ ; Figure 2.3) was calculated using trigonometry in 3D. The occlusal plane is defined as the plane on the mandible containing points at the posterior edge of the tooth row and points at the medial and lateral sides of the third mandibular molar. The angle between the occlusal plane and the line connecting the fulcrum and bite point (dashed line in Figure 2.3) was then calculated using the dot product:

$$\theta = \sin^{-1} \left(\frac{\mathbf{n} \cdot \mathbf{m}}{|\mathbf{n}| |\mathbf{m}|} \right)$$

Where \mathbf{n} is the normal vector to the occlusal plane and \mathbf{m} is the vector of the line representing the distance from the fulcrum to the incisor bite point. As the occlusal plane runs parallel to the JMA, θ is equivalent to the angle between JMA and the line representing the distance between fulcrum and incisor bite point. The JMA can then be calculated using standard trigonometry.

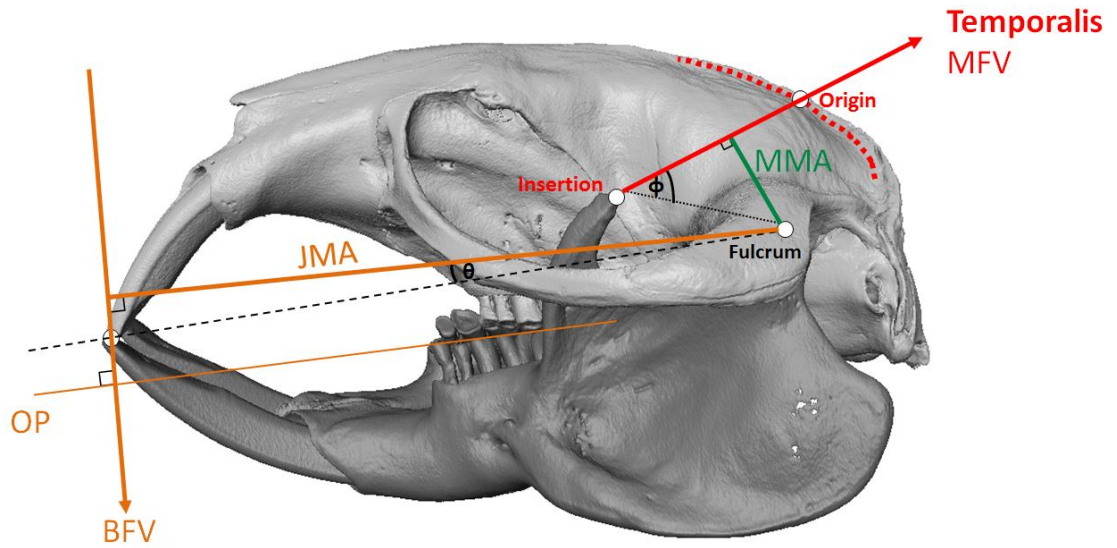


Figure 2.3 Calculation of muscle moment arm (MMA) of temporalis and jaw moment arm (JMA) to evaluate mechanical advantage of temporalis. Abbreviations: BFV, bite force vector; JMA, jaw moment arm; MFV, muscle force vector; MMA, muscle moment arm; OP, occlusal plane.

MMA is calculated as the perpendicular distance from the fulcrum to the muscle force vector (MFV). MFV was defined by a line going through the centre of the origin and insertion of each muscle (see Figure 2.3). The origin and insertion of each muscle was defined by placing a curve on the dorsal border of each muscle origin on the cranium and the ventral border of each muscle insertion on the mandible. The curve was placed via a B-spline in Avizo 8.0, and automatically divided into 100 equidistant points. Thus the centre of each origin and insertion could be established to represent the directionality of the muscle force. Note that no curve was placed on the insertion of temporalis or the origin of superficial masseter as these muscle attachment areas were small enough to be represented as a single point. MMA was then calculated using standard trigonometry.

In order to evaluate the effect of gape on mechanical advantage, a rotation matrix was used to rotate the co-ordinates lying on the mandible around an axis running through the landmarks representing the dorsal points on the condylar surfaces on the left and right side of the mandible (thus simulating mandibular rotation):

$$\begin{bmatrix} (a(v^2 + w^2) - u(bv + cw - ux - vy - wz))(1 - \cos \sigma) + x \cos \sigma + (-cv + bw - wy + vz) \sin \sigma \\ (b(u^2 + w^2) - v(au + cw - ux - vy - wz))(1 - \cos \sigma) + y \cos \sigma + (cu - aw + wx - uz) \sin \sigma \\ (c(u^2 + v^2) - w(au + bv - ux - vy - wz))(1 - \cos \sigma) + z \cos \sigma + (-bu + av - vx + uy) \sin \sigma \end{bmatrix}$$

Where (x, y, z) is the point being rotated about the line through (a, b, c) with a direction vector of (u, v, w) by angle σ . The direction vector is defined by the tips of the left and right condyles.

It is also worth noting that the theoretical maximum gape of this model was deemed to be the angle where mechanical advantage was a minimum. This assumption originates from the fact that beyond a certain angle of rotation, the mandibular insertion of the muscle will move posterior to the fulcrum, and therefore from that point would operate to open the jaw, not close it. Limitations of this model will also be discussed below.

2.3 Results

2.3.1 Morphological predictors of bite force (including upper incisor procumbency)

The results of the comparisons of head height, cranial width, procumbency angle and rostral length between bathyergid genera are displayed in Figure 2.4, Figure 2.5, Figure 2.6 and Figure 2.7. Unequal variance t-tests indicated that there are significant differences in relative head height ($t=-10.37$, $P<0.01$) and relative cranial width ($t=-8.51$, $P<0.01$) between chisel-tooth and scratch digging genera. Chisel-tooth digging bathyergids have relatively taller and wider crania than the scratch digging genus, *Bathyergus*. Upper incisor procumbency angle also appeared to be larger in chisel-tooth digging genera compared to *Bathyergus* ($t=-4.03$, $P<0.01$). However, Figure 2.6, which represents upper incisor procumbency angles according to each genus, shows that some of the lowest procumbency angles were recorded in specimens of the chisel-tooth digging genus *Heterocephalus*, the naked mole-rat. In comparison, rostral length failed to separate chisel-tooth and scratch diggers. Although *Bathyergus* was predicted, as a scratch digger, to have a relatively shorter rostrum than the chisel-tooth digging genera, no statistically significant difference between the groups was found. Interestingly, *Heterocephalus* also appears to display the shortest rostrum according to Figure 2.7, but owing to small sample sizes in some genera, the differences between genera could not be tested statistically.

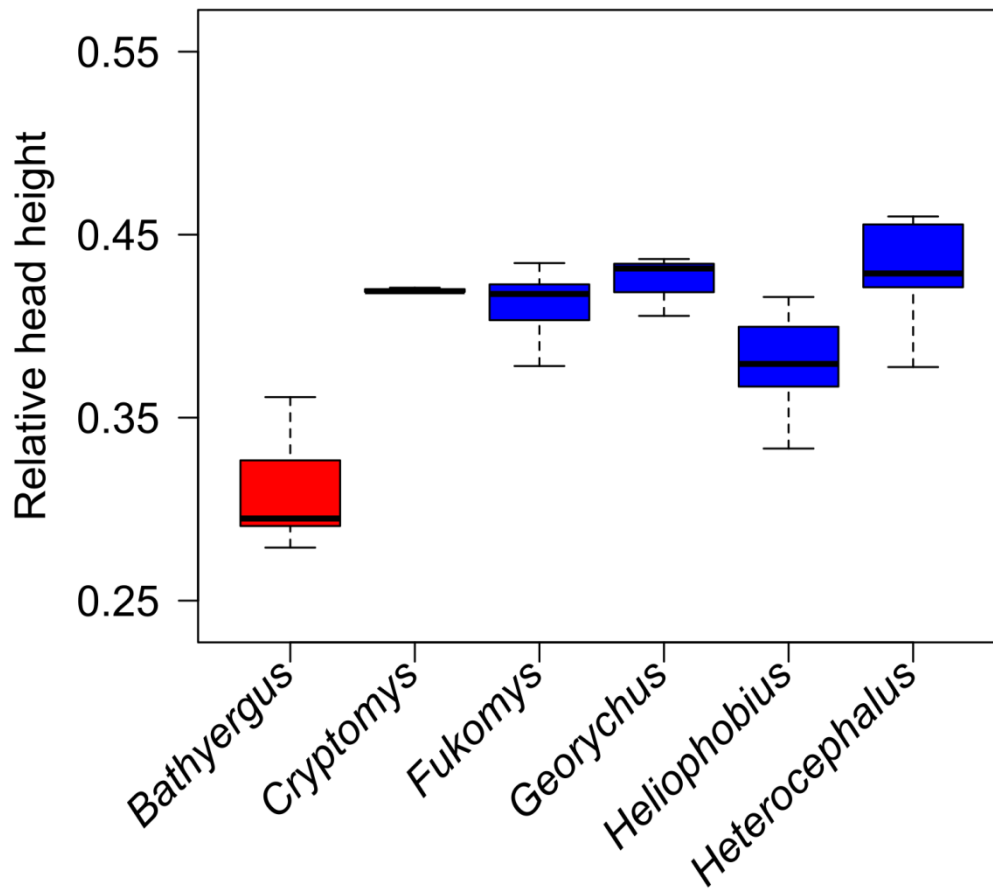


Figure 2.4 Box plot showing head height (relative to cranial length) in chisel-tooth digging (blue) and scratch digging (red) bathyergid genera. Black lines within boxes represent median values. Boundaries of boxes represent 25th and 75th quartiles. Whiskers extend to 1.5 times the interquartile range and white dots represent outliers that fall outside this range.

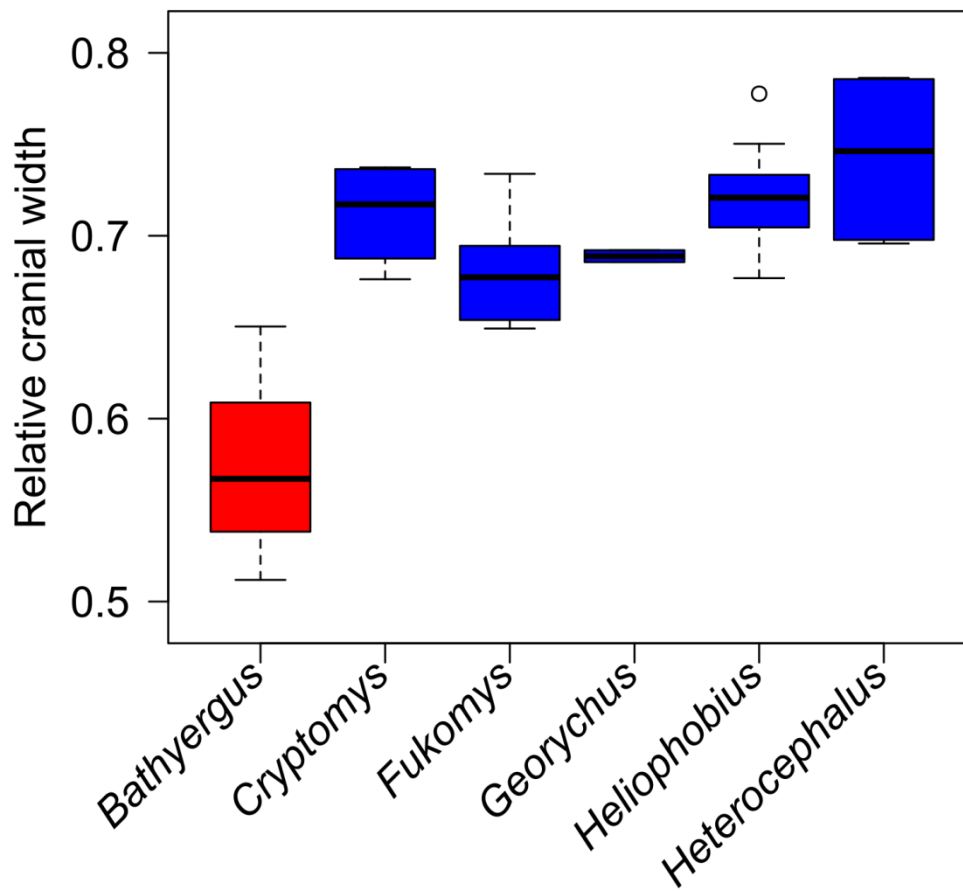


Figure 2.5 Box plot showing cranial width (relative to cranial length) in chisel-tooth digging (blue) and scratch digging (red) bathyergid genera. Black lines within boxes represent median values. Boundaries of boxes represent 25th and 75th quartiles. Whiskers extend to 1.5 times the interquartile range and white dots represent outliers that fall outside this range.

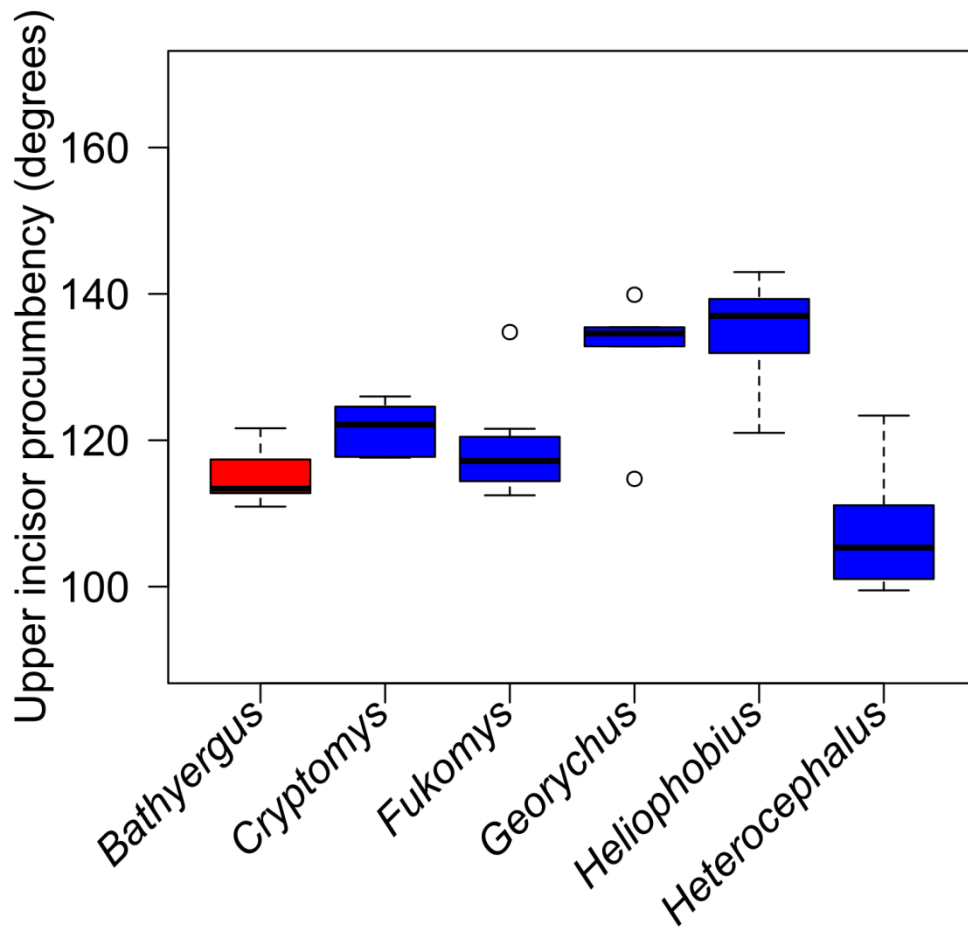


Figure 2.6 Box plot showing upper incisor procumbency in chisel-tooth digging (blue) and scratch digging (red) bathyergid genera. Black lines within boxes represent median values. Boundaries of boxes represent 25th and 75th quartiles. Whiskers extend to 1.5 times the interquartile range and white dots represent outliers that fall outside this range.

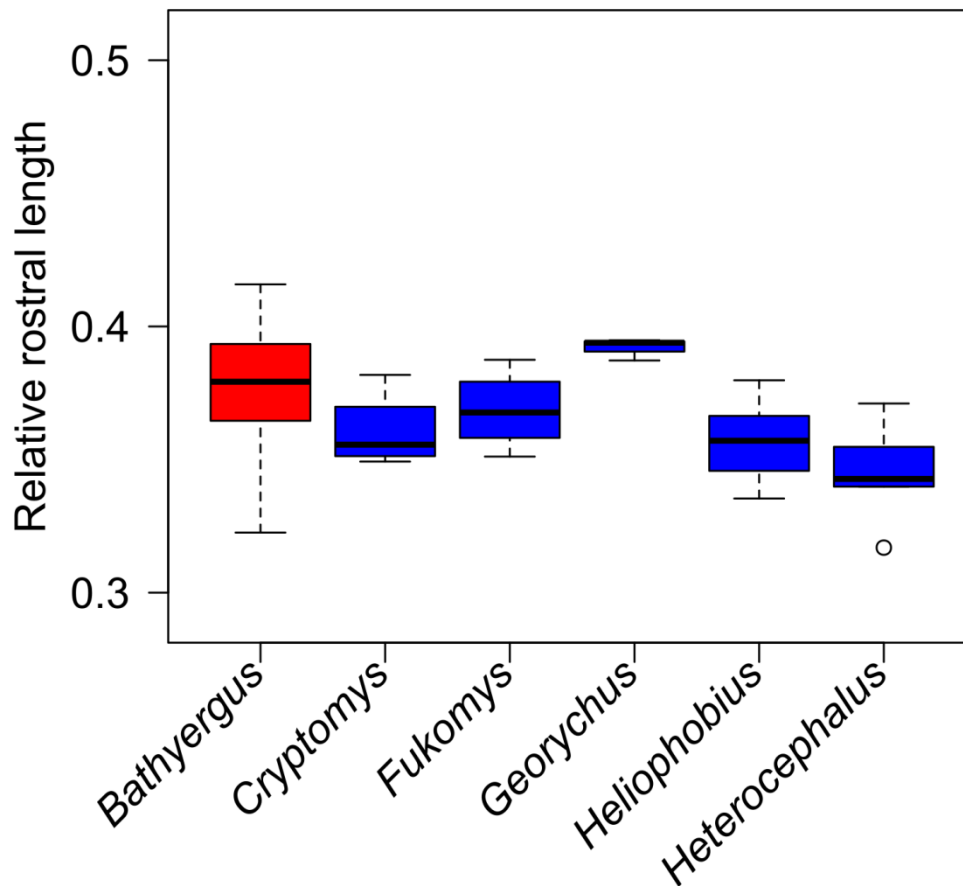


Figure 2.7 Box plot showing rostral length (relative to cranial length) in chisel-tooth digging (blue) and scratch digging (red) bathyergid genera. Black lines within boxes represent median values. Boundaries of boxes represent 25th and 75th quartiles. Whiskers extend to 1.5 times the interquartile range and white dots represent outliers that fall outside this range.

2.3.2 Morphological predictors of gape

The visual comparisons of jaw length, condyle length and condyle height between bathyergid genera are displayed in Figure 2.8, Figure 2.9 and Figure 2.10. Chisel-tooth diggers exhibit significant differences in all morphological predictors of gape compared to scratch diggers. A Mann-Whitney U test showed that chisel-tooth digging bathyergids have relatively longer lower jaws ($U=0$, $P<0.01$). Unequal variance t -tests showed that chisel-tooth diggers have relatively longer condyle articulating surfaces ($t=-13.58$, $P<0.01$) and relatively increased condyle heights ($t=-2.71$, $P<0.05$).

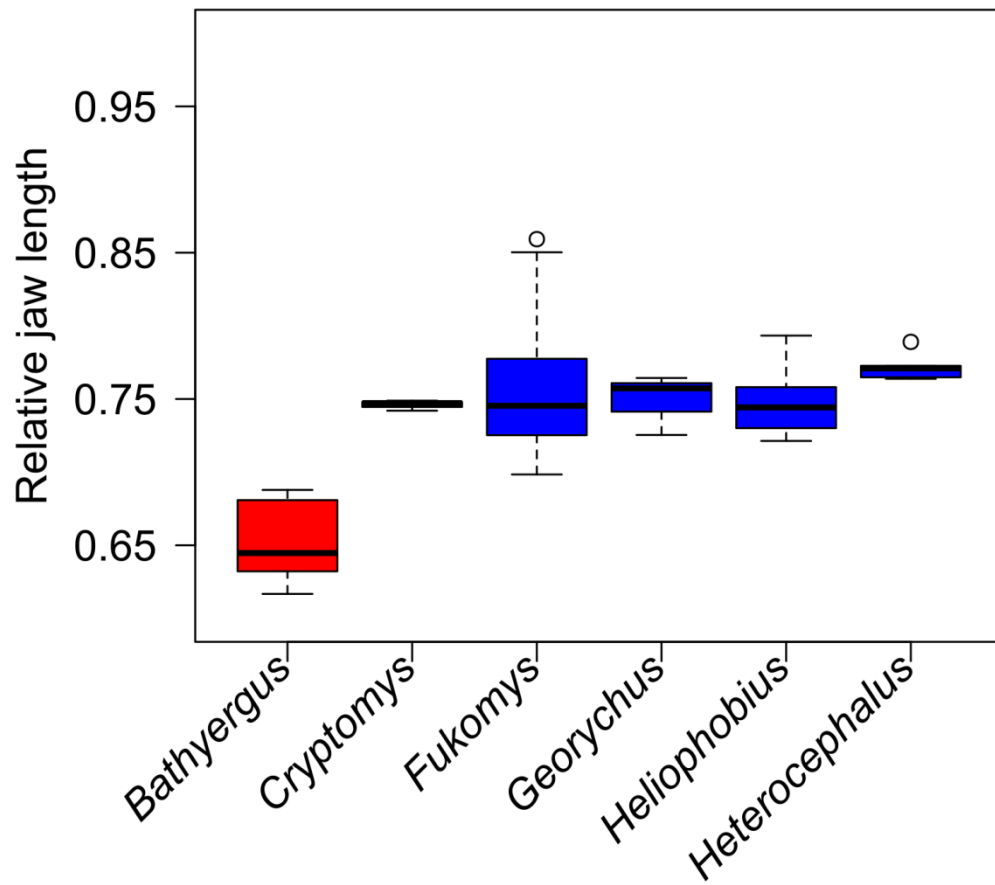


Figure 2.8 Box plot showing jaw length (relative to cranial length) in chisel-tooth digging (blue) and scratch digging (red) bathyergid genera. Black lines within boxes represent median values.

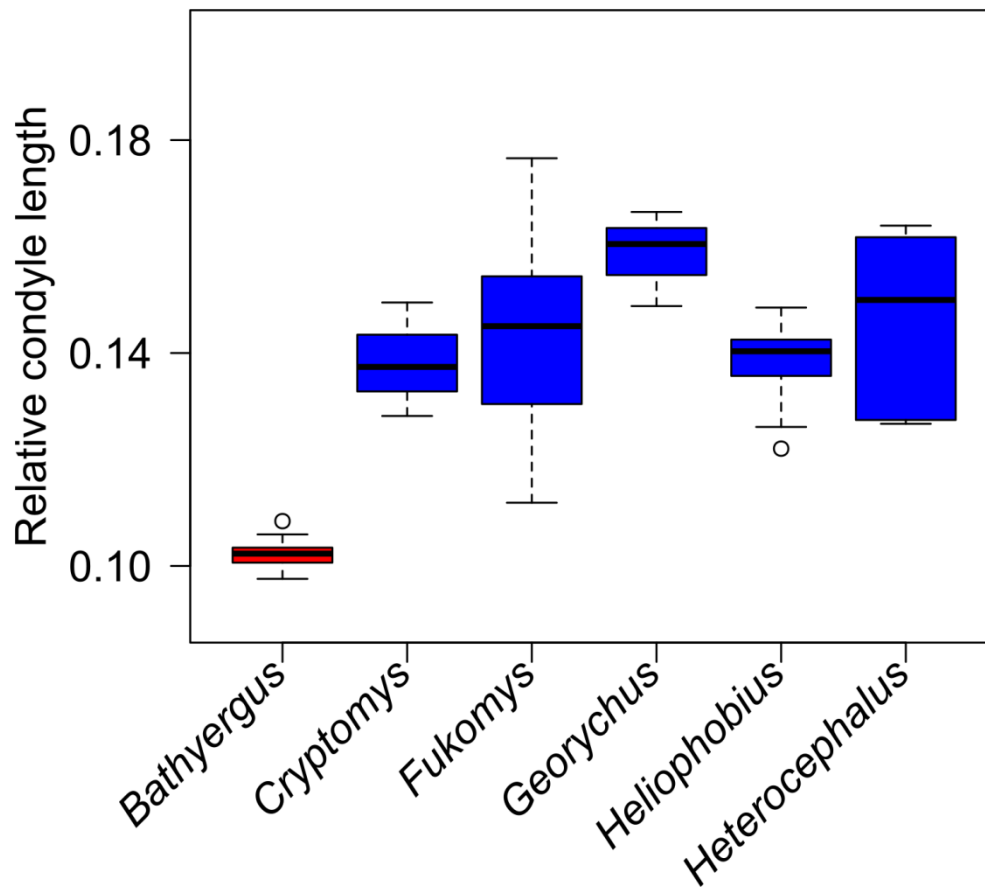


Figure 2.9 Box plot showing condyle length (relative to cranial length) in chisel-tooth digging (blue) and scratch digging (red) bathyergid genera. Black lines within boxes represent median values. Boundaries of boxes represent 25th and 75th quartiles. Whiskers extend to 1.5 times the interquartile range and white dots represent outliers that fall outside this range.

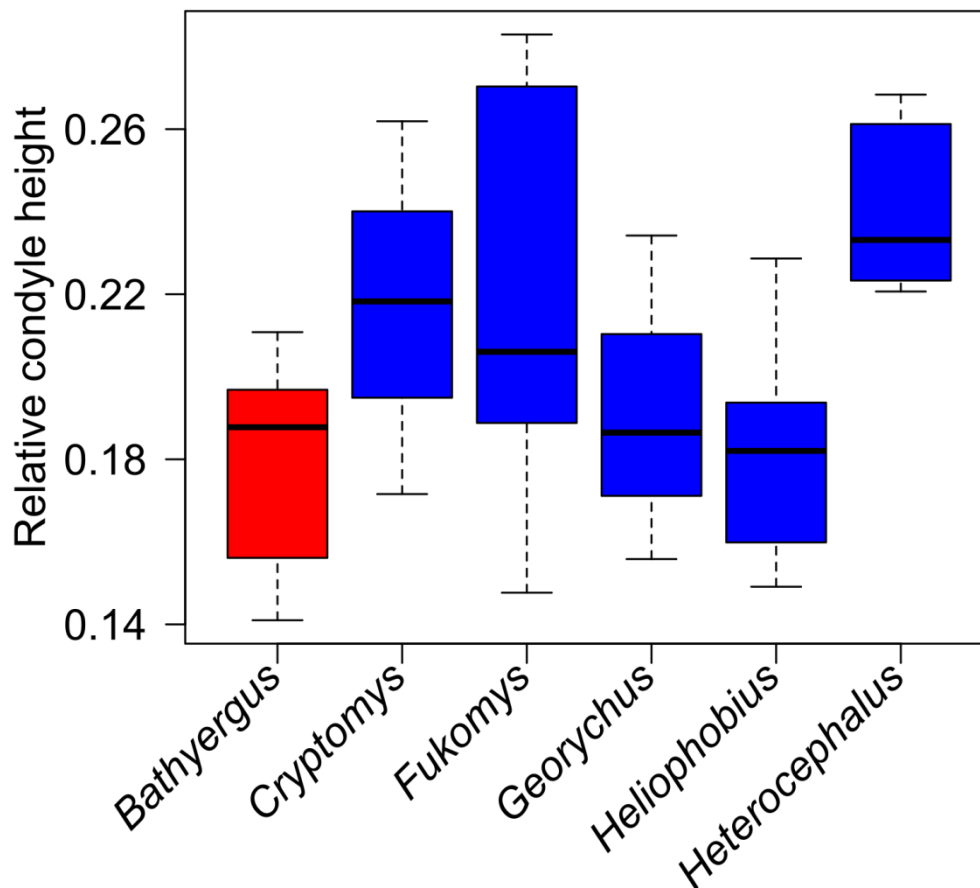


Figure 2.10 Box plot showing condyle height (relative to cranial length) in chisel-tooth digging (blue) and scratch digging (red) bathyergid genera. Black lines within boxes represent median values. Boundaries of boxes represent 25th and 75th quartiles. Whiskers extend to 1.5 times the interquartile range and white dots represent outliers that fall outside this range.

2.3.3 Allometric relationship of morphological traits

The allometric equations of the morphological predictors of bite force and gape are displayed in Table 2.4. All variables were found to be strongly correlated with basilar length except for upper incisor procumbency. The mandibular measurements (condyle height, condyle length and jaw length) all scaled with negative allometry (slope<1). Within the cranium, head height and cranial width also scaled with negative allometry. However, rostral length scaled with slightly positive allometry (slope>1). Upper incisor procumbency was not significantly correlated with basilar length ($P>0.05$).

Figures 2.11-16 represent the residuals from the allometric equations in Table 2.4. Upper incisor procumbency residuals were not calculated due to non-significance of allometry. The results show a similar pattern to the isometrically scaled morphological predictors of bite force and gape. A Mann-Whitney U test showed that chisel-tooth digging bathyergids have relatively larger head heights ($U=14$, $P<0.01$; Figure 2.11)

and cranial widths ($U=44$, $P<0.01$; Figure 2.12). Similarly to the isometrically scaled rostral length measurements, there was no significant difference between the two bathyergid groups in rostral length corrected for allometry ($P>0.05$; Figure 2.13).

A Mann-Whitney U test showed that chisel-tooth digging bathyergids have relatively longer jaw lengths ($U=8$, $P<0.01$; Figure 2.14) and condyle lengths ($U=0$, $P<0.01$; Figure 2.15). However, condyle height corrected for allometry showed no difference between the two groups ($P>0.05$; Figure 2.16).

Table 2.4 Allometric equations ($y=axb$; reduced major axis regression) to assess influence of size (x =basilar length) on morphological variables.

Variable (y)	Equation	R^2	P
Head height	$y=-0.01x^{0.75}$	0.83	<0.01
Cranial width	$y=0.22x^{0.75}$	0.93	<0.01
Rostral length	$y=-0.63x^{1.12}$	0.98	<0.01
Upper incisor procumbency	$y=1.63x^{0.29}$	0.02	>0.05
Jaw length	$y=0.05x^{0.88}$	0.95	<0.01
Condyle length	$y=-0.63x^{0.84}$	0.71	<0.01
Condyle height	$y=-0.63x^{0.96}$	0.67	<0.01

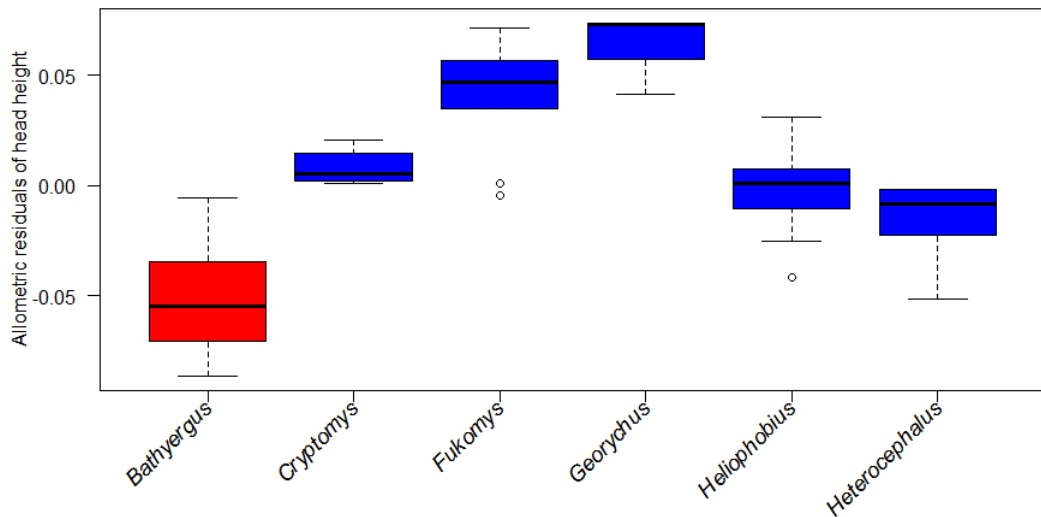


Figure 2.11. Box plot showing allometric residuals of head height from equation in Table 2.4 in chisel-tooth digging (blue) and scratch digging (red) bathyergid genera. Black lines within boxes represent median values. Boundaries of boxes represent 25th and 75th quartiles. Whiskers extend to 1.5 times the interquartile range and white dots represent outliers that fall outside this range.

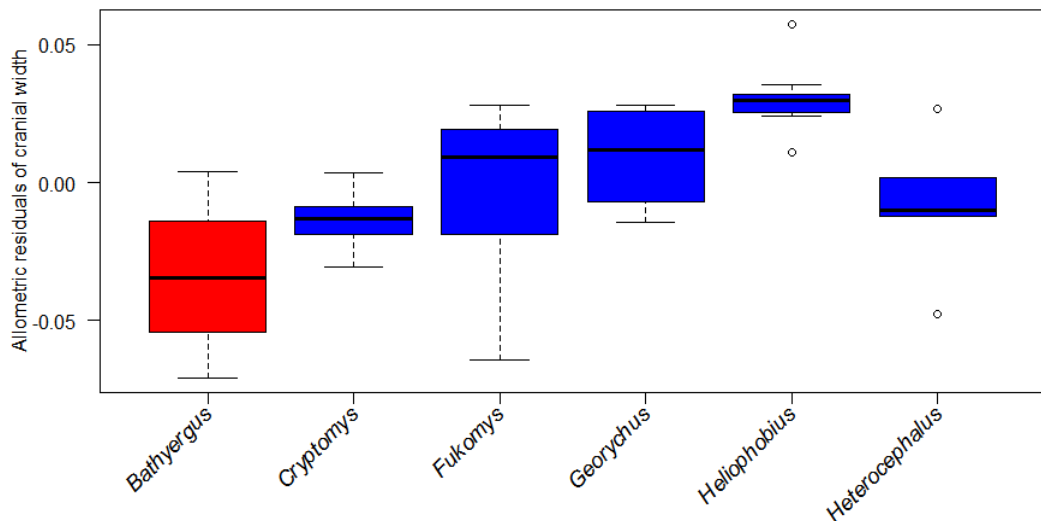


Figure 2.12 Box plot showing allometric residuals of cranial width from equation in Table 2.4 in chisel-tooth digging (blue) and scratch digging (red) bathyergid genera. Black lines within boxes represent median values. Boundaries of boxes represent 25th and 75th quartiles. Whiskers extend to 1.5 times the interquartile range and white dots represent outliers that fall outside this range.

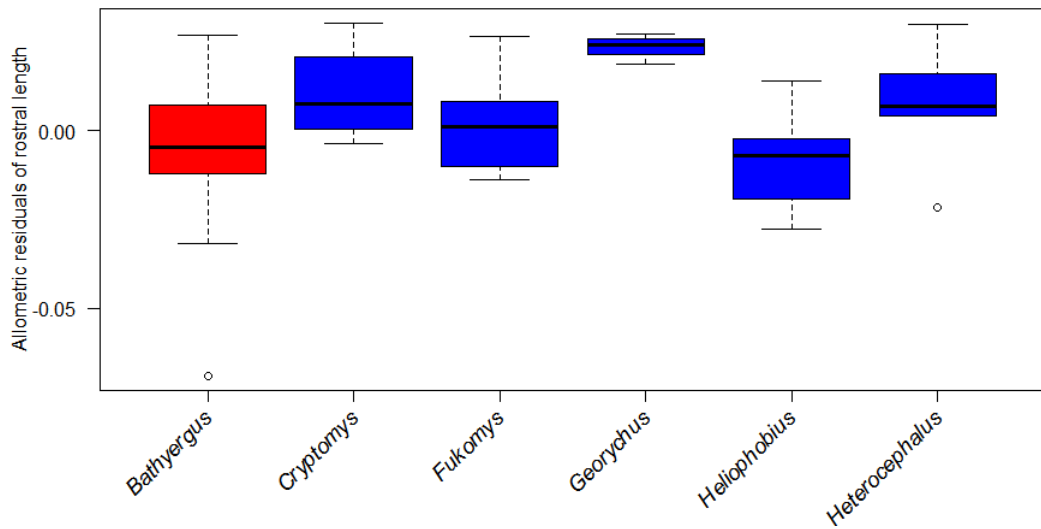


Figure 2.13 Box plot showing allometric residuals of rostral length from equation in Table 2.4 in chisel-tooth digging (blue) and scratch digging (red) bathyergid genera. Black lines within boxes represent median values. Boundaries of boxes represent 25th and 75th quartiles. Whiskers extend to 1.5 times the interquartile range and white dots represent outliers that fall outside this range.

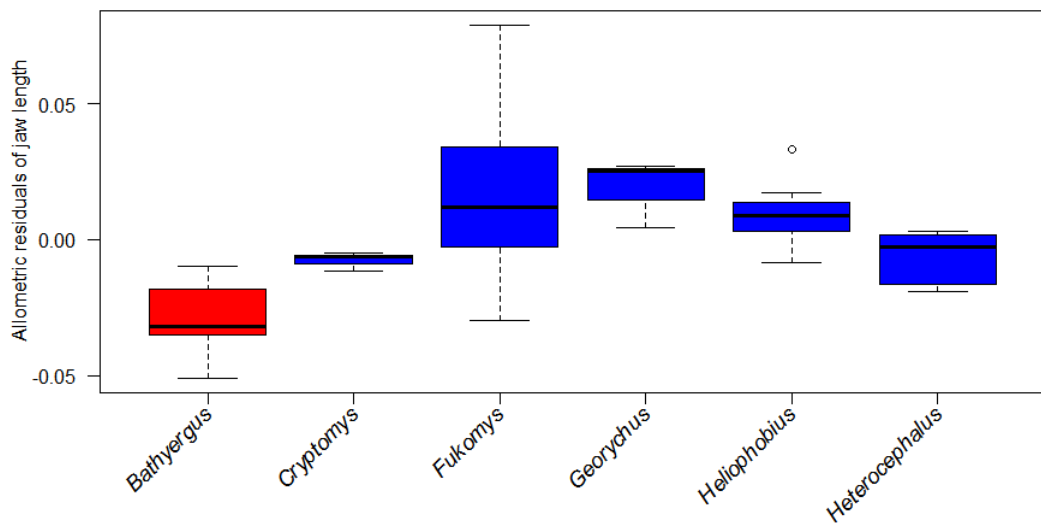


Figure 2.14 Box plot showing allometric residuals of jaw length from equation in Table 2.4 in chisel-tooth digging (blue) and scratch digging (red) bathyergid genera. Black lines within boxes represent median values. Boundaries of boxes represent 25th and 75th quartiles. Whiskers extend to 1.5 times the interquartile range and white dots represent outliers that fall outside this range.

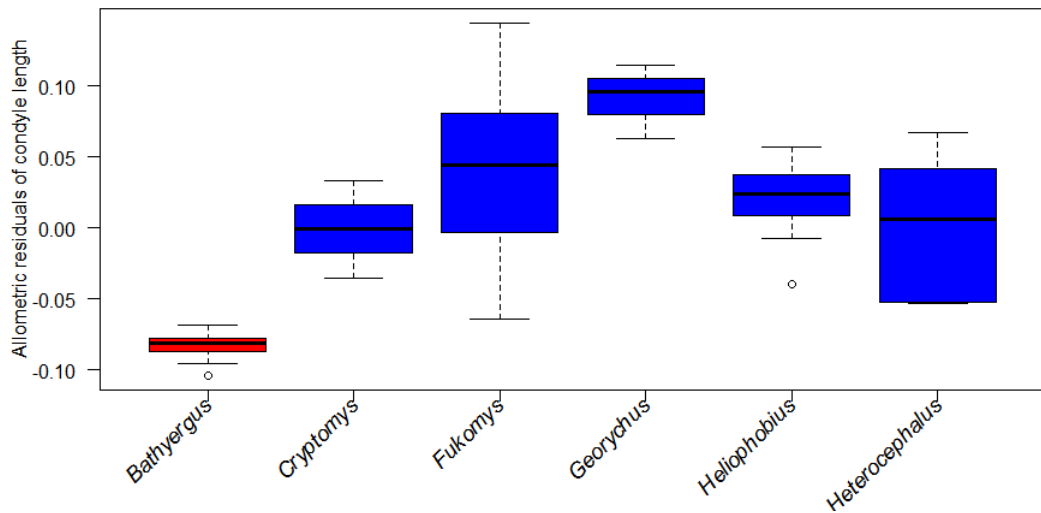


Figure 2.15 Box plot showing allometric residuals of condyle length from equation in Table 2.4 in chisel-tooth digging (blue) and scratch digging (red) bathyergid genera. Black lines within boxes represent median values. Boundaries of boxes represent 25th and 75th quartiles. Whiskers extend to 1.5 times the interquartile range and white dots represent outliers that fall outside this range.

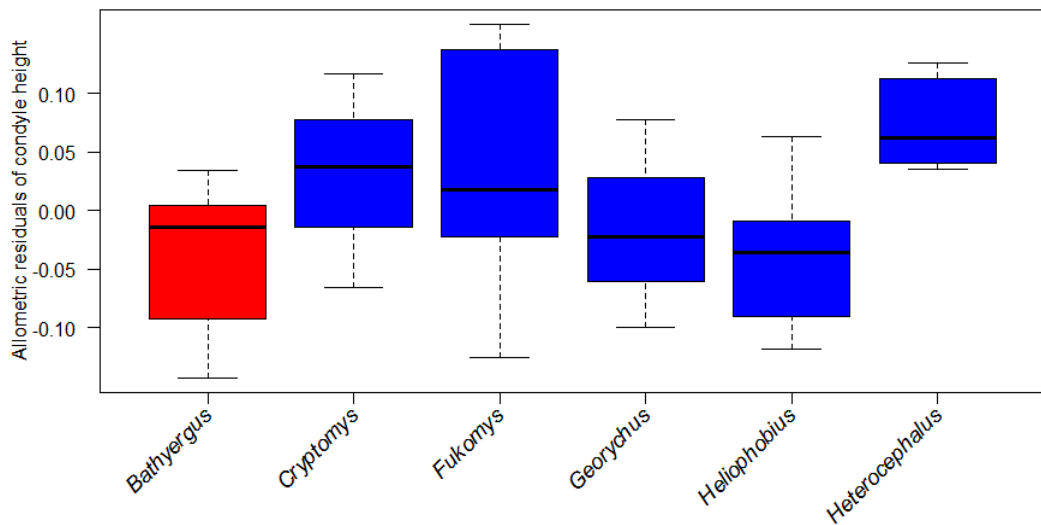


Figure 2.16 Box plot showing allometric residuals of condyle height from equation in Table 2.4 in chisel-tooth digging (blue) and scratch digging (red) bathyergid genera. Black lines within boxes represent median values. Boundaries of boxes represent 25th and 75th quartiles. Whiskers extend to 1.5 times the interquartile range and white dots represent outliers that fall outside this range.

2.3.4 Biomechanical implications of morphological traits

Biomechanically modelling the moment arms of the three selected muscles showed the potential impact on the digging/masticatory system from the morphological differences found between chisel-tooth and scratch diggers. At 0° gape, the MA of the temporalis muscle was shown to be significantly different between *Bathyergus* and the chisel-tooth digging bathyergids ($U=6$, $P<0.01$). No such statistical difference was found for the MA of the superficial or deep masseters.

The effect of gape on the mechanical advantage of the three selected masticatory muscles was tested by applying rotation matrices to the landmarks representing muscle insertion points on the mandible. The results show that for each muscle, increasing gape decreases the mechanical advantage to a minimum point, which varies depending on the genus, beyond which the MA starts to rise again. For example at 0° gape, the mechanical advantage of the temporalis muscle shows a significant difference between chisel-tooth digging and scratch digging genera. However, at around 40° this changes and the mechanical advantage of the scratch digging genus *Bathyergus* begins to increase from its lowest point (Figure 2.17). The mechanical advantages of the chisel-tooth digging genera reach their lowest points at higher gape angles, with *Heliophobius* only reaching its lowest MA close to 90°, before increasing.

The effect of gape on the superficial and deep masseters is slightly different compared to the temporalis. Increasing gape decreases mechanical advantage of both masseter muscles at a faster rate compared to the temporalis in all genera. The mechanical advantages of the masseter muscles also reach their lowest values at a larger gape than the temporalis. The lowest MA of the superficial masseter for all genera is in the range of 80-90° before it begins to increase (Figure 2.18), and the MA of deep masseter does not seem to reach a minimum for any genus at gapes up to 100° (Figure 2.19). It is worth noting at this point that all gape angles are theoretical and may not be achievable in reality. The problems of interpretation of these graphs will be discussed below.

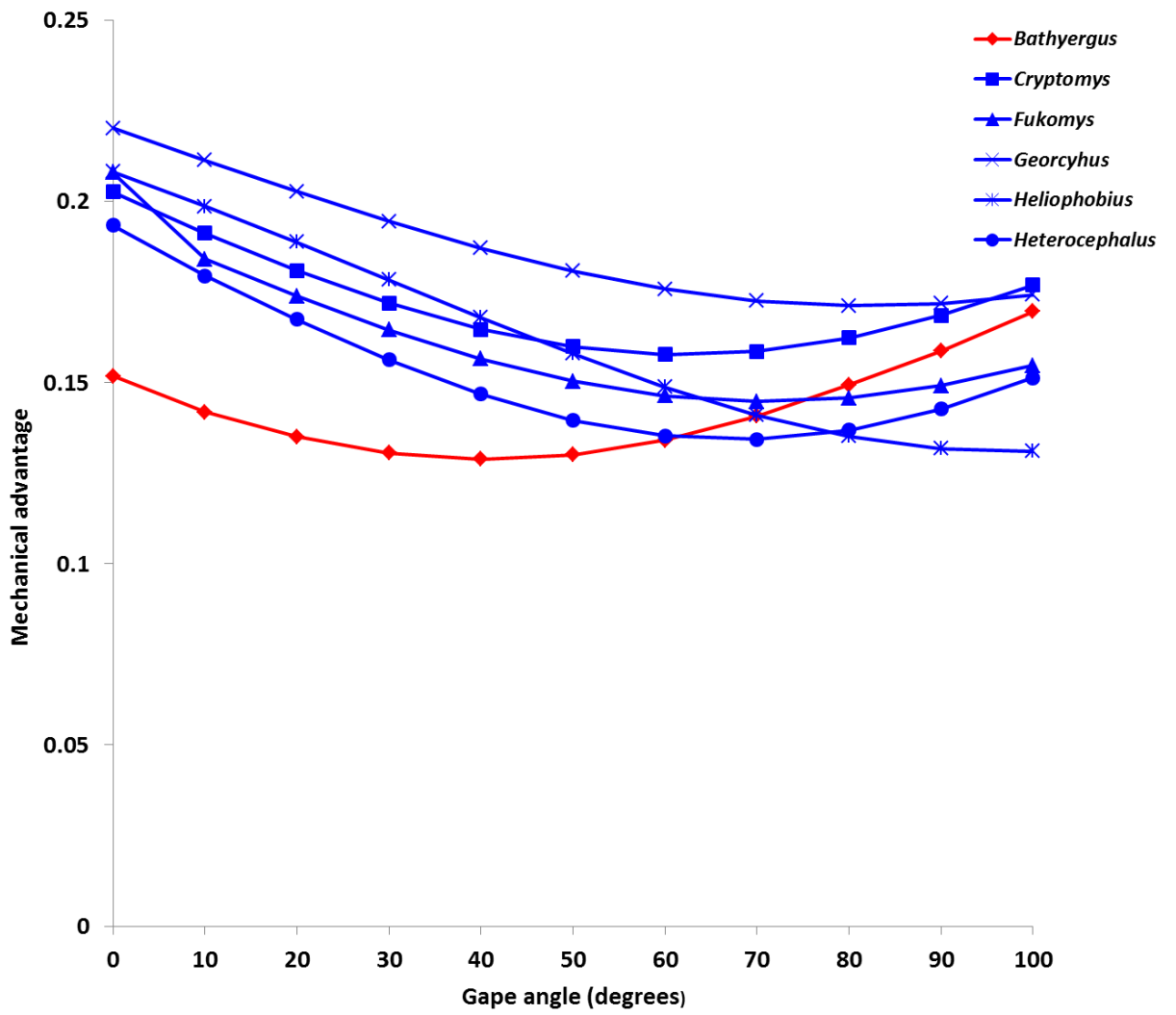


Figure 2.17 Mechanical advantage of the temporalis at gapes between 0° and 100° in chisel-tooth digging (blue) and scratch digging (red) bathyergid genera. Species means are represented.

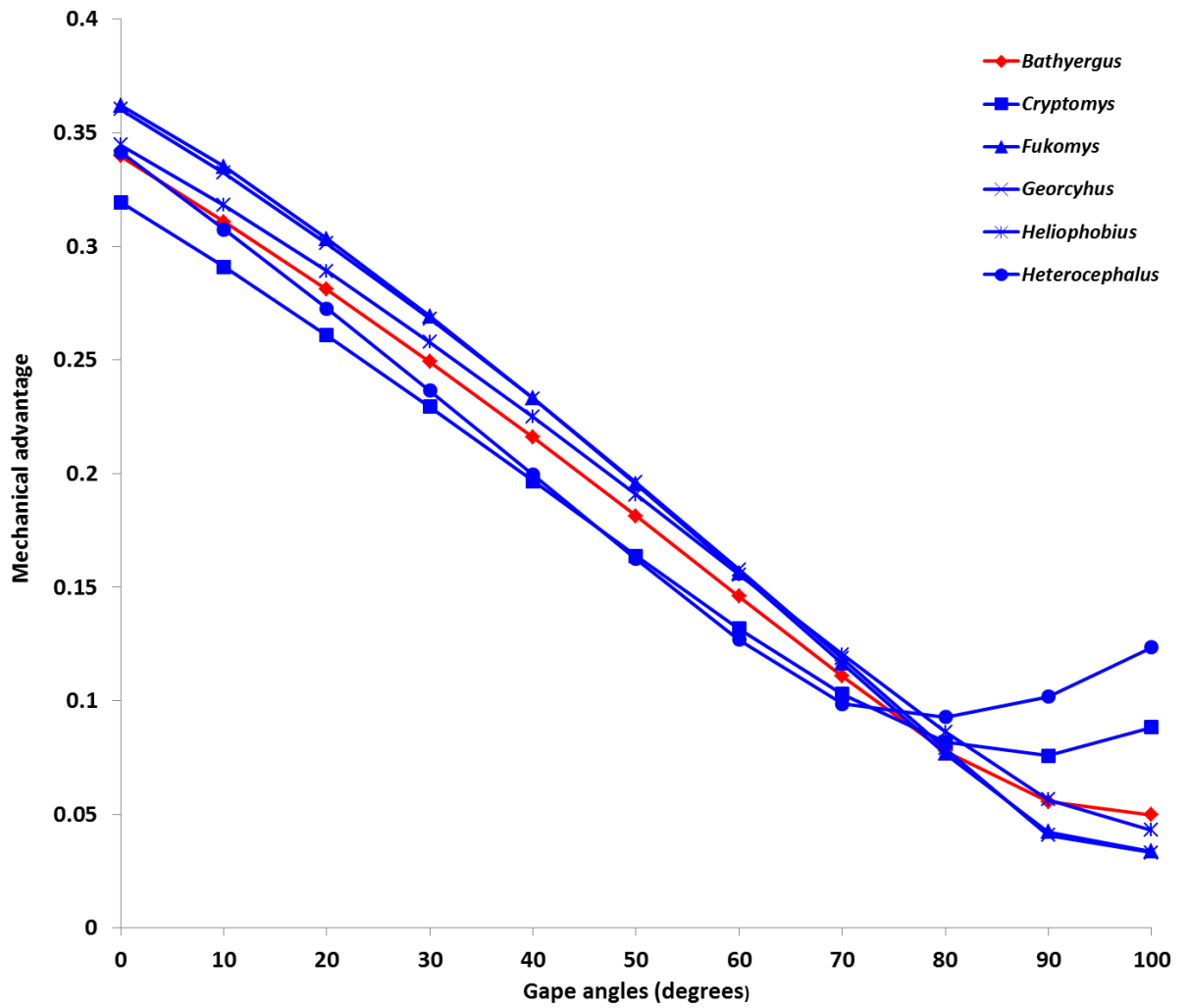


Figure 2.18 Mechanical advantage of the superficial masseter at gapes between 0° and 100° in chisel-tooth digging (blue) and scratch digging (red) bathyergid genera. Species means are represented.

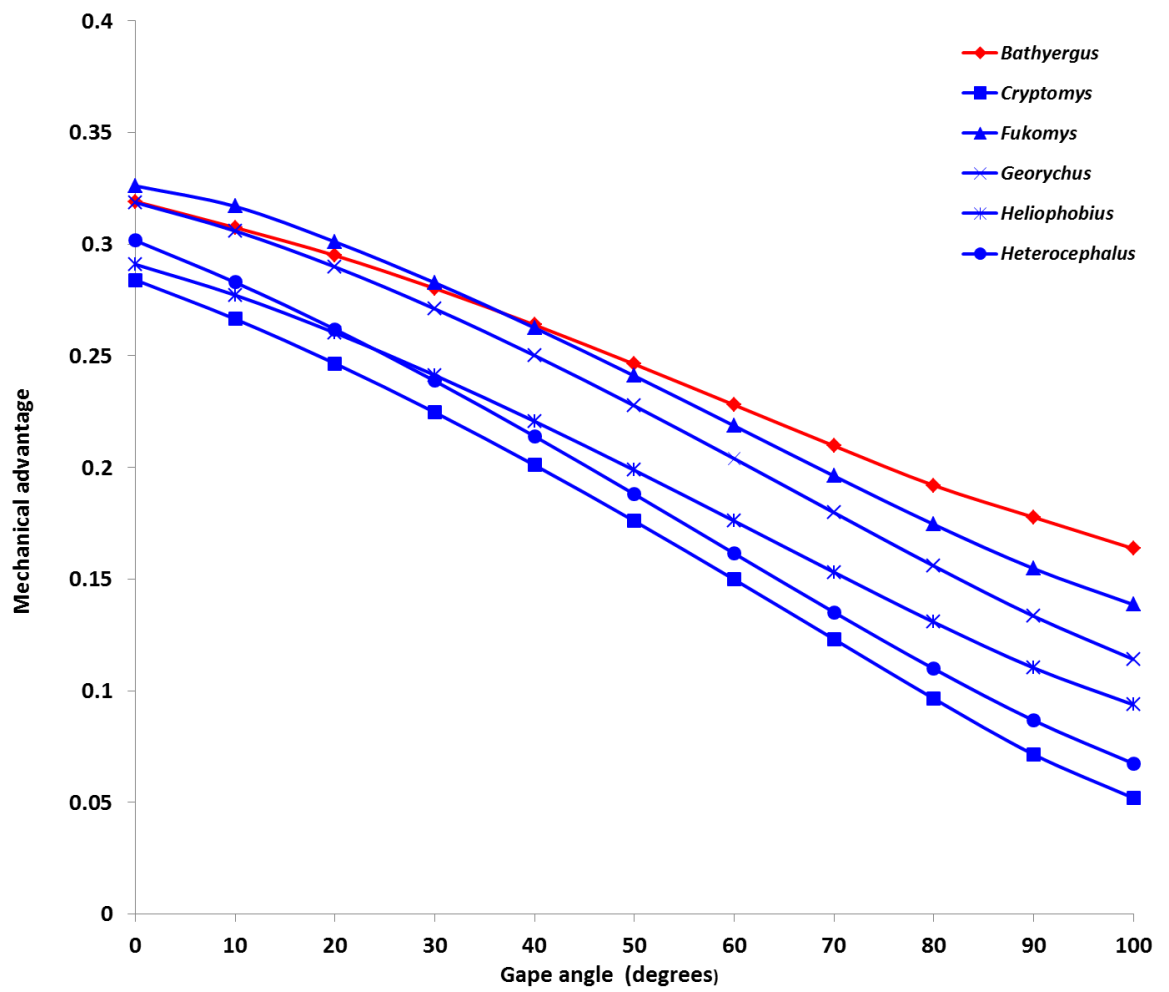


Figure 2.19 Mechanical advantage of the deep masseter at gapes between 0° and 100° in chisel-tooth digging (blue) and scratch digging (red) bathyergid genera. Species means are represented.

2.4 Discussion

2.4.1 Bite force

My results indicate that the cranium and mandible of chisel-tooth digging bathyergids are able to produce a larger bite force at the incisors than the scratch digging *Bathyergus*. I found that chisel-tooth diggers had significantly wider crania and taller heads (relative to basilar length) compared with the scratch digger *Bathyergus*. Subterranean rodents tend to have larger skulls than their terrestrial counterparts in order to accommodate larger, more powerful masticatory muscles (Stein, 2000). This trend has accelerated in chisel-tooth diggers, with Samuels and Van Valkenburgh (2009) finding that the skulls of chisel-tooth diggers showed broader rostra, wider zygomatic arches and larger temporal fossae compared to scratch digging rodents, including *Bathyergus*. This supports the results presented in this study, adding to the evidence that chisel-tooth digging is associated with relative enlargement of both the masseter and temporalis muscles (Stein, 2000).

Head height has previously been shown to be a strong indicator of bite force in *Fukomys* by Van Daele et al (2009). However, the authors did not explain exactly how they measured this variable. In my study, head height only included the cranium, from the posterior margin of the palate to the bregma, which may have been different to the measurement reported by Van Daele et al (2009). Nevertheless, head height measured here differentiated the chisel-tooth diggers from the scratch diggers. An increase in the relative head height of chisel-tooth diggers is probably the result of enlarged temporal fossae, as the variable incorporates this region of the skull. The temporalis muscle has been shown to be the dominant masticatory muscle in the chisel-tooth digger *Heterocephalus*, with temporalis accounting for 32% of all masticatory muscles (Cox and Faulkes, 2014). Similar dominance of the temporalis muscle is also seen in *Fukomys*, accounting for a range of around 25% (Van Daele et al, 2009). This proportion of the masticatory muscle is very large in comparison to other hystricognathous rodents e.g. *Cavia* (11%: Cox and Jeffery, 2011), *Hydrochoerus* (5%: Müller, 1933) and *Hystrix* (17%: Turnbull, 1970). Interestingly, temporalis dominance similar to mole-rats is also reported in sciuriform rodents (25-30%: Druzinsky, 2010) which, like *Fukomys*, have a large bite force for their size (Freeman and Lemen, 2008). Furthermore, a comparative study of the chisel-tooth digger *Georychus* and scratch digger *Bathyergus* found that *Georychus* had a relatively larger temporalis than

Bathyergus (Kouame et al, 2006). It is clear that the temporalis muscle, along with the other masticatory muscles, is dominant in chisel-tooth digging mole-rats, and may be one of the driving factors behind a relatively increased head height.

The biomechanical impact of this presumed difference in temporalis size was measured by calculating the MA of the muscle (along with that of the superficial and deep masseters). The results show that there is a significant increase in temporalis MA in chisel-tooth diggers compared with the scratch digger. This may be a result of the change in the temporal fossa morphology, which potentially explains why the temporalis takes up a larger proportion of the masticatory muscles in chisel-tooth diggers compared to other rodents. Enlarged temporal fossae are a characteristic that distinguishes the cranial shape of chisel-tooth and scratch digging rodents (Samuels and Van Valkenburgh, 2009). However, Stein (2000) notes that the crania of subterranean rodents are usually dorsally flattened compared to non-subterranean rodents. This study suggests that this flattening is reversed in chisel-tooth diggers in order to increase the size of the temporal fossa and hence produce greater bite forces at the incisors. So why doesn't *Bathyergus*, the only scratch digger genus within the Bathyergidae, retain this chisel-tooth digging cranial shape, given that its phylogenetic position within the family (Figure 2.1) suggests evolution from a chisel-tooth digging ancestor? *Bathyergus* lives in soft soils in Southern Africa, so it is possible that a dorsally flattened skull is an optimum shape to move efficiently through an underground burrow in such a substrate. In order to exploit areas with harder soils, chisel-tooth digging mole-rats have had to adapt their skulls to incorporate a larger temporalis for improved bite force at the incisors. The relaxation of this selection pressure for high bite force may have driven the cranium of *Bathyergus* to revert to the more usual morphology for subterranean rodents.

In addition to changes in muscle attachment areas, there are a number of other potential forces that could have resulted in this increased head height in chisel-tooth diggers. It is possible that variation in head height amongst bathyergids may also be a result of variation in relative brain size. Previous work has indicated that subterranean rodents have relatively small brains (Mace et al, 1981; Vassallo and Echeverría, 2009). However, *Bathyergus* is the largest genus of the Bathyergidae and so its brain is likely to be relatively even smaller owing to the negative allometry between brain and body size. Thus, a relatively smaller brain in *Bathyergus* would require a relatively smaller braincase, which would lead to a reduction in head height. Another alternative is

evident in how the upper incisor is positioned within the skull of the bathyergids. Chisel-tooth digging rodents require a longer upper incisor within the skull in order to increase the angle of procumbency. In non-bathyergid chisel-tooth digging rodents (e.g. *Ctenomys* and *Spalacopus*), these large incisors are located in alveolar sheaths that are lateral to the cheek teeth and avoid the internal cranial space (Lessa, 1990). Chisel-tooth digging bathyergids incorporate this enlarged incisor high on the rostrum and orbit, before inserting behind the cheek teeth, as is shown in Figure 2.3. This configuration may have influenced the overall architecture of the skull by increasing height head in chisel-tooth digging bathyergids. Within *Bathyergus*, the incorporation of an upper incisor is exclusive to the rostrum and inserts anterior to the cheek teeth and so does not require a modification to the rest of the cranium. These explanations and the scenario based on temporalis size are not necessarily mutually exclusive and may all be in operation.

Rostral length did not differentiate between chisel-tooth and scratch digging (Figure 2.7; 2.13), which was rather surprising considering the significant increases found in chisel-tooth digger jaw length (Figure 2.8; 2.14) and the covariation found between the cranium and mandible of hystricognath rodents (Hautier et al, 2012). Samuels and Van Valkenburgh (2009) also found that chisel-tooth diggers have longer rostra compared to scratch diggers, but this pattern has not been found within the context of the bathyergids here. In fact the only notably different rostral length was that of the chisel-tooth digger *Heterocephalus*, which appears to have a relatively shorter rostrum compared to the other bathyergids (Figure 2.7). An increase in relative rostral length has been associated with an increase in incisor procumbency in some subterranean rodents (Lessa and Patton, 1989; Mora et al, 2003). However, such an increase would not be necessary in chisel-tooth digging bathyergids with procumbent incisors owing to the displacement of the incisor roots posteriorly within the skull (Landry, 1957a). Overall, rostral length was shown to be positively allometric in Bathyergidae, which has previously been noted in other mammalian orders (Radinsky, 1985).

2.4.2 *The curious case of the naked mole-rat*

The apparent reduction of rostral length in *Heterocephalus* has previously been proposed to have occurred to shorten the out-lever of the masticatory system and hence increase the mechanical advantage of the masticatory muscles (Cox and Faulkes, 2014). This is probably not the case for two reasons: firstly, the relative reduction in the rostrum would be likely to be seen in the other chisel-tooth digging bathyergids, which

it is not; secondly, as chisel-tooth digging is accomplished primarily by the lower incisors (Stein, 2000), a decrease in the out-lever of the masticatory system would require a decrease in lower jaw length, not rostral length. However, lower jaw length has actually increased in all chisel-tooth diggers (see Figure 2.8; 2.14).

The reduced rostrum found in *Heterocephalus* may be partly explained by allometric scaling: rostral length scales with positive allometry (Table 2.4; Figure 2.13) and *Heterocephalus* is the smallest species of mole-rat. However, the short rostrum could also be a further adaptation towards chisel-tooth digging, required by this particular species due to its particularly small size. In fact, *Heterocephalus* is one of the smallest subterranean mammals, with a body mass range of 30-50 g (Jarvis and Sherman, 2002). Bite force has been shown to correlate strongly with body mass in rodents (Freeman and Lemen, 2008; Van Daele et al, 2009; Becerra et al, 2014). However, there must be a minimum amount of power produced at the incisors in order to break through the hard soils in which chisel-tooth diggers are known to burrow. Therefore, small rodents such as *Heterocephalus* must modify their chisel-tooth digging apparatus further than larger sized chisel-tooth diggers in order to produce an adequate amount of force at the incisors to break through the soil. Cox and Faulkes (2014) report that the total masticatory muscle mass of *Heterocephalus* is 75% of that reported for the rat (Cox and Jeffery, 2011), despite *Heterocephalus* being only 14-23% of the body mass of the rat specimen used in Cox and Jeffery (2011). These examples show that *Heterocephalus* has evolved a form that can accommodate large masticatory muscles despite its small size.

Heterocephalus may have evolved to accommodate these larger masticatory muscles in a number of ways: A reduction of the eyes is a common synapomorphy seen amongst subterranean mammals (Darwin, 1859), with subterranean rodents being no exception (Nevo, 1979; Burda et al, 1990; Stein, 2000). This reduction of the eye has potentially made available space for an anterior expansion of the temporalis into the unoccupied orbit (Lavocat, 1973; Cox and Faulkes, 2014), although this is probably not an adaptation exclusive to *Heterocephalus*.

Secondly, *Heterocephalus* may have evolved these larger masticatory muscles by taking advantage of its unusual cranial musculature. Almost all living rodents can be classified into three (non-phylogenetic) groups, based on their masticatory morphology: sciuriform (squirrel-like), myomorph (mouse-like) or hystricomorph (porcupine-like)

(Brandt, 1855; Wood, 1965). However, the Bathyergidae are unusual as their masticatory morphology does not conform to any of these morphotypes. Unlike most other rodents, no part of the masticatory musculature attaches to the rostrum. This unusual morphology is termed protrogomorph, and is thought to be the ancestral condition of rodents (Wood, 1965), but has probably been secondarily acquired in the Bathyergidae (Landry, 1957b; Maier and Schrenk, 1987; Cox and Faulkes, 2014). The larger mole-rats have retained a long rostrum as there is enough space available in the temporal fossa to accommodate large muscles to provide adequate bite forces; and a reduction of the rostrum would require a reduction in jaw length, which is necessary to produce a large gape (see below). Smaller subterranean rodents such as *Heterocephalus* do not have this luxury; they are constrained by the limited space they have to accommodate muscles that provide a minimum bite force necessary to break through tough soils. They have managed to do so by expanding the zygomatic arches anteriorly, reducing the relative length of the rostrum, and providing more space for the masticatory muscles. Similar issues with constraints of space are found during ontogenetic development of subterranean rodents. Naturally, when animals are born, they are much smaller than fully grown adults. Not long after birth however, juveniles must be able to masticate efficiently to break down food and, in the case of subterranean rodents, assist in burrow construction. This means that they also must be able to produce enough force at the incisors, despite having the disadvantage of a greatly reduced masticatory musculature arrangement. Previous research has shown that digging behaviour occurs soon after birth in *Ctenomys* (Vassallo, 2015), with some pups weighing less than 40g (a similar weight to *Heterocephalus* adults) participating in burrow construction. In-levers of the masseteric muscles of *Ctenomys* showed negative allometric growth, so that juveniles are more efficient than adults at producing bite forces (Verzi et al, 2010). Vassallo et al (2016) also showed that relative incisor bending strength did not change throughout ontogeny of *Ctenomys*, and so coupled together with muscles, the masticatory apparatus can create enough power at the incisor to break through soil at a young age. These examples show the adaptability of small subterranean rodents that have either evolved into small adults (*Heterocephalus*) or rodents that can contribute to borrow construction at a very early stage of ontogeny (*Ctenomys*).

2.4.3 Incisor procumbency in chisel-tooth digging rodents

Previous research has suggested that increased upper incisor procumbency is a trait associated with chisel-tooth digging (Lessa, 1990; Van der Merwe and Botha, 1998; Vassallo, 1998; Stein, 2000). This study agrees with the extensive literature as I showed that most chisel-tooth digging bathyergids have a larger upper incisor procumbency angle than the scratch digging *Bathyergus*. However, an examination of Figure 2.6 shows that some specimens of *Heterocephalus* (a chisel-tooth digger) have a smaller upper incisor procumbency angle than the other chisel-tooth diggers. There was no difference found between the upper incisor procumbency of *Heterocephalus* and the scratch digger *Bathyergus*, despite a significant difference being found between the two digging groups overall. Lessa and Patton (1989) postulated that incisor procumbency is coupled by two main evolutionary mechanisms. First, incisor procumbency has been linked to rostral allometric growth (e.g. Mora et al, 2003), i.e. the longer the rostrum, the higher the incisor procumbency. Second, Landry (1957a) proposed that procumbent incisors require large incisor canals with extended roots at a posterior position within the skull (and procumbency is therefore more of a structural issue rather than a size issue). So, in non-procumbent rodents the incisor root only extends back to a position above the cheek teeth (Landry, 1957a), whereas increased procumbency is found in rodents that have shifted their incisor roots more posteriorly. The incisor root of *Heterocephalus* (like all chisel-tooth digging bathyergids) is positioned as far back in the skull as possible. I therefore hypothesise that, as it appears to have a greatly shortened rostrum, *Heterocephalus* has the most procumbent incisors it can possibly have, given the size of its skull, whereas *Bathyergus* has a relatively reduced procumbency, given its large size (up to 2 kg; Stein, 2000). The varying position of the incisor within the skull has probably led to the lack of clear allometric scaling of incisor procumbency across the Bathyergidae (Table 2.4).

2.4.4 Gape

My results indicate that the cranium and mandible of chisel-tooth digging bathyergids are able to produce a larger gape than the scratch digging *Bathyergus*. I found that chisel-tooth diggers had significantly greater relative jaw lengths, condyle lengths and condyle heights than *Bathyergus*. However, when the data was corrected for allometric scaling, there was no difference found in condyle height between the two groups (Figure 2.16). Jaw length is a strong predictor of gape in many animals including snakes (Hampton and Moon, 2013), primates (Hylander, 2013) and mice (Vinyard and

Payseur, 2008). Functional gapes are typically measured from the tips of the maxillary incisor to tips of the mandibular incisor, and therefore an increased mandible relative to skull length will lead to an increased gape for the same angle of rotation of the mandible. However, it is worth noting that this rule is the case when only considering the geometry of the mandible. Other factors such as muscle stretch of the masseter (Herring and Herring, 1974) have a considerable effect on gape and have not been considered in this study. Masseter fibre lengths taken from the literature however suggest that the chisel-tooth digger *Fukomys* possesses longer masseter muscle fibres (Van Daele et al, 2009) than *Callithrix jacchus*, a common marmoset comparable in size to the mole-rat and with known abilities to produce wide gapes (Eng et al, 2009).

Condyle length has also been found to be associated with increased gape in mice (Vinyard and Payseur, 2008). It is unclear if an increased condyle length relates to an increase in condyle surface area or in condyle curvature, as both these factors can have an effect on joint mobility (Swartz, 1989). Either way, an antero-posteriorly elongated condyle appears to increase potential rotation at the jaw joint, thus facilitating a wider gape. In a number of other chisel-tooth digging rodents in the Ctenomyidae and Spalacidae, this characteristic is correlated with the presence of some kind of postglenoid articulation of the mandible, which provides stability during incisor biting with high forces (Verzi and Olivares, 2006). However, no postglenoid fossa for such an articulation could be identified in the bathyergid species under study here.

Condyle height also differed between chisel-tooth and scratch digging bathyergids when isometrically scaled, with chisel-tooth digging rodents having larger condyle heights than the scratch digger. This was a rather surprising result as it is contrary to my initial hypothesis, that a low condyle height will facilitate a wider gape by reducing stretch in the masseter muscle (Herring and Herring, 1974). However, when corrected for allometric scaling, there was found to be no difference in condyle height between the two digging groups (Figure 2.16). Interestingly, although it was found in primates as a strong morphological predictor of gape, this was not found to be the case in mice (Vinyard et al, 2003; Vinyard and Payseur, 2008).

It has been well established that increasing gape decreases bite force in mammals with a generalized morphology (Maynard Smith and Savage, 1959; Turnbull, 1970; Herring, 1975; Dumont and Herrel, 2003; Bourke et al, 2008; Williams et al, 2009). In the context of my results, this trade-off is clear when considering that, although it will

increase gape, an increased jaw length will also decrease the muscle out-lever, therefore reducing the muscle's MA. In order to examine how gape theoretically affects the mechanical advantage of each masticatory muscle, the mandible was rotated around the skull of each specimen. The results show that continually increasing gape drastically reduces MA of both the superficial and deep masseter, but that a rather different pattern is found with regard to the temporalis muscle (Figure 2.17, Figure 2.18 and Figure 2.19). First, the rate of change (declination) of the temporalis MA is smaller compared to the masseter muscles. This implies that temporalis is better at maintaining MA at increased gapes compared to the masseters. However, it should be noted that the MA of both masseters at low gapes is around a third higher than the temporalis. Second, the temporalis MA decreases as gape increases down to a minimum point, after which it begins to increase again. Interestingly, the point where MA is lowest is different depending on the species; *Bathyergus* reaches its minimum MA at a narrower gape than its chisel-tooth digging relatives. Before anything can be inferred from this result, it is important to discuss what is actually happening at this point of minimum MA. Mathematically, the reason why MA decreases with increasing gape is related to the positioning of the muscle force vector (MFV) relative to the condyle (or the muscle moment arm). Rotating the mandible to mimic jaw opening causes the MFV to change in such a way that the perpendicular distance between the MFV and the condyle is reduced (this distance is the muscle moment arm). As the muscle moment arm is reduced and the jaw moment arm stays the same, the MA of the muscle is reduced (as MA is defined as the ratio between muscle moment arm and jaw moment arm). The minimum MA represents the MFV being as close as possible to the condyle in 3D space. If the mandible is theoretically rotated further after this point, the MA of the muscle will increase again, as the perpendicular distance of the MFV to the condyle increases in the opposite direction. Although this is what happens in theory, this cannot occur in a biologically functional sense because parts of the skull begin to obstruct the path of the muscle. For this reason, the gape at which MA is lowest represents the theoretical maximum gape relevant to each muscle. Looking at the impact of gape on MA of temporalis muscle of the scratch digger *Bathyergus* (Figure 2.17), it can be seen that MA of temporalis reaches its lowest point around 40° . This is in contrast to the chisel-tooth diggers, who reach their lowest points around $70-80^\circ$. This figure for maximum gape is in the *in vivo* range of gape reported for chisel-tooth digger *Fukomys*, which had an average maximum gape of 71° (Heindryckx, 2014). My model prediction of maximum gape is similar to the *in vivo* result for *Fukomys*, despite only considering

the temporalis muscle, and not taking into account other variables such as muscle stretch, which highlights the importance of craniomandibular form in constraining gape.

So why does the temporalis seem to restrict gape in the scratch digger *Bathyergus* more than in chisel-tooth diggers? It appears that a restriction of gape is related to the morphology of the coronoid process, where the temporalis inserts. In the scratch digger *Bathyergus*, the coronoid process has greatly shortened to a level equal to the condyle, creating a shallow mandibular notch. The chisel-tooth digger on the other hand has a much longer fin shaped coronoid process, and displays a much deeper mandibular notch (see Figure 2.20). In terms of gape constrained by the temporalis, the shape of the coronoid process of the chisel-tooth digger is more advantageous. The long fin shape of the coronoid process means that even at high gape the insertion of the temporalis does not become wrapped around the zygomatic process. The greater length of the coronoid process, along with the larger and deeper temporal fossa, also causes the muscle vector to be more vertical, increasing the muscle moment arm of the temporalis muscle.



Figure 2.20 Lateral view of the mandibles of *Heliophobius argenteocinereus* (above) and *Bathyergus suillus* (below). Arrows indicate the coronoid process.

2.4.5 Conclusions

The results here support previous research indicating that the cranial and mandibular morphology of the scratch digging genus *Bathyergus* is very different to that of chisel-tooth digging members of the Bathyergidae (Samuels and Van Valkenburgh, 2009; Gomes Rodrigues et al. *in press*). It is not possible, with the methods employed in this study, to say if the change in morphology of *Bathyergus* represents selection or genetic drift, but it is possible to test the functional implications of the morphological change. The results show that the morphology seen in the chisel-tooth digging genera better facilitates the production of high bite force and wide gape, thus enabling more efficient digging with the incisors than could be achieved by *Bathyergus*. Clearly as a change in digging behaviour has occurred on the lineage leading to *Bathyergus*, an associated change in morphology has also taken place.

Chapter 3: The effect of digging on craniodental morphology in rodents

3.1 Introduction

Rodentia is by far the largest mammalian order with more than 2200 species (Wilson and Reeder, 2005) and accounts for 41% of extant mammalian diversity (Hautier and Cox, 2015). This broad diversification has led the order to radiate into arboreal, semi-aquatic, subterranean and terrestrial niches and it is represented on every continent except Antarctica. The evolutionary success of the rodents, especially mice and rats, is thought to be down to their efficient masticatory apparatus (Cox et al., 2012; Tiphaine et al., 2013). Despite their extensive ecological and phylogenetic radiation, all rodents are united by a common morphology, diprotodonty. This morphology is characterised by a pair of enlarged upper incisors embedded in the cranium and a pair of lower incisors in the mandible. Rodent incisors are open-rooted and continue to grow throughout life (Nowak, 1999). The incisors are separated from the cheek teeth by a diastema, due to the loss of incisors I^1 , I^3 and I^4 and all canines and mesial premolars. Rodent incisors have also lost enamel on the lingual side of the incisor, leaving the dentine exposed. Due to this loss of lingual enamel, rodents are able to sharpen the tips of their incisors by wearing away the softer dentine using the adjacent incisor (Osborn, 1969), a process unique to rodents (Druzinsky, 2015). This sharp tip is beneficial for feeding, defensive strategies and in the case of some subterranean rodents, for digging burrows (Becht, 1953; Nevo, 1969; Hildebrand, 1985).

Subterranean rodents, a specialized group of rodents that live almost exclusively underground, experience a very different type of selection pressure to terrestrial rodents. For instance, burrowing underground requires 360-3400 times the energy of moving a similar distance above ground (Vleck, 1979; Jarvis and Bennett, 1991). This extent of energy expenditure has required subterranean rodents to evolve efficient methods of soil excavation. The majority of subterranean rodents show one of two types of digging method: chisel-tooth digging and scratch digging (Hildebrand, 1985). Chisel-tooth digging involves the rodent using their incisors to excavate the soil whereas scratch digging rodents only use their forelimbs. The ability to use incisors for digging has

allowed chisel-tooth digging rodents the freedom to exploit environments of varying soil quality (Lessa and Thaeler, 1989; Lessa, 1990).

Noticeable craniodental modifications have been associated with subterranean rodents that have adopted chisel-tooth digging methods. Such modifications include larger temporal fossae; wider and taller crania; enlarged zygomatic arches; longer rostra; more procumbent incisors and incisors that are more resistant to bending stresses (Landry, 1957a; Agrawal, 1967; Samuels and Van Valkenburgh, 2009; Becerra et al., 2012, 2013, 2014; McIntosh and Cox, 2016; Gomes Rodrigues et al., *in press*; Chapter 2). It is thought that some of these modifications improve bite force and gape in subterranean rodents that use their incisors to dig in hard soils (McIntosh and Cox, 2016; Chapter 2).

An extensively studied modification in chisel-tooth digging rodents is variation of upper incisor procumbency, that is, the angle of anterior projection of the upper incisors (Landry, 1957a; Agrawal, 1967; Lessa and Thaeler, 1989; Lessa and Patton, 1989; Vassallo, 1998; van der Merwe and Botha, 1998; Fernandez et al., 2000; Mora et al., 2003). These studies have shown that subterranean rodents that primarily use their incisors to dig tend to have larger angles of procumbency in the upper incisors compared to subterranean rodents that primarily use their forelimbs to dig. Vassallo (1998) hypothesised that this increased angle of procumbency allows for a more favourable angle to break harder soils. Incisor procumbency in rodents is governed by overall curvature of the incisor and its placement within the rostrum (Landry, 1957a; Akersten, 1981). Landry (1957a) points out that to keep the incisor in its functional plane, the only way the procumbency could change without changing incisor morphology (incisor curvature) is by raising or lowering the posterior end of the incisor. However, rostral space in rodents is nearly completely occupied by the incisor, and so this type of incisal movement would not be possible (Landry, 1957a)(Figure 3.1).

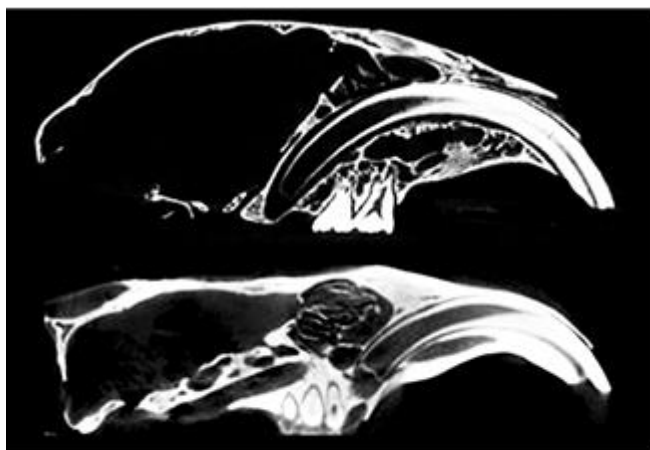


Figure 3.1 Mid-sagittal slice of CT scan in two subterranean rodents: chisel-tooth digging *Georychus capensis* (above) and scratch digging *Bathyergus suillus* (below). Notice the posterior displacement of the incisor root in *Georychus capensis* compared with *Bathyergus suillus*. Figure scaled to cranial length of *Georychus capensis*.

Chisel-tooth digging members of the subterranean rodent family Bathyergidae (African mole-rats) exhibit some of the most procumbent upper incisors that are seen in any rodent (Ellerman, 1940; Landry, 1957a). The upper incisors also extend far back into the cranium, and are rooted behind the cheek teeth. Interestingly, this family also contains a scratch digging genus of rodent, *Bathyergus*. The upper incisors of this genus are less procumbent than those of the chisel-tooth digging genera (van der Merwe and Botha, 1998; Nowak, 1999; Stein, 2000; McIntosh and Cox, 2016; Chapter 2). This reduction in procumbency is also associated with a change of incisor morphology where the incisor root is placed further forward (Figure 3.1). The cranium of the scratch digging *Bathyergus* has also been shown to be morphologically different from the chisel-tooth digging family members (Samuels and Van Valkenburgh, 2009; Gomes Rodrigues et al., *in press*). This is despite the fact that *Bathyergus* is not the basal genus of the family and is likely to have evolved from a chisel-tooth digging ancestor (Faulkes et al., 2004; Deuve et al., 2008; Figure 3.2). Chisel-tooth digging has evolved independently a number of times, including at least once in all six families of modern subterranean rodents (Nowak, 1999). Furthermore, Samuels and Van Valkenburgh (2009) showed chisel-tooth diggers from several families of subterranean rodent converge in cranial shape, although they did not take phylogeny into account, imperative for statistical tests using inter-specific data (Felsenstein, 1985).

The rodent cranium is a complexly integrated structure (Hallgrímsson et al., 2009) and understanding how different structures covary within the cranium could potentially

explain morphological diversity in some clades and constraints in others. Covariation of incisor morphology and cranial shape has never been studied in rodents, and as the incisor takes up such a large space within the craniofacial structure of the rodent, it is potentially an underlying factor in chisel-tooth digging cranial convergence.

In order to address this issue, I will quantify incisor morphology in a diverse number of rodents from both a terrestrial and subterranean background to show how chisel-tooth digging influences incisor morphology. Secondly, I will quantify cranial shape and attempt to verify the findings of Samuels and Van Valkenburgh (2009) using phylogenetic comparative methods (Felsenstein, 1985; Rohlf, 2001). I will then assess how incisor morphology and cranial shape covary and show the extent of morphological integration between the upper incisor and cranium in rodents.

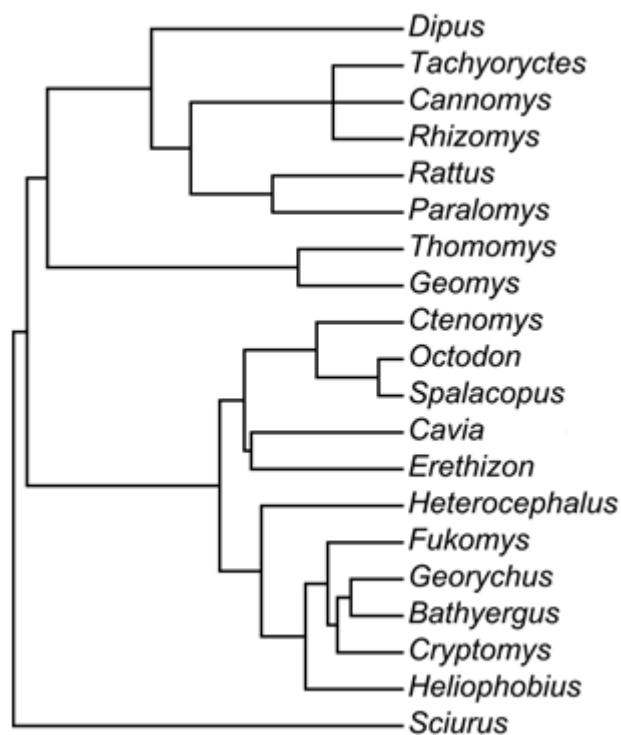


Figure 3.2 Phylogeny of sample used in this study. Modified from Fabre et al. (2012).

3.2 Materials and Methods

3.2.1 Rodent sample

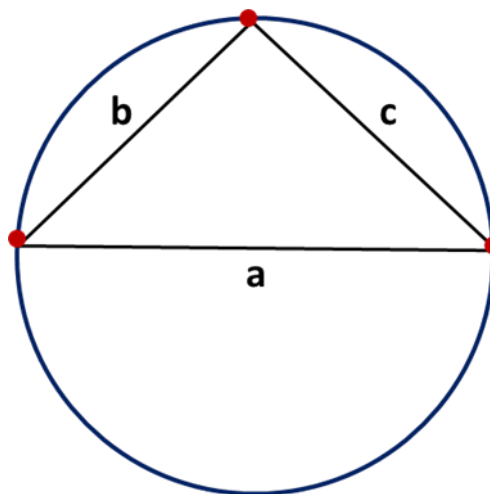
This study analysed 65 adult crania from a diverse group of rodents representing 20 genera and 11 families: Bathyergidae, Caviidae, Cricetidae, Ctenomyidae, Dipodidae, Erethizontidae, Geomyidae, Muridae, Octodontidae, Scuridae and Spalacidae (Table 3.1; Figure 3.2). The study focuses on the influence of chisel-tooth digging on incisor morphology. However, other factors such as diet, habitat and phylogeny have been shown to influence cranial and incisor morphology in rodents (Samuels, 2009; Croft et al., 2011; Hautier et al., 2012). In order to account for these potential unwanted influences, the sample contains phylogenetically distant subterranean and terrestrial rodents with different ecologies (Table 3.1). The specimens were scanned on an X-Tek Metris microCT scanner at the University of Hull (Medical and Biological Engineering Research Group). The resulting scans had isometric voxels with dimensions ranging between 0.01mm and 0.07mm.

Table 3.1 List of genera analysed including specimen number, diet and mode of digging. Abbreviations for dietary categories: O, omnivore; GH, generalist herbivore; SH, specialist herbivore. Dietary categories follow method of Samuels (2009). Subterranean rodent genera are in bold.

Family	Genus #	Genus	N	Diet	Mode of digging
Bathyergidae	1	<i>Bathyergus</i>	10	SH	Scratch
	2	<i>Cryptomys</i>	1	SH	Chisel-tooth
	3	<i>Fukomys</i>	9	SH	Chisel-tooth
	4	<i>Georchus</i>	3	SH	Chisel-tooth
	5	<i>Heliophobius</i>	10	SH	Chisel-tooth
	6	<i>Heterocephalus</i>	5	SH	Chisel-tooth
Caviidae	7	<i>Cavia</i>	2	SH	
Cricetidae	8	<i>Paralomys</i>	1	GH	
Ctenomyidae	9	<i>Ctenomys</i>	1	SH	Scratch
Dipodidae	10	<i>Dipus</i>	1	GH	
Erethizontidae	11	<i>Erethizon</i>	1	SH	
Geomyidae	12	<i>Geomys</i>	1	SH	Scratch
	13	<i>Thomomys</i>	1	SH	Scratch
Muridae	14	<i>Rattus</i>	2	O	
Octodontidae	15	<i>Octodon</i>	1	GH	
	16	<i>Spalacopus</i>	1	SH	Chisel-tooth
Spalacidae	17	<i>Cannomys</i>	1	SH	Chisel-tooth
	18	<i>Rhizomys</i>	3	SH	Chisel-tooth
	19	<i>Tachyoryctes</i>	4	SH	Chisel-tooth
Scuiridae	20	<i>Sciurus</i>	7	O	

3.2.2 Assessing incisor morphology

Rodent cranial surfaces were automatically created from the microCT scans using a predefined grey scale in Avizo 8.0 (FEI, Hillsboro, Oregon). One upper incisor from each specimen was manually segmented into a separate material using the segmentation module in Avizo and a separate surface for the incisor was created. Incisor morphology was quantified using a number of measurements. Firstly, incisor curvature was measured by fitting a circle to the surface outline of the incisor. As any three non-linear points describe a circle, three points were equidistantly placed on the surface midline of the incisor via a B-spline (at the apex, tip and most dorsal point of curve) using Avizo. This method assumes that incisor growth leads to circular incisor form. This is not strictly the case as a rat upper incisor grows helically (Herzberg and Schour, 1941). However, Lin et al. (2010) analysed the lateral profile of the incisor using a geographic information system (GIS) programme and their results were identical to results modelling the incisor as a circular arc. As incisor curvature depends on both radius of curvature and length (Landry, 1957a), the relationship between these two variables was assessed using ordinary least squares (OLS) regression to show which had a greater influence on incisor curvature within the sample. Radius of curvature (RoC) of incisors was calculated from the fitted circle using an equation derived from Heron's formula (Figure 3.3). Length of incisor [straight line distance from apex to tip (**a** in Figure 3.3)] was calculated using standard Pythagoras' formula.



$$\text{RoC} = \frac{abc}{\sqrt{(2a^2b^2 + 2b^2c^2 + 2c^2a^2 - a^4 - b^4 - c^4)}}$$

Figure 3.3 Measuring radius of curvature. The length of the incisor (L) is measured using the base of the triangle (**a**). Red points represent the 3 the points placed on to surface of the incisor.

Rodent incisors are long relative to their diameter (i.e. take up a large proportion of a circle) and so can be affected by bending stresses (Bacigalupe et al., 2002). Second moment of area (SMA) is a geometric measurement that defines the resistance to bending of a cross-section of an object and is a good indicator of structural strength, a potentially important property for incisors used to dig through hard soils. Each incisor surface was aligned to a global axis in Avizo using the three points to fit a circle. This ensures that the root, tip and lingual side of each incisor were aligned on the same axis. The surfaces were then converted to volumes to create a stack of slices. The median slice of each incisor was then exported into ImageJ (Schneider et al., 2012). As the points used to align the incisors were placed equidistantly using a B-spline, each individual slice representing the cross section of each incisor was homologous. SMA of each cross-section was calculated using the ImageJ macro, BoneJ (Doubé et al., 2010).

The sample included a large range of body masses (e.g. *Paralomys* can be as small as 12g, whereas *Bathyergus* can grow up to 2kg) and past studies have shown that variables such as SMA of rodent incisors correlate strongly with size (e.g. Verzi et al., 2010). It was therefore decided to include size as a covariate to account for scaling. The size surrogate chosen was cranial length which was defined as basilar length (BL) (from the posterior margins of the alveoli of the upper incisors to the anteriormost point on the border of the foramen magnum). BL was calculated using Pythagorean methods from Cartesian points placed in Avizo. Incisor morphology variables were also logged in all analyses due to size differences and the necessity to linearize variables to carry out statistical procedures.

As closely related species tend to be more similar to each other than to more distantly related species they cannot be considered as completely independent units (Felsenstein, 1985; Garland et al., 2005), a prerequisite for standard statistical tests. On top of this, any study considering the influence of function on form in an inter-specific context, must take into account any other factors, such as phylogeny, that could inflate type 1 errors. Phylogenetic Generalized Least Squares (PGLS) (Grafen, 1989; Martins and Hansen, 1997) analysis was performed to show if any relationship between size and incisor morphology existed after phylogeny was accounted for. PGLS is a phylogenetic regression method (Grafen, 1989) which accounts for phylogeny via the error constant in the regression equation and is mathematically equivalent to the more commonly used comparative method, Felsenstein's (1985) independent contrasts (Garland and Ives, 2000; Rohlf, 2001). PGLS is preferred over independent contrasts in this case as it is a

more accurate technique when polytomies are found in the phylogeny (Rüber and Adams, 2001). It is also advantageous when wanting to graphically display an individual species contribution to a statistical test, such as generalized phylogenetic ANCOVA, as independent contrasts only represent the evolutionary differences between species and not the species itself.

It is possible to test how much phylogenetic signal is present in my data, a statistical procedure that quantifies the expected covariation of species traits under a selected evolutionary model (e.g. Brownian motion) on a phylogeny (for review see Blomberg and Garland, 2002). For the univariate analyses in this study, Pagel's λ (Pagel, 1999) was used to estimate the phylogenetic signalling in the data. Pagel's λ is a scaling parameter that measures the correlation of traits relative to expected correlation under a Brownian motion model of evolution. Normally, λ ranges from zero (no phylogenetic signal and data is equivalent to a "star" phylogeny) to one (data consistent with selected phylogenetic tree). Pagel's λ and PGLS regressions in this study are quantified simultaneously using the method proposed by Revell (2010). Phylogenetic ANCOVA models using PGLS (to test for differences between chisel-tooth digging incisors and incisors that are not used for this purpose) are fitted using genus means of the sample and the nlme (Pinheiro et al. 2016) and ape (Paradis et al., 2004) packages in R (R core team, 2016). The phylogeny used in all phylogenetically informed analyses in this study was modified from Fabre et al. (2012; Figure 3.2)

3.2.3 *Assessing cranial morphology*

The cranium of each specimen was quantified using 3D landmark coordinates. The *Geomys* specimen was not used in this study due to extensive damage of the cranium. Each landmark represented homologous anatomical points between specimens. Cranial surfaces were constructed from microCT scans and landmarked in Avizo (Figure 3.4 and Table 3.2). From this landmark data, variation in the shape of the crania was analysed with geometric morphometrics (for review see O'Higgins, 2000; Adams et al., 2004; Slice, 2007). The landmark co-ordinates were subjected to the Procrustes method of generalized least squares (GLS) superimposition (Rohlf and Slice, 1990). This process involves translating, scaling and rotating the landmark configurations and minimising inter-landmark distances, quantifying the differences in shape of each specimen. This Procrustes transformation represents the landmark configurations on Kendall's shape space (Kendall, 1984; Rohlf, 2000) which are now represented by Procrustes coordinates (a non-Euclidean shape space). A principal component analysis

(PCA) of genus averaged Procrustes coordinates allowed 2-D visualisation of the data and essentially shows the largest shape variation between genera. Surface warps of the extreme ends of the principal components axes were also included to visualise the shape variation within the data. The phylogenetic signal in the data was quantified by calculating the κ statistic (Blomberg et al., 2003), generalized to accept multivariate shape data (Adams, 2014a). Although the κ statistic and λ statistic are derived differently (κ is a scaled ratio of variance and λ is a scaling metric) their outcomes are normally similar i.e. <1 implies data is less phylogenetically correlated than expected under Brownian motion and >1 is more phylogenetically correlated than under Brownian motion. This multivariate κ statistic is the only developed method that predicts phylogenetic signal in multivariate data (Adams, 2014a). Measuring phylogenetic signalling simultaneously with the phylogenetic regression has been shown to outperform non-phylogenetic procedures in univariate data, even if the data has low phylogenetic signal (Revell, 2010). This has yet to be shown in multivariate data and as such both phylogenetic and non-phylogenetic procedures will be applied to my multivariate data sets to show the effect of phylogenetic correction.

A phylogenetic principal components analysis was also performed on the Procrustes coordinates. This analysis centres the data on the ancestral root of a phylogeny (“phylogenetic mean”) and extracts principal components from the variance covariance matrix corrected for phylogenetic propinquity, so that the major axes represent the non-phylogenetic residual shape variation, after the removal of phylogenetic covariation from the data (Revell, 2009; Polly et al., 2013; but see Uyeda et al., 2015). To calculate surface warps associated with extremes of phylogenetic principal components (PPC) axes, an average surface calculated from Procrustes coordinates is warped to an ancestral state reconstruction at the root of the phylogeny (Yang et al., 1995). Appropriately scaled eigenvectors from the corresponding PPC are then used to show the shape differences along the PPC axes.

Procrustes ANOVAs (analysis of variance) and phylogenetically informed Procrustes ANOVAs (Adams, 2014b) were performed on Procrustes coordinates to test for differences between skull shapes of chisel-tooth diggers and non-tooth diggers. Procrustes ANOVA is identical to a MANOVA on PC scores but performs better on multivariate data when the number of variables exceeds number of specimens (Adams, 2014b). GLS superimposition, phylogenetic signal testing, principal components analysis, ANOVAs and surface warps were processed using the geomorph package in R

(Adams and Otárola-Castillo, 2013). Phylogenetic principal components analysis was performed using the phytools package in R (Revell, 2012).

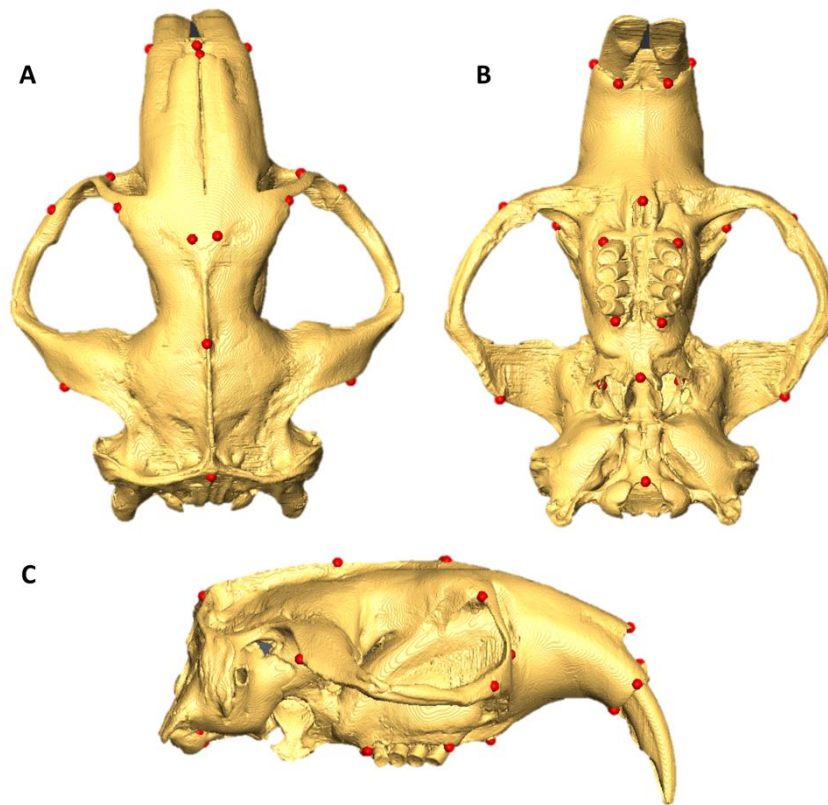


Figure 3.4 Landmark configuration represented on *Fukomys mechowii*. A, dorsal view. B, ventral view. C, lateral view. List of landmarks and anatomical descriptions in Table 3.2.

Table 3.2. 29 cranial landmarks and a description of their anatomical positions.

Number	Landmark definition
1	Antermost point on internasal suture
2	Midpoint of ventral margin of nasal opening
3	Dorsalmost point on left incisal alveolar margin
4	Dorsalmost point on right incisal alveolar margin
5	Ventral margin of left incisal alveolus
6	Ventral margin of right incisal alveolus
7	Midpoint of anterior extremity of incisive foramina
8	Lateralmost aspect of left infraorbital foramen
9	Lateralmost aspect of right infraorbital foramen
10	Antermost point on left orbital margin
11	Antermost point on right orbital margin
12	Posteriormost point of left naso-frontal suture
13	Posteriormost point of right naso-frontal suture
14	Antermost point of left maxillo-jugal suture
15	Antermost point of right maxillo-jugal suture
16	Posterior tip of left zygomatic arch
17	Posterior tip of right zygomatic arch
18	Anterolateral extremity of left cheek tooth row
19	Anterolateral extremity of right cheek tooth row
20	Posterior extremity of left cheek tooth row
21	Posterior extremity of right cheek tooth row
22	Posteriormost point of left foramen ovale
23	Posteriormost point of right foramen ovale
24	Bregma
25	Point of maximum curvature on the posterior edge of the palatine
26	Inferiormost point on margin of foramen magnum
27	Posteriormost point on dorsal midline
28	Lateralmost point of left hypoglossal foramen
29	Lateralmost point of right hypoglossal foramen

3.2.4 *Assessing covariation between incisor and cranial morphology*

Morphological integration and covariation of biological forms has been extensively studied using geometric morphometrics and partial least squares (PLS) (e.g. Rohlf and Corti, 2000; Bookstein et al., 2003; Bastir et al., 2005; Marugán-Lobón and Buscalioni, 2006; Hautier et al., 2012; Mitteroecker et al., 2012; Klingenberg, 2014). PLS quantifies the maximum amount of covariation between two sets of variables, using a correlation or covariance (for geometric morphometric studies) matrix of traits (Rohlf and Corti, 2000). An advantage PLS has over regression methods for studies of integration and covariation is that the dependency of the variables does not need to be established, beneficial in studies in which the direction of influence is not known. In this study, one set of variables contains the Procrustes coordinates of cranial shape. The second set of variables is the standardized incisor measurements, incisor radius of curvature and second moment of area. Generalized Procrustes analysis removes size from the cranial shape variables. It was therefore decided to account for size differences among taxa by isometrically scaling the incisor variables when measuring covariation between cranium and incisors. Size was defined by cranial length which was used as the independent variable to regress against incisor variables following the method by Revell (2009). The residuals calculated from these regressions were then used in PLS analyses with cranial shape variables to measure covariation.

As in the methods above, any inter-generic analysis must also account for the non-independence of the data. Incorporating phylogeny whilst quantifying morphological integration at the inter-generic level shows how morphological covariation has evolved along a tree (Klingenberg and Marugán-Lobón, 2013). Furthermore, the level of morphological integration can influence phenotypic variation and evolvability (Goswami, 2006; Goswami et al., 2014). Phylogenetic PLS is calculated by incorporating the evolutionary covariance matrix from PGLS to calculate PLS scores (Adams and Felice, 2014). Phylogenetic and non-phylogenetic PLS results will be compared to show if the cranium and incisors always covary in a similar way or if adaptive radiations have occurred. The strength of association between cranial and incisor variables is quantified using the RV coefficient (Klingenberg, 2009). RV coefficient ranges from 0 (variables are independent) to 1 (variables are dependent). Phylogenetic and non-phylogenetic PLS analyses, accompanying surface warps and RV coefficient calculations are implemented in the geomorph package in R (Adams and Otárola-Castillo, 2013).

3.3 Results

3.3.1 Incisor morphology

The relationship between upper incisor length and upper incisor radius of curvature in each genus is displayed in Figure 3.5. Incisor curvature can be changed by radius of curvature, or by the proportion of the circle taken up by the incisor (represented by incisor length). OLS model fitted to origin (Figure 3.5) shows a positive relationship between the two variables ($R^2=0.998$, $P<0.01$). The gradient between the two variables was nearly half (0.52, $P<0.01$). This means that every upper incisor measured in this sample was taking up about a semi-circle of differently sized circles i.e. the incisors were the same shape but different sizes.

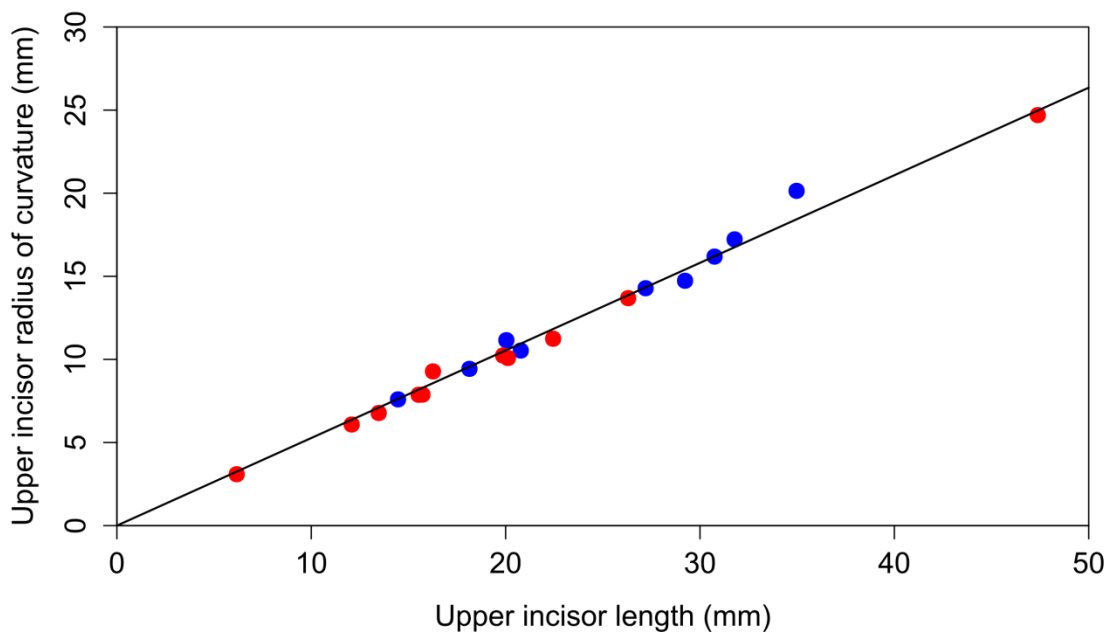


Figure 3.5. OLS model fitted through origin showing the relationship between upper incisor length and upper incisor radius of curvature. Chisel-tooth digging genera are in blue. Non-tooth digging genera are in red.

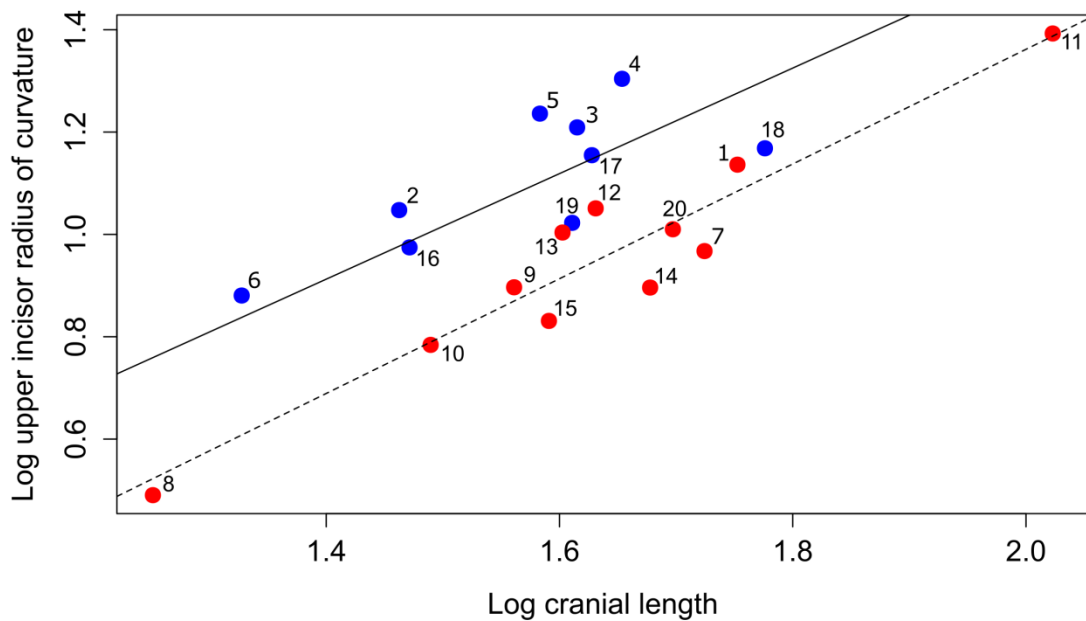


Figure 3.6. Phylogenetic ANCOVA representing the relationship between cranial length, upper incisor radius of curvature and digging method. Chisel-tooth digging genera are in blue. Non-tooth digging genera are in red. Genus numbers are given in Table 3.1. Solid line represents PGLS of chisel-tooth digging and dashed line represents PGLS of non-tooth digging.

Figure 3.6 shows the relationship between cranial length and upper incisor radius of curvature. Incisor length was not measured due to its strong relationship with radius of curvature (Figure 3.5). Interaction between log cranial length (covariate) and digging method (categorical-variable) was not significant ($P > 0.05$) i.e. similar slopes between groups. Generalized phylogenetic ANCOVA revealed that chisel-tooth digging rodents have a significantly larger upper incisor radius of curvature ($P < 0.01$) than other rodents. Phylogenetic signal in this data, measured simultaneously with PGLS model using λ , was 0.60.

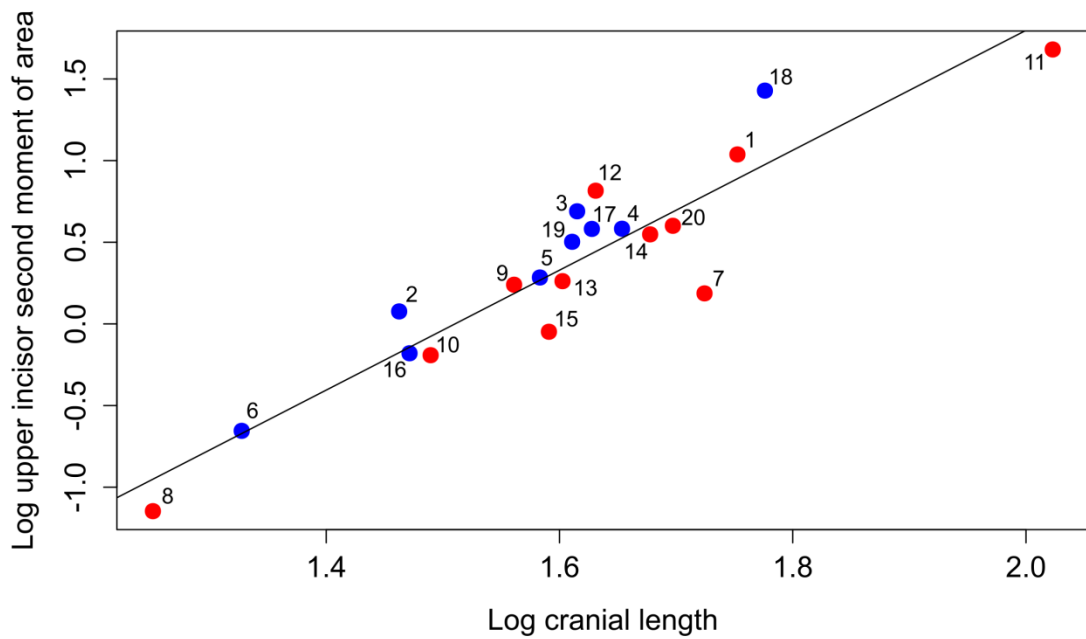


Figure 3.7. PGLS representing the relationship between cranial length and upper incisor second moment of area. Chisel-tooth digging genera are in blue. Non-tooth digging genera are in red. Genus numbers are given in Table 3.1. Line represents PGLS through all data.

Figure 3.7 shows the relationship between cranial length and second moment of area of upper incisors. Interaction between log cranial length (covariate) and digging method (categorical-variable) was significant ($P < 0.01$). This meant an ANCOVA could not be applied to the data as the slopes were not similar between groups (a prerequisite for ANCOVA models). PGLS was applied to the data instead and the residuals were examined to show the relationship between the data (Figure 3.8). The residuals of the PGLS of cranial length and upper incisor SMA show that not only do the chisel-tooth digging rodents have a relatively larger upper incisor SMA, but so do the other subterranean rodents in the data (see Table 3.1 for groupings). Phylogenetic signal in this PGLS analysis was 0.51.

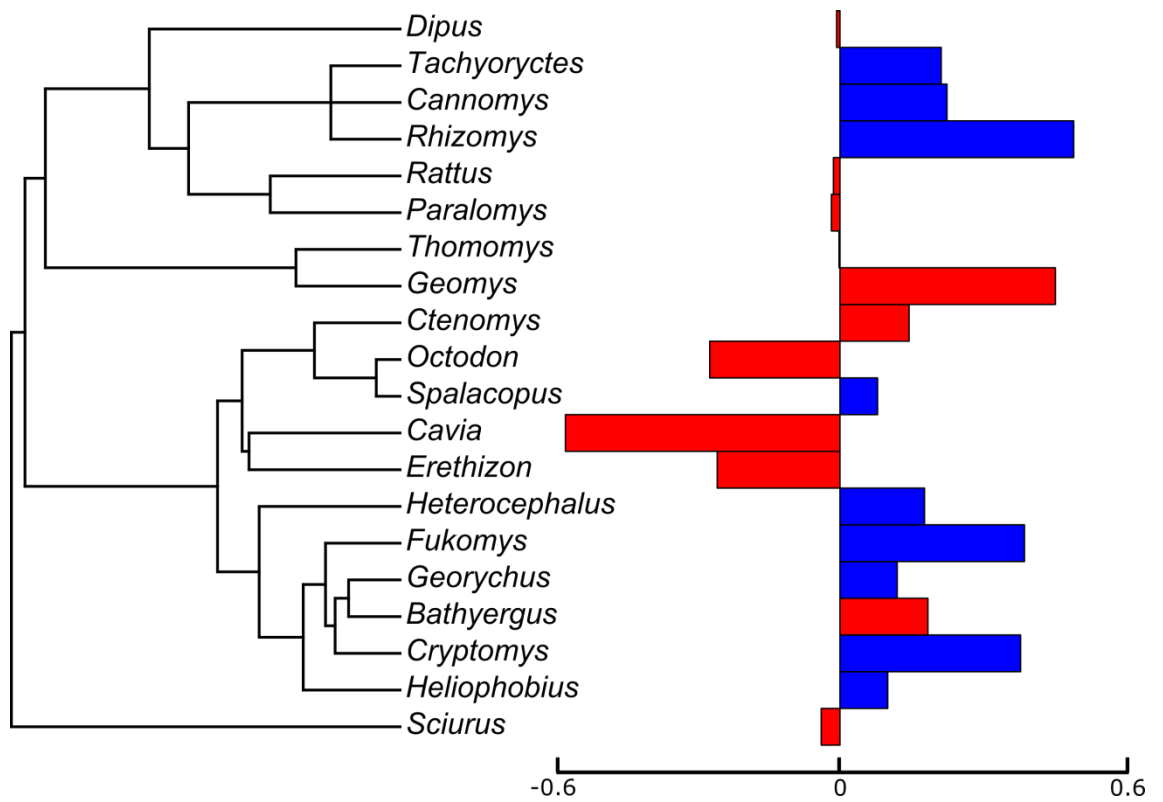


Figure 3.8 Phylogeny of data with accompanying SMA residual values from PGLS of cranial length and upper incisor SMA. Chisel-tooth digging genera residuals are in blue. Non-tooth digging genera residuals are in red.

3.3.2 Cranial morphology

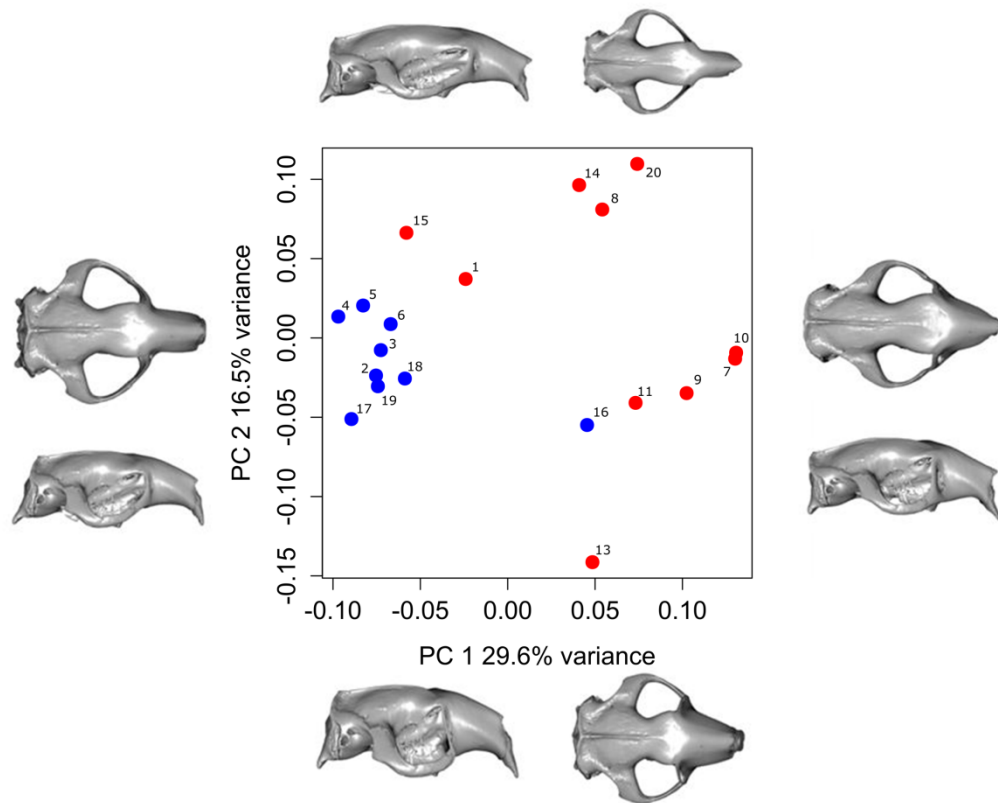


Figure 3.9 Principal components analysis with surface warps representing shape variation across PC1 and PC2 axes. Chisel-tooth digging genera are in blue. Non-tooth digging genera are in red. Genus numbers are given in Table 3.1.

Figure 3.9 and Figure 3.10 represent some of the variation in cranial shape (Figure 3.9) and non-phylogenetic cranial shape (Figure 3.10). Both types of principal component methods represent a very similar pattern of shape variation (although PPC1 represents a larger variance relative to PC1). However, phylogenetic signal in the data is significant ($\kappa_{\text{mult}}=0.49$, $P<0.01$). As the pattern of shape variation is similar in both phylogenetic PCA and PCA, the ordinary PCA results will be referred to (Figure 3.9). From Figure 3.9 it can be seen that most of the chisel-tooth digging rodents group in the same part of the subspace (towards negative end of PC1). The only chisel-tooth digging rodent that departs from the group is *Spalacopus* (which lies positively on PC1 with respect to the rest of the chisel-tooth digging group). The non-tooth digging rodents do not group tightly and are spread over different parts of the subspace. A Procrustes ANOVA indicates that chisel-tooth and non-tooth digging groups can be distinguished in morphospace ($F=3.57$, $P<0.01$). However, a Procrustes ANOVA incorporating the

phylogeny leads to insignificance between groups ($F= 2.25, P>0.05$), unsurprising due to the significant amount of phylogenetic signal in the data. Shape variation across the two PC axes is represented by the warps on the extremes of the PC axes. Positive PC1 scores are associated with a rounder, narrower, more gracile skull shape and a wider rostrum. More negative PC1 scores are associated with a flatter, wider skull shape and a thinner rostrum.

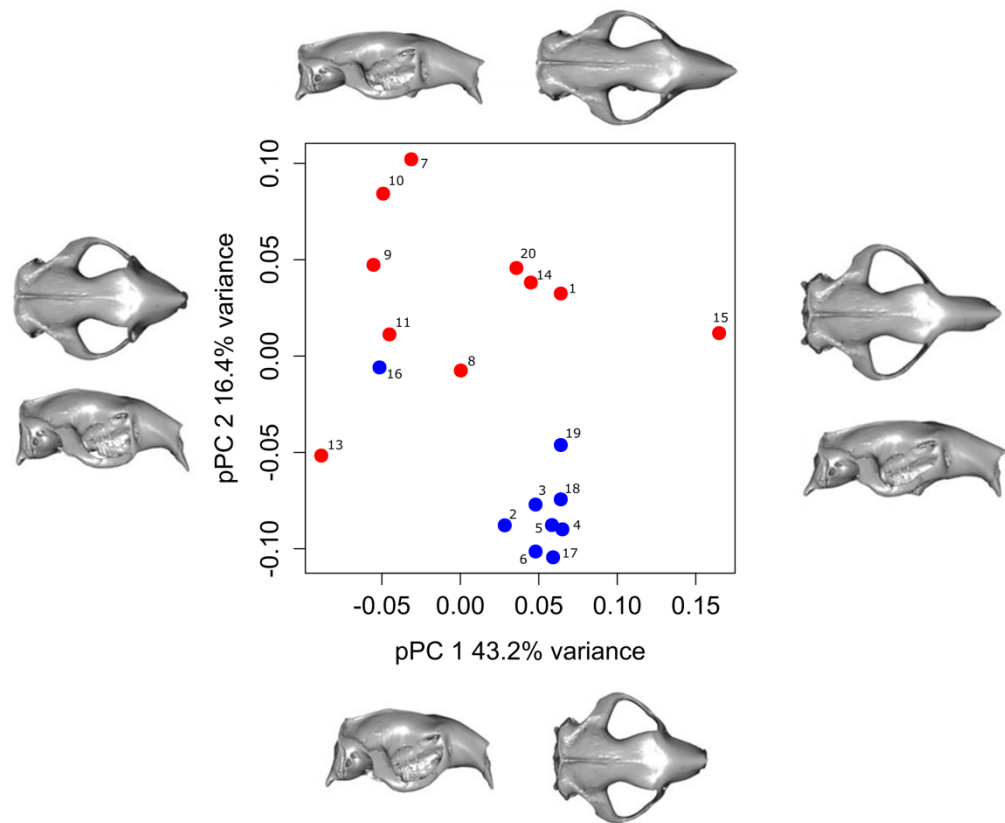


Figure 3.10 Phylogenetic principal components analysis with surface warps representing non-phylogenetic shape variation across PC1 and PC2 axes. Chisel-tooth digging genera are in blue. Non-tooth digging genera are in red. Genus numbers are given in Table 3.1.

3.3.3 Covariation of incisor and cranial morphology

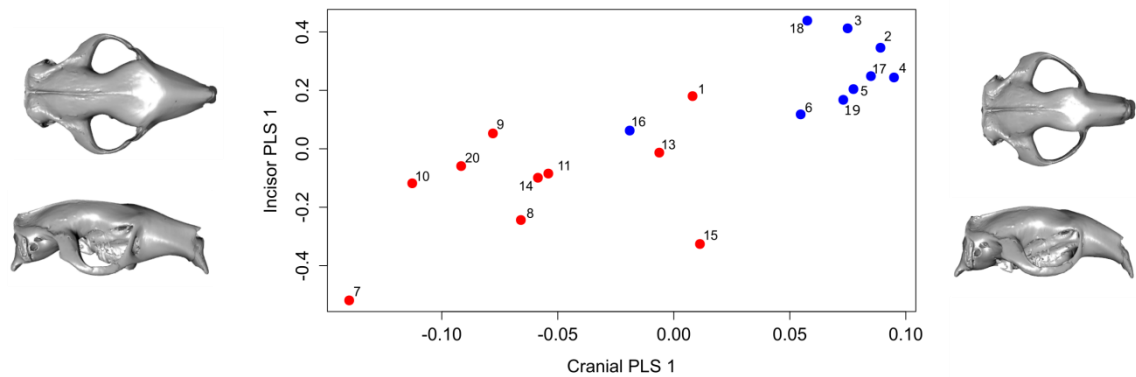


Figure 3.11 Partial least squares analysis with cranial surface warps representing cranial shape and incisor covariation across PLS 1 (accounts for 93.7% squared covariance). Chisel-tooth digging genera are in blue. Non-tooth digging genera are in red. Genus numbers are given in Table 3.1.

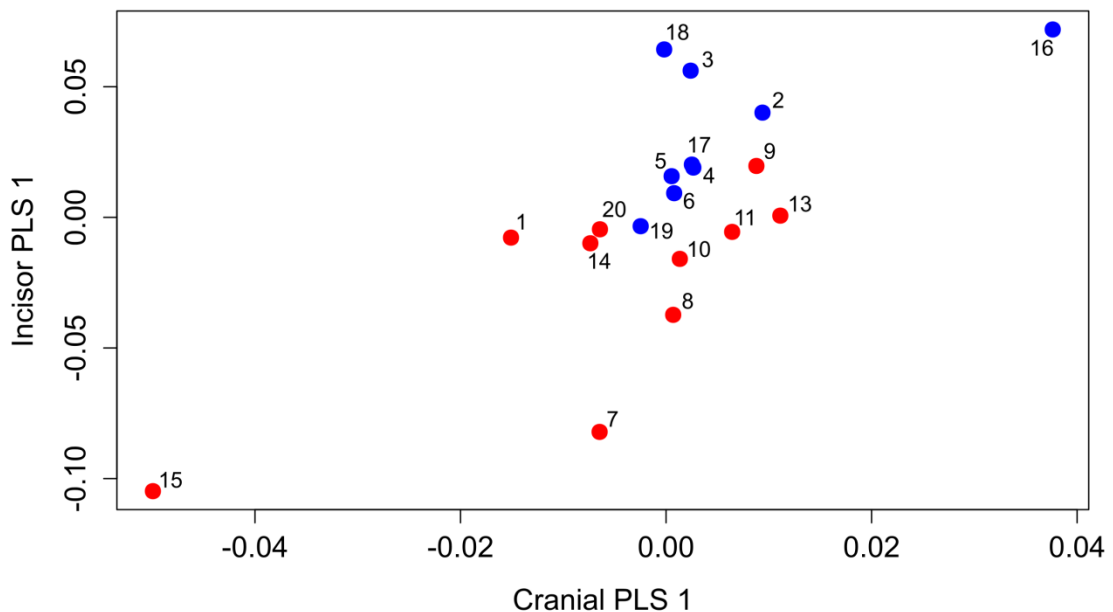


Figure 3.12 Phylogenetic partial least squares analysis representing cranial shape and incisor covariation across PLS 1). Chisel-tooth digging genera are in blue. Non-tooth digging genera are in red. Genus numbers are given in Table 3.1.

The results of the non-phylogenetic PLS show that there is strong covariation between cranial shape variables and incisor variables (PLS correlation: 0.8, $P < 0.05$). The strength of association between the cranial shape and incisor variables was moderately high, at 0.45 (measured using the RV coefficient, $P < 0.01$). Negative PLS 1 scores are associated with non-tooth digging genera, whereas positive PLS 1 scores are associated

with chisel-tooth digging genera. The surface warps associated with the PLS plot (Figure 3.11) show the cranial shape covariation with the incisor variables at the extreme ends of PLS 1 axis. Negative PLS 1 scores are associated with elongated, narrow crania and wide rostra. Positive PLS 1 scores are associated with shorter, wider crania and narrow rostra. Phylogenetic PLS analysis (Figure 3.12) was non-significant and is shown only to compare with the results of the non-phylogenetic PLS.

3.4 Discussion

3.4.1 *Incisor morphology*

This study has shown that there is a clear correlation between size, radius of curvature of the upper incisor and digging method in rodents (Figure 3.6). However, as λ was less than one (0.60), it can be said that although the evolution of incisor radius of curvature was closer to Brownian motion model than a star phylogeny, other ecological variables are also influencing incisor radius of curvature. Despite the seemingly complicated relationship between phylogeny and ecology on the evolution of incisor radius of curvature, it is clear that chisel-tooth digging rodents have acquired a larger radius of curvature of incisor for their size compared to rodents that do not require their incisors to dig. Landry (1957a) assessed upper incisor radius of curvature in a phylogenetically diverse group of rodents and concluded that a large upper incisor radius of curvature (and arc length) is required to improve upper incisor procumbency. McIntosh and Cox (2016) and Chapter 2 of this thesis, showed that a family of chisel-tooth digging rodents have a craniomandibular morphology that facilitates a wide gape. A wide gape coupled with more procumbent incisors would allow the incisor tip to be perpendicular to the soil at the rodent's widest gape. This would allow the incisor tip to be in contact with the soil throughout a complete gape motion and hence remove a larger amount of soil relative to a rodent with reduced procumbent incisors.

Increasing the radius of curvature of the upper incisor requires the root of the incisor to be further displaced into the pterygoid region of the skull. The cranium is a complex structure which plays host to the brain and other sensitive sensory structures. As the cranium is highly integrated (Cheverud, 1982; Hallgrímsson et al., 2007; Klingenberg and Marugán-Lobón, 2013), any cranial morphological change could have an effect on

these systems (see below). However, as mentioned earlier, incisor procumbency is governed by changes in incisor length and radius of curvature. Increasing incisor procumbency could also be achieved by moving the incisor root forward; keeping the radius of curvature constant, and decreasing the arc length of the incisor [see Landry (1957a) for further discussion]. This would mean the root of the incisor would not be required to expand further back into the skull. Another strategy would be to increase the length of the rostrum to incorporate the larger incisor, but this would result in a loss of mechanical efficiency of the major masticatory muscles (see McIntosh and Cox, 2016 and Chapter 2 for discussion of this situation). Chisel-tooth diggers having longer incisors originating further back into the skull is probably an adaptation to using their incisors to dig in hard soils. An increased incisor length within the alveolus gives a larger surface area in contact with the skull that can then dissipate the larger forces generated at the tip during chisel-tooth digging (Landry, 1957a; Becerra et al., 2012). Indeed, due to the positive relationship between incisor length and radius of curvature of all the rodents in this sample (Figure 3.5), this could be true for the whole order.

Interestingly, the second moment of area, an indicator of bending strength, did not correlate in the same way as incisor radius of curvature. Firstly, studying the residuals of the analysis (Figure 3.8), it is clear that this variable does not show differences between chisel-tooth digging rodents and non-tooth digging rodents. Instead, it seems that the difference lies between the subterranean and terrestrial rodents. The subterranean rodents have a larger incisor second moment of area for their size compared with the terrestrial rodents in my sample. For example, one of the largest (for its size) incisor second moment of areas was measured in *Geomys*, a subterranean, scratch digging rodent. Subterranean rodent diets are mostly made up of geophytes and other subterranean plants, which tend to be hard and fibrous materials (see Busch et al., 2000). Therefore, it appears that subterranean rodents have adapted to resist the increased pressure at the incisor tip due to their hard food diet by making the incisor more resistant to bending. Incisor morphology has been shown to strongly correlate with diet in caviomorph rodents (Croft et al., 2011). Becerra et al. (2012) found that second moment of area correlated with incisor root length (equivalent to incisor radius of curvature) in caviomorphs. This observation was not directly studied in this chapter. However, incisor radius of curvature significantly differed between chisel-tooth digging and non-tooth digging rodents, whereas incisor second moment of area did not, so correlation between these two variables would have probably been weak. Caviomorpha

includes a wide variety of subterranean rodents including the claw and chisel-tooth digging genus *Ctenomys* (Lessa et al., 2008; Becerra et al., 2013). However, Becerra et al. (2012) did not include any genera that exclusively use their incisors to dig, which are labelled as chisel-tooth diggers in my own sample (*Ctenomys* is labelled as a scratch digger in my sample). I therefore propose that subterranean rodent incisors are resistant to bending due to their hard food diets, but chisel-tooth digging rodents also have an adaptation to deal with the additional forces exhibited during incisor digging in hard soils by increasing their incisor length to dissipate these forces.

3.4.2 Cranial morphology

It is clear from examining both PCA and PPCA plots (Figure 3.9 and Figure 3.10, respectively) that cranial shape has significantly converged in chisel-tooth diggers (with the exception of *Spalacopus*). Although *Spalacopus* is a chisel-tooth digging rodent with large incisors equivalent to other chisel-tooth diggers (Figure 3.6), it does not have a similar cranial shape. This could be due to the arrangement of the incisor in the cranium of *Spalacopus*. The incisors of *Spalacopus* are located in alveolar sheaths that are lateral to the cheek teeth and thus avoid the internal cranial space (Lessa, 1990). Other chisel-tooth diggers do not have this lateralization of the alveolar sheath and incorporate the incisor alveolus into internal cranial spaces, potentially constraining cranial shape in other chisel-tooth digging rodents. However, only one specimen of *Spalacopus* was used in this study, so more need to be included in order to address this issue thoroughly.

This convergence of cranial shape with digging methods has already been shown in rodents (Samuels and Van Valkenburgh, 2009) and was also found in this study (Procrustes ANOVA, $P < 0.01$). However, Samuels and Van Valkenburgh (2009) did not take into account phylogenetic similarity between species. In my own data, the phylogenetic signal of cranial shape was significant ($\kappa = 0.49$, $P < 0.01$). This was a surprising result given the amount of cranial convergence of chisel-tooth digging crania shown in the morphospace (Figure 3.9 and Figure 3.10) and the fact chisel-tooth digging has arisen independently in the sample used (in spalacids and bathyergids, see Figure 3.8). However, when phylogeny of the data is accounted for, chisel-tooth digging crania are not dissimilar to non-tooth digging crania (phylogenetically informed

Procrustes ANOVA, $P > 0.05$), a result showing how important it is to include phylogeny into inter-generic analyses.

Inferring from the phylogenetically and non-phylogenetically informed results, the significant differences of cranial shape found using the non-phylogenetic methods are mostly down to chisel-tooth digging relationships amongst phylogenetically similar genera. From the phylogeny, it can be seen that even though chisel-tooth digging has occurred independently, the chisel-tooth digging genera cluster in two separate groups (Figure 3.8). *Spalacopus*, the only chisel-tooth digging genus that isn't part of these two phylogenetic groups, does not have a similar cranial morphology to the other chisel-tooth diggers (Figure 3.9 and Figure 3.10), which is may be why the phylogenetic correction on the data does not detect a significant difference between chisel-tooth and non-tooth digging crania. However, cranial morphology probably adapted to chisel-tooth digging independently in earlier lineages of rodent evolutionary history. If chisel-tooth digging genera were spread out evenly throughout the phylogeny then perhaps a significant difference may have been found, a potential lesson in data sampling. A second lesson that needs to be highlighted from this study is the size of the sample. Phylogenetic comparative methods reduce the weighting of genera/species that are more closely related relative to genera/species that are phylogenetically more distant. My sample only consisted of nine chisel-tooth digging genera and combined with potential downsampling due to phylogenetic similarity, may not have been large enough to highlight any biological signal that potentially was occurring.

3.4.3 Covariation of incisor and cranial morphology

Cranial and incisor morphology covary with moderate strength in rodents when phylogenetic affinities are not included in the analysis (Figure 3.11). Comparing the PCA and PPCA of cranial shape (Figure 3.9 and Figure 3.10, respectively) with the non-phylogenetic PLS (Figure 3.11), it can be seen that chisel-tooth digging rodents group tightly (except *Spalacopus*). The cranial PCA and PPCA show the variation in cranial shape within the sample whereas PLS shows the covariation between incisor and cranial shape within the sample. The fact that chisel-tooth digging rodents group tightly in both analyses implies that the covariation and integration of incisor and cranial morphology is a key factor in chisel-tooth digging cranial shape variation and thus incisor morphology could potentially be constraining cranial shape in chisel-tooth digging rodents.

Interestingly, when phylogeny was taken into account, any covariation between incisor and cranial morphology becomes non-significant (Figure 3.12); a similar outcome when phylogenetic comparative methods were incorporated into analysing variation of the crania (see above). Again, this could be down to similar sampling errors as described above. Indeed other studies that compare analyses with and without phylogenetic comparative methods have seen similar outcomes to this study i.e. significance without including phylogeny and nonsignificance including phylogeny (e.g. Cardini and Elton, 2008; Perez et al., 2011; Baab et al., 2014). Having said this, comparing the two methods has delivered some interesting insights into why taking account of phylogeny makes these results non-significant. Applying phylogenetic comparative models to analyses that measure covariation in a sample effectively tries to model how the variables covary throughout the selected phylogeny, if Brownian motion is assumed (Klingenberg and Marugán-Lobón, 2013; Adams and Felice, 2014). However, chisel-tooth digging is probably an adaptation to hard soils, and therefore using a random walk method (Brownian motion) is probably oversimplifying what is occurring in the evolutionary covariation of incisor and cranial morphology in this sample (for further discussion see chapter 5).

3.4.4 Conclusion

This study has shown that incisor radius of curvature is significantly larger in chisel-tooth digging rodents and is probably an adaptation to dissipate extra forces across the cranium, incurred by the tip of the incisor digging in hard soils. Second moment of area of incisors was also found to be larger in subterranean rodents, and is probably an adaptation to the hard food diets of fossorial rodents. Also, when phylogeny is not accounted for, incisor and cranial morphology are part of an integrated system that potentially affects diversity of form in rodents. However, it was also highlighted how important it is to test for phylogenetic influences in data that consists of different species and that much more work needs to be done to model evolutionary processes in multivariate data accurately.

Chapter 4: Digging biomechanics of the cranial form in African mole-rats (Family: Bathyergidae)

4.1 Introduction

The cranial morphology of subterranean rodents is strongly constrained compared to their non-fossorial counterparts and is clearly linked to a subterranean lifestyle (Gomes Rodrigues et al., *in press*). Furthermore, studies have shown that there are distinctions of cranial morphology between subterranean rodents of differing digging methods (Samuels and Van Valkenburgh, 2009, McIntosh and Cox, 2016; Chapter 2). There are two main modes of digging in subterranean rodents: chisel-tooth digging, which involves the use of incisors to remove soils; and scratch digging, which involves the use of the forelimbs and claws. Chisel-tooth digging is thought to have evolved in order to exploit harder soils as incisors are covered in hard enamel and fixed within the cranium and mandible. This is in contrast to the claws, which are made up of softer keratin and have more flexibility (Lessa and Thaeler, 1989) and so would deal less well in the removal of harder soils during burrow construction. Morphological differences in the cranium of chisel-tooth digging rodents include: more procumbent incisors, wider crania, enlarged zygomatic arches and larger temporal fossae (Landry, 1957a, Agrawal, 1967, Lessa and Stein, 1992, Samuels and Van Valkenburgh, 2009). Chisel-tooth digging mandibles are associated with higher coronoid processes, reduced condyle heights and deep incisor roots (Verzi and Olivares, 2006; McIntosh and Cox, 2016; Gomes Rodrigues et al., *in press*; Chapter 2).

As chisel-tooth digging has arisen independently in all six subterranean rodent families (Stein, 2000), this morphological constraint is probably related to function. For example, bite force, a measure strongly associated with an animal's ecology (e.g. Smith, 1970; Christiansen and Wroe, 2007) has been shown to be larger (relative to body size) in chisel-tooth digging rodents than other mammals (Van Daele et al., 2009; Becerra et al., 2014). An increase in bite force in chisel-tooth diggers is expected due to the extra force required to break through hard soils at the incisor.

Interestingly, cranial shape constraints are found in types of carnivores that also require a high bite force (Wroe et al., 2005; Wroe and Milne, 2007; Figueirido et al., 2013). For

example, Figueirido et al (2013) showed that bamboo-feeding and bone-cracking carnivores, two phylogenetically distant groups, converge in cranial morphospace. Morphological traits associated with this convergence includes enlarged areas for masticatory muscle attachments (e.g. wide zygomatic arches, deep crania, enlarged sagittal crests), characteristics associated with production of high bite forces and dissipation of stress in carnivores (Ewer, 1973; Biknevicius and Van Valkenburgh, 1996; Figueirido et al., 2013). Similar characteristics have been found in chisel-tooth digging rodents (relative to other rodents) (Samuels and Van Valkenburgh, 2009; McIntosh and Cox, 2016; Gomes Rodrigues et al., *in press*; Chapter 2). Also, the temporalis has also been shown to be a key muscle in carnivoran mastication, as animals that require both a large bite force and a wide gape, require a dominant temporalis (Turnbull, 1970; Emerson and Radinsky, 1980). McIntosh and Cox (2016) and Chapter 2 also found that the mechanical advantage of temporalis is significantly larger in chisel-tooth digging rodents, offering strong evidence that the temporalis is a driving force in constraining skull shape in these phylogenetically distant groups.

As in the above examples, comparative studies traditionally have taken place in a univariate context, looking at single traits in relation to an organism's performance (e.g. Vinyard et al., 2003; Morgan and Verzi, 2011; Hampton and Moon, 2013). Although these types of analyses are helpful in showing how a trait has potentially evolved to perform a task that increases the chances of survival of a species in a particular environment, they lack any information on how this one trait perturbs an overall highly integrated system. Integration and modularity amongst morphological traits is a concept that has been given much attention recently due to the advancement of geometric morphometrics (for review of integration and modularity in morphological traits, see Klingenberg, 2008). As an organism's overall shape is inherently integrated and multivariate, it is important to also assess the performance of an organism's shape in an all-encompassing method. Studies of vertebrate morphology have turned to finite element analysis (FEA) to address this issue of complexity. FEA breaks down a biological structure's infinite complexity by dividing it into a large number of discrete, simple elements, which are connected via nodes. These elements are then assigned material properties that will accurately respond via stress, strain and deformations under an applied loading and constraining condition (for review of FEA use in biology see Richmond et al., 2005; Rayfield, 2007). This method has been used to investigate masticatory biomechanics in a diverse range of organisms, including bats (Dumont et

al., 2005), dinosaurs (e.g. Button et al., 2014), ostriches (e.g. Rayfield, 2011), primates (e.g. Fitton et al., 2012), lizards (Curtis et al., 2013) and rodents (Cox et al., 2011, 2012, 2013).

In Chapter 2 of this thesis (McIntosh and Cox, 2016), chisel-tooth digging rodents were shown to have multiple morphological traits in the cranium and mandible that are linked to increased bite force and gape capabilities. In this study, FEA is used to elucidate the overall performance of a chisel-tooth digging rodent (*Fukomys mechowii*) relative to a scratch digging rodent (*Bathyergus suillus*). These two subterranean rodents are from the same family (Bathyergidae) and are known to have very similar diets of roots and tubers (Bennett and Faulkes, 2000), making them a good choice for a comparative study of digging performance of the cranium.

It is hypothesised that the constrained shape of the cranium seen in chisel-tooth digging rodents has an improved performance for digging at the incisors compared to scratch digging rodents. Using FEA, digging will be statically simulated by modelling the cranium at different angles of gape and assessing the biomechanical response to each loading condition. Using a novel technique of integrating geometric morphometrics (GMM) with FEA (O'Higgins et al., 2011; O'Higgins et al., 2012), it will also be possible to quantify the differences in overall deformations (of size and shape) in each species to specific loading scenarios. I predict that, compared to the scratch digging species, the chisel-tooth digging cranium will: (1) exhibit lower stress; (2) be more efficient at converting muscle forces to bite forces; (3) experience less deformation; and (4) have an improved performance (measured using metrics from hypotheses 1-3) at higher gapes, relative to the scratch digging cranium.

4.2 Materials and Methods

4.2.1 Sample and model construction

Finite element (FE) models were created from microCT scans of two adult African mole-rat skulls: the chisel-tooth digging *Fukomys mechowii* (MNHN [Muséum National d'Histoire Naturelle] ZM-MO-1911-664) and the scratch digging *Bathorygus suillus* (University of Pretoria 631). The specimens were scanned on an X-Tek Metris microCT scanner at the University of Hull (Medical and Biological Engineering Research Group). The scans had isometric voxels of 0.0417 mm (*Fukomys*) and 0.0532mm (*Bathorygus*). Using Avizo 8.0 (FEI, Hillsboro, OR) the scans were resampled to double their original voxel sizes to ensure a reasonable processing time during FE model creation and solving stages. 3D volume reconstructions of the skulls were created by a combination of automated and manual thresholding of materials that depicted the most accurate representation of skull geometry and the removal of unwanted material such as scanning artifacts and nasal turbinates, as they were not considered to be load-bearing. Bone, teeth, and incisor pulp cavity were segmented into separate materials so they could be assigned different elastic properties. All bone was modelled as cortical bone, as recent work on macaques indicates that there is little difference in performance between solid models and models incorporating trabecular bone (Fitton et al., 2015). Enamel, dentine and periodontal ligament were not modelled separately as the scans were not of high enough quality to accurately segment these materials. Also, studies have shown that varying these material properties have little effect on the overall deformation of the skull (Cox et al., 2011; Wood et al., 2011). The reconstructions were then converted to an 8-noded cubic mesh directly from voxels using VOX-FE, in-house custom-built FEA software (Liu et al., 2012). The *Fukomys* and *Bathorygus* models comprised 9481075 and 6796670 elements, respectively.

4.2.2 Material properties

Based on previous nano-indentation work on rodents (Cox et al., 2011, 2012) and other mammals (Kupczik et al., 2007), bone and teeth were assigned Young's moduli of 17 and 30 GPa, respectively. Pulp was assigned a Young's modulus of 2 MPa (Williams and Edmundson, 1984). All materials were modelled as homogeneous and isotropic with a Poisson's ratio of 0.3 being assigned to bone and teeth and a ratio of 0.45 to pulp (Williams and Edmundson, 1984). No data is available for material properties of bathyergids. However, it was considered appropriate to use these properties as this

study is primarily concerned with the relative digging performance between two species, and therefore is less concerned with absolute output values. Also, variation of material properties seem to have less of an impact on global patterns of stress and strain than does variation in geometry (Ross et al., 2005, Strait et al., 2005, Wroe et al., 2007, Walmsley et al., 2013).

4.2.3 *Constraints*

As the models were representing static simulations, they had to be prevented from motion when muscle loads were applied. In order to model chisel-tooth digging, the models were constrained at the point of contact of the incisor tip with the soil in the direction of the bite. Due to the close apposition of the incisors in rodents, the nodes assigned as bite point constraints were spread equally between both incisors' medial edges. An equal number of nodes were constrained at each temporo-mandibular joint (TMJ) in all three axis. The TMJ in rodents is situated on the ventral side of the zygomatic process of the squamosal and represents the point on the skull where reaction forces occur between the mandibular condyles and the skull when the model is loaded. In both models, 40 nodes were assigned to each area of constraint.

4.2.4 *Modelling muscle loads and changes in gape*

Loads were applied bilaterally for the following muscles, as rodents generally demonstrate a bilateral masticatory pattern at the incisors (Offermans and de Vree, 1990; Satoh, 1998): temporalis; superficial masseter; deep masseter; zygomaticomandibularis (ZM: anterior, infraorbital and posterior parts); lateral pterygoid; and medial pterygoid. The masseter muscle was divided into 3 parts (superficial; deep and ZM) following (Turnbull, 1970; Cox and Jeffery, 2011). Muscle attachment sites were assigned based on dissections by Van Daele et al. (2009) and virtual muscle reconstructions by Cox and Faulkes (2014). The Bathyergidae family members have a somewhat rare masticatory musculature arrangement in comparison to the rest of Rodentia. The majority of rodents are usually classified into three (non-phylogenetic) groups, based on their masticatory musculature: sciurormorph (squirrel-like); myomorph (mouse-like) and hystricomorph (porcupine-like) (Brandt, 1855; Wood, 1965). However, the Bathyergidae have a musculature arrangement which does not fit into any of these classifications. Unlike in the three traditional rodent groups, the masseter in bathyergids does not have a rostral origin. Instead, the bathyergids are thought to resemble the ancestral condition of rodents, known as protrogomorphy (Wood, 1965), where the masseter originates posterior to the infraorbital foramen. This

condition has probably been secondarily acquired in the bathyergids who likely evolved from a hystricomorph ancestor (Landry, 1957b; Maier and Schrenk, 1987; Cox and Faulkes, 2014). This is of particular interest in this study due to the slight differences of the origin of the infraorbital part of the zygomaticomandibularis (IOZM) within the two specimens used in this study. The chisel-tooth digging *Fukomys* has a larger, more hystricomorphous infraorbital foramen when compared to the scratch digging *Bathyergus*, where the foramen is significantly reduced. As such, in *Fukomys*, a small proportion of the IOZM passes through the infraorbital foramen. This is not the case in *Bathyergus*, where the IOZM attaches posterior to the infraorbital foramen. The anterior and posterior ZM originate on the jugo-squamosal suture on the medial surface of the zygomatic arch and the glenoid fossa, respectively. The temporalis, the largest masticatory muscle in bathyergids (Morlok, 1983; Van Daele et al., 2009; Cox and Faulkes 2014), originates across the entirety of the parietal bone and some of the frontal and squamosal. The superficial masseter begins on the anteroventral surface of the zygomatic arch, where the arch meets the skull and the deep masseter originates along the length of the ventral border of the zygomatic arch. Finally, the medial and lateral pterygoids originate within the pterygoid fossa and on the lateral side of the pterygoid plate, respectively.

The direction of pull of each muscle (i.e. muscle directional vector) was determined by placing a reconstruction of the specimen's mandible in a position of incisor occlusion (0°) using Avizo. The *Bathyergus* and *Fukomys* mandibles were automatically segmented in Avizo from microCT scans (0.0481 and 0.0350 mm isometric voxel sizes, respectively). Landmarks representing the insertion of each muscle were placed onto the mandible and loaded into VOX-FE in order to accurately represent the direction of pull. The temporalis insertion was modelled as inserting at the tip of the coronoid process. As the superficial masseter insertion fans out over the entirety of the ventral border of the mandible, a B-spline was placed on the ventral border and a landmark was placed on the mid-point of the B-spline to represent the directional vector of the superficial masseter. The deep masseter also fans out over the mandible and its insertion is directly dorsal to the superficial masseter, so was modelled using the same method as the superficial masseter. IOZM inserts at the base of the coronoid process lateral to the distal molar. The anterior ZM inserts on the ventral part of the coronoid process and the posterior ZM on the mandibular ramus. The medial pterygoid inserts on the medial part of the mandibular angle. Lastly, the lateral pterygoid inserts on the medial part of the

mandibular condyle. In VOX-FE, the origin of the muscle directional vector is assigned by calculating the centroid of the selected area of nodes defining the muscle origin. Each selected muscle node then runs parallel to the centroid vector. To calculate muscle magnitudes, PCSA values for *Fukomys mechowii* were taken from Van Daele et al, 2009 and then multiplied by an intrinsic muscle stress value of 0.3N mm^{-2} (van Spronsen et al., 1989; Weijjs and Hillen, 1985). No PCSA data was available for *Bathyergus*, so the *Fukomys* muscle forces, scaled to model area, were used instead (the limitations of this are discussed below). To replicate different angles of gape, the landmarks representing each muscle insertion were rotated about an axis running between the left and right TMJ (see McIntosh and Cox, 2016 and Chapter 2 for further details of method) and the muscle directional vectors changed accordingly to simulate the effects of gape on the performance of the models. Condyle translation has been shown to occur in the terrestrial rodent, *Pedetes capensis* during different stages of mastication (Offermans and de Vree, 1990). However, condyle movement during digging at the incisors has been shown to be stable in *Ctenomys*, a South American subterranean rodent (Verzi and Olivares, 2006). For this reason, condyle translation has not been included in the model, and the mandible has been simply rotated around an axis (TMJ).

4.2.5 Comparison of performance indicators between finite element models

In order to establish which model performed better under a chisel-tooth digging simulation, performance indicators must be comparable. In this study, von Mises (VM) stress was used as a key indicator of performance. VM stress is an accurate predictor of failure in ductile materials such as bone, with VM stresses that exceed the strength of the material, leading to permanent plastic deformation. Structures which exhibit overall lower VM stresses in a comparative context are therefore less likely to fail under a given loading. If two models of the same shape but of different sizes have equal loads, the larger model will exhibit less stress (as stress equals force applied over the area of the model). To consider the effect of difference in shape on stress between two models, the effect of size must be controlled for, which can be achieved by keeping the ratio of force to surface area constant between the two models (Dumont et al., 2009). As PCSA values were not available for *Bathyergus*, surface area for both models were calculated in Avizo, and the ratio of the two surface areas was used to scale forces applied to the *Bathyergus*, thus making the resultant VM stress values for each model comparable. In order to quantify VM stress across the skull, the VM stress of each element from each model was extracted and the median VM stress for both models was calculated. Using

the median, rather than the mean, to compare VM stress prevents outlying values that can arise from modelling artifacts from artificially increasing the average and gives a good indicator of overall spread of VM stress across the cranium.

Although scaling the FE models to force:area ratio allows an assessment of the significance of model shape, it is also of interest to show how the models perform when scaled to an ecologically relevant bite force. This is possible as deformations increase linearly and proportionately with applied loading conditions (O'Higgins and Milne, 2013; Fitton et al., 2015). *Fukomys* has been shown to have an *in vivo* bite force of 40N (Van Daele et al., 2009) and as such both models' were scaled using absolute bite force outputs (Table 4.1) in order to produce a bite force of 40N at all gape angles. As one loaded model condition created a negative absolute bite force output (*Bathyergus* model at 90°; Table 4.1), it could not be scaled and was discarded from this part of the study (see discussion for further explanation).

The mechanical efficiency of incisor biting in each model was also calculated to assess the performance of both models. Mechanical efficiency is the ratio of predicted bite force to total muscle input force and provides a single value with which to assess the efficiency of the masticatory system in transforming muscle to bite force (Dumont et al., 2011; Cox et al., 2012). Mechanical efficiency is dimensionless and is therefore independent of size, which is why it is a useful variable with which to compare models.

4.2.6 Geometric morphometric analysis of cranial deformations

When ductile materials have forces applied to them, they will elastically deform, meaning they will return to their original form when forces are removed. However, as explained above, if an object experiences stress that exceeds the object's strength, it will plastically deform, meaning that the object will not return to its original form. The further a loaded object is from its original form, the more likely it is to plastically deform, and so an object's global deformation is of particular interest to biologists trying to assess the performance of morphology during different loading conditions.

Visually, it can be rather difficult to assess variation between FE models as deformations between unloaded and loaded models are small. Recently, geometric morphometrics (GMM), a landmark based form analysis method (for review, see O'Higgins, 2000) has been applied to finite element analyses in order to quantify global

deformations between loaded and unloaded models (O'Higgins et al., 2011, 2012; Cox et al., 2011; Gröning et al., 2011; O'Higgins and Milne, 2013; Fitton et al., 2015). It should also be noted that GMM analyses cannot predict material failures (which is done by strain analysis), as they can only quantify the differences of size and shape between the deformations, and not the processes that achieve these deformations (O'Higgins and Milne, 2013). Therefore, the term deformation used throughout refers to differences in size and shape of models and not rigid body motion (as rigid body displacement is removed during GMM analysis). A set of landmarks (3-D coordinate data) were placed onto selected nodes of each unloaded model (the same landmark set used in Chapter 3; see Figure 3.4 and Table 3.2). The landmarks were then extracted from displaced nodes from the loaded models and analysed to quantify the size and shape difference between the unloaded and loaded models.

The majority of GMM analyses concentrate on the shape of an object and as such 'remove' the size aspect of an object. This is achieved by scaling all configurations to unit centroid size: the square root of the sum of squared landmark differences to the centroid. Each landmark configuration is also translated to an arbitrary axis coordinate system, normally centralized at (0, 0, 0). Each configuration is then rotated with respect to an average configuration in order to minimize the distance between corresponding landmarks. This process is called a generalized Procrustes analysis (Dryden and Mardia, 1998) and the resulting landmark coordinates (Procrustes coordinates) are now represented on Kendall's shape space (Kendall, 1984). However, deformations that occur in FEA have arisen due to differences in size as well as shape. In a mechanical context, it makes little sense to attribute deformations to shape alone (O'Higgins and Milne, 2013). Past studies that have applied GMM to FEA circumvent this problem by not scaling each landmark configuration to its centroid size during the Procrustes procedure, minimizing the landmark differences between unscaled configurations (Milne and O'Higgins, 2012; O'Higgins and Milne, 2013, Fitton et al., 2015). This method represents the Procrustes coordinates in "size and shape" space (Dryden and Mardia, 1998; Dryden et al., 2007) instead of Kendall's shape space. This is a potential problem, as methods that are not based on Kendall's shape space have been shown to strongly constrain the possible results obtained by ordination methods (Rohlf, 2000). To overcome this issue, landmark coordinates (of both unloaded models and all loaded models) were subjected to a full Procrustes analysis and were not projected onto a tangent space in order to keep the coordinates (Procrustes) on the surface of Kendall's

shape space (see Rohlf, 1999 for more information on this). To include the effect of size, the Procrustes coordinates of each model were then scaled to their respective centroid sizes.

In order to quantify the differences in deformation between two specimens in a comparative analysis, the difference in size and shape between the two unloaded models must be discarded, as these differences will far outweigh the differences found between the unloaded and loaded models (Fitton et al., 2015). To compare how two different models deform, both models' landmark coordinates (unloaded and loaded) are subjected to the same Procrustes analysis and scaled according to their centroid sizes (as above). The difference in Procrustes coordinates (after centroid size scaling) between each loaded and unloaded model were calculated to obtain their residuals (these residuals represent the displacement of selected nodes on each model after the FE analysis). In order to visualise the differences in deformations between the two models, the residuals were added to a mean unloaded landmark configuration, which is calculated from the two unloaded model configurations after Procrustes fitting and scaling (from the above analysis). This mean configuration (which represents the mean unloaded model) and the loaded models' configurations (mean unloaded model plus each loaded models' residuals) are subjected to a second Procrustes analysis, without scaling or tangent projection (O'Higgins and Milne, 2013), essentially carrying out a principal components analysis on the above coordinates to represent the multivariate data on a graph. Size and shape differences between the mean model and the loaded models were visualized firstly by warping the *Bathyergus* surface (using Avizo) to the mean configuration of the unloaded models, therefore creating a *Bathyergus-Fukomys* hybrid surface. This hybrid surface was then used together with transformation grids, calculated via the thin plate spline (TPS) method (Bookstein, 1989) to visualize the size and shape deformations. As these deformations are very small, to aid visual interpretation, the deformations are magnified 500 times. This therefore means the resulting bending energy represented on the transformation grid is not absolute, but is rather used as a visual device (Weber et al., 2011; O'Higgins and Milne, 2013).

To compare the deformations of the models that were scaled to bite force, the residuals of the above analysis should be scaled to the bite force ratio. However, as one model was missing from this part of the analysis (see below), new residuals were calculated (as different numbers of variables affects how the models are superimposed during the Procrustes fit). These new residuals were added to a mean model (as above) and the

models were Procrustes fitted to calculate new centroid sizes (as they will be slightly different from the original GPA). Visualisations of these scaled deformations, represented using TPS, were magnified 50 times. All geometric morphometric analyses were carried out using the EVAN toolbox (<http://www.evan-society.org>).

It should be noted that the models did not contain PCSA values of the individual specimens used in model creation. For this reason, it was not possible to validate either model accurately and so the model outputs should not be considered to be reproducing biological reality. Instead, the scaling of the muscle forces allows conclusions to be drawn on the relative impact of changing muscle orientations in species with different cranial morphologies, similar to Dumont et al (2011).

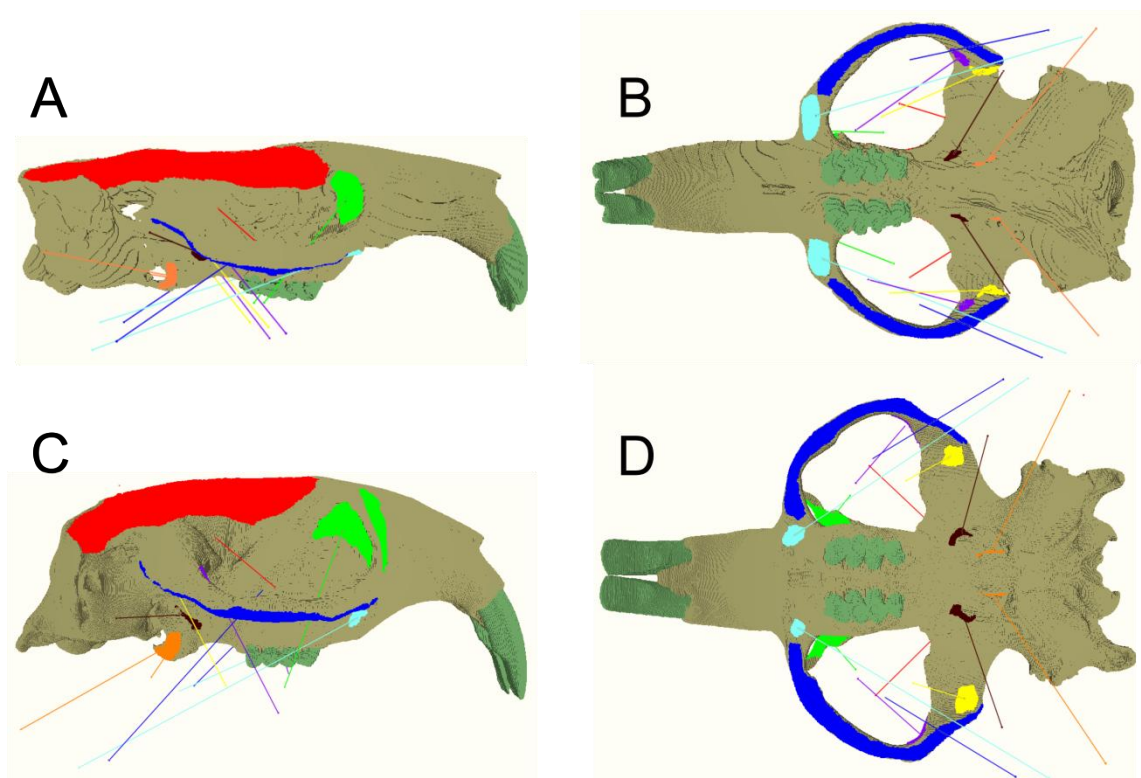


Figure 4.1 Muscle arrangements and muscle vectors of the masticatory muscles represented in both FE models. A, *Bathyergus* model in lateral view. B, *Bathyergus* model in ventral view. C, *Fukomys* model in lateral view. D, *Fukomys* model in ventral view. Colours of muscle vectors: temporalis, red; superficial masseter, cyan; deep masseter, royal blue; IOZM, green; anterior ZM, purple; posterior ZM, yellow; lateral pterygoid, brown; medial pterygoid, orange.

4.3 Results

4.3.1 Models scaled to force:area ratio

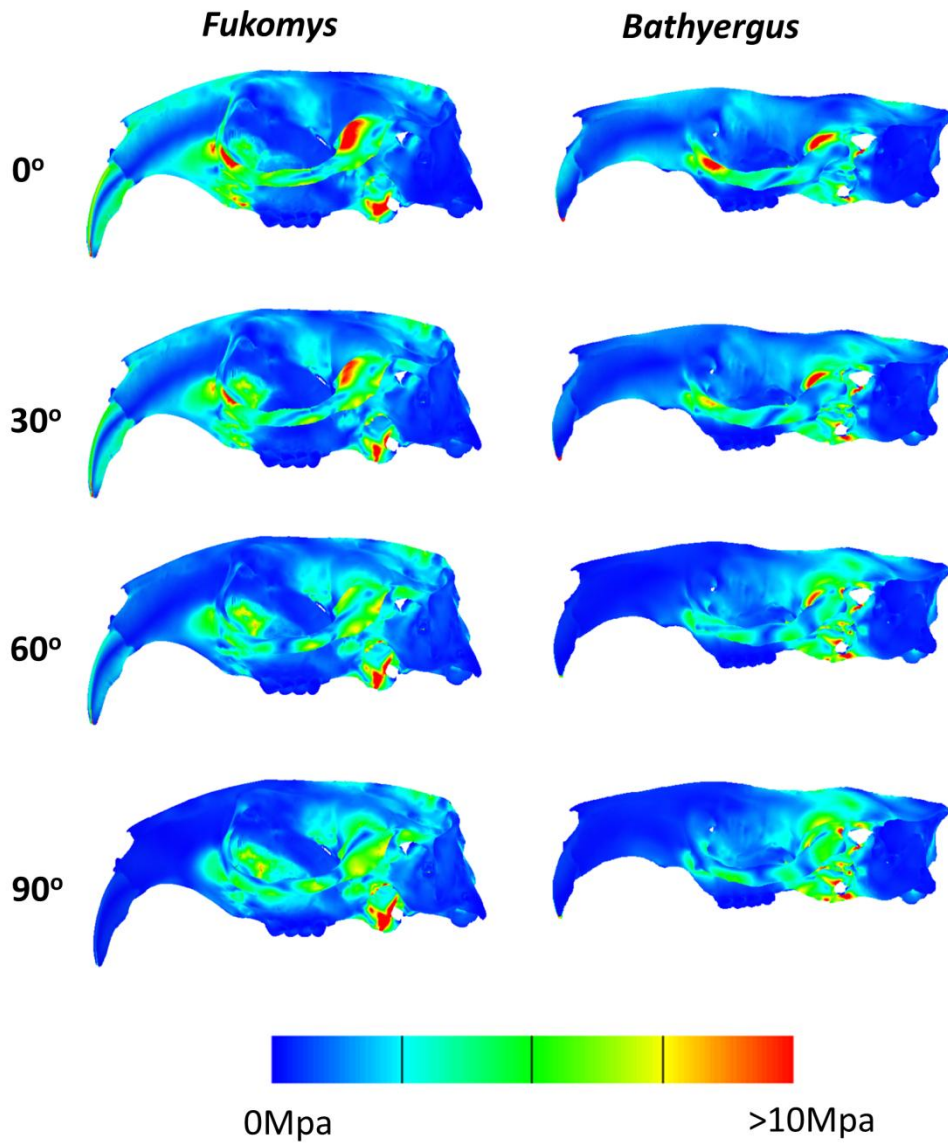


Figure 4.2 Von Mises stress contour maps across models scaled to force:area in lateral view. Left column is *Fukomys* model, right column is *Bathyergus* model at differing gape angles.

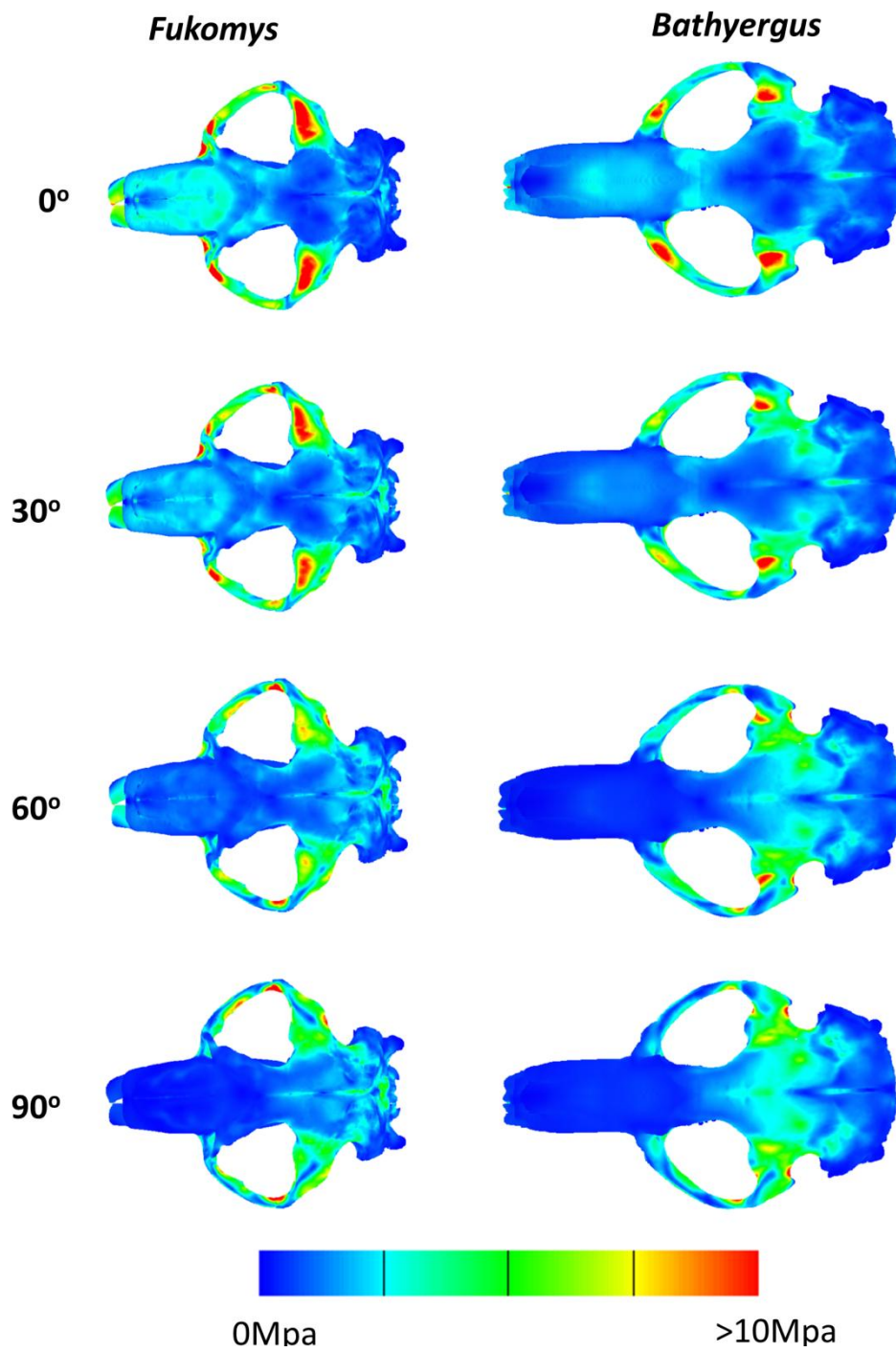


Figure 4.3 Von Mises stress contour maps across models scaled to force:area in dorsal view. Left column is *Fukomys* model, right column is *Bathyergus* model at differing gape angles.

Table 4.1. Median von Mises stress, bite force output and mechanical efficiency across both models at increasing gape.

Gape angle (degrees)	Median VM(MPa)		Bite force (N)		Mechanical efficiency	
	<i>Fukomys</i>	<i>Bathyergus</i>	<i>Fukomys</i>	<i>Bathyergus</i>	<i>Fukomys</i>	<i>Bathyergus</i>
0	1.06	0.88	18.83	15.09	0.18	0.13
30	1.04	0.76	15.26	9.73	0.15	0.08
60	0.85	0.52	9.13	3.04	0.09	0.03
90	0.63	0.59	1.95	-3.84	0.02	-0.03

Figure 4.2 and Figure 4.3 represent the results of VM stress across the crania of the two models (lateral and dorsal, respectively) when scaled to the same force: surface area ratio. The distribution of VM-stress differs slightly between the two crania. Both models appear to be most stressed at the zygomatic arch, especially around the area of the glenoid fossa, where joint reaction forces take place between the cranium and mandibular condyles. However, the stress at the glenoid fossa reduces when gape angles are increased. *Fukomys* is more stressed across the rostrum compared to *Bathyergus*. *Fukomys* also seems to be experiencing more stress around the infraorbital foramen, probably due to infraorbital part of the zygomandibularis extending slightly through the foramen, something which does not occur in *Bathyergus*. Both models appear also to experience quite high stresses at the attachment of the pterygoid muscles, with slightly higher stresses occurring in the *Fukomys* model. At increasing angles of gape, stress appears to transfer posteriorly through the cranium in both models, with stress at the rostrum being reduced. From occlusion to 60° gape angle, the incisor in *Fukomys* appears to be more stressed than in *Bathyergus*. Studying median VM stresses (Table 4.1) shows that increasing angles of gape reduces the stress in the cranium. However, *Fukomys* experiences higher VM stress in the cranium at each pairwise gape compared to *Bathyergus*.

Table 4.1 includes mechanical efficiency differences between the two species. As gape increases, mechanical efficiency decreases in both specimens. However, *Fukomys* is 1.2 times more efficient at 0° but 3 times more efficient at 60° compared to *Bathyergus*. *Fukomys* is also more efficient than *Bathyergus* at converting input forces to output forces at all gape angles.

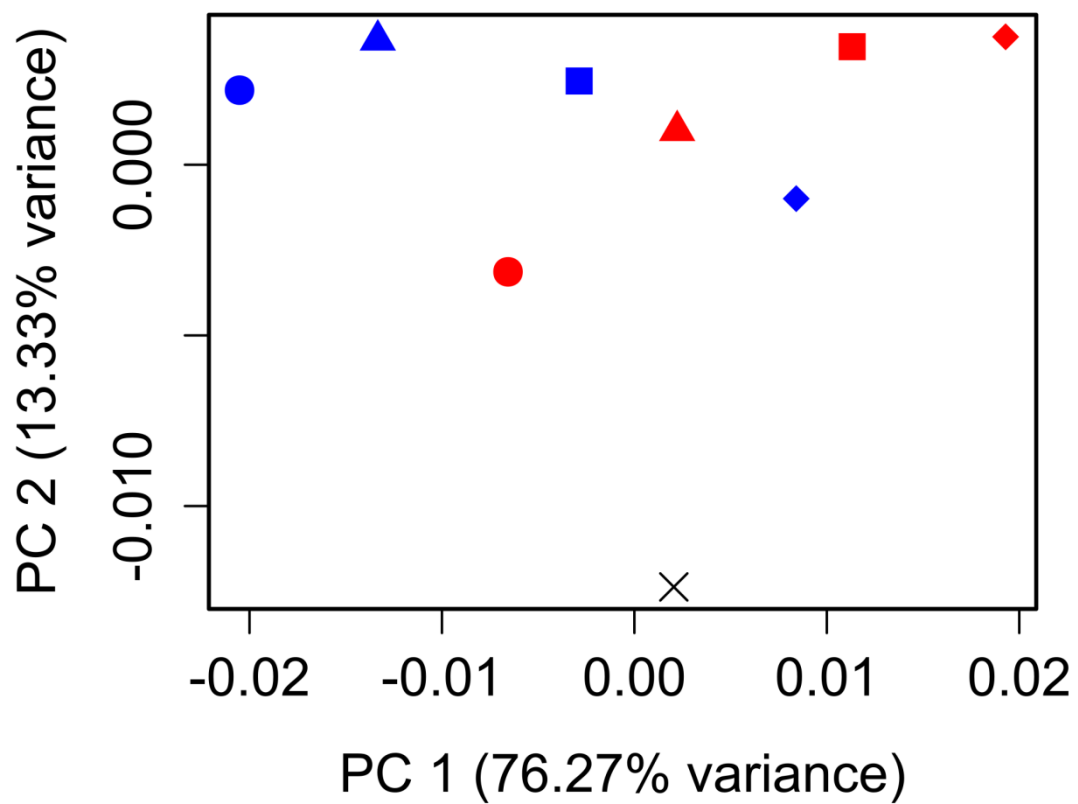


Figure 4.4 PCA plot representing the deformations between the two models scaled to force:area ratio. Mean unloaded model represented as a black cross. Blue points represent *Fukomys* models and red points represent *Bathyergus* models. Models at occlusion (circles), at 30° gape (triangles), 60° gape (squares) and 90° gape (diamonds).

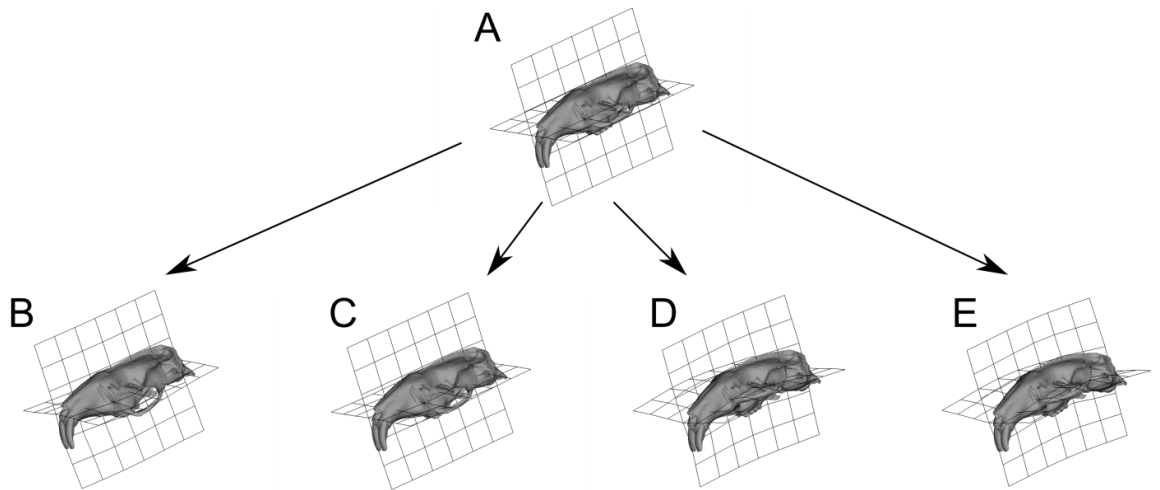


Figure 4.5 Transformation grids and surface warps associated with PCA plot (Figure 4.4) representing the deformation between the two models scaled to force:area ratio. Arrows represent the change in size and shape between unloaded mean model and target. A, unloaded mean model; B, size and shape change from unloaded model to *Fukomys* model in occlusion; C, size and shape change from unloaded model to *Bathyergus* model in occlusion; D, size and shape change from unloaded model to *Fukomys* model at 90° gape; E, size and shape change from unloaded model to *Bathyergus* model at 90° gape

Figure 4.4 shows the size and shape deformations between the two model types at varying degrees of gape. PC1 represents 76.27% variance and PC2 13.33%. PC1 is dominated by the differences between the loaded models at differing angles of gape whilst PC2 shows the difference between the unloaded mean and the loaded models. Figure 4.5A, B and C show the deformation between the mean unloaded model and the two models at occlusion using thin plate splines. The differences between the mean unloaded model and the loaded models at occlusion seem to be ventral deflexion of the zygomatic arch. *Bathyergus* in occlusion and *Fukomys* at 90° gape appear to be the least deformed from the mean unloaded model; whereas *Bathyergus* at 90° gape and *Fukomys* in occlusion are the most deformed from the mean unloaded model. Figure 4.5D and E show cranial deformations from unloaded mean to 90° gape in both models. The deformations between the two models are shown to be rather similar, with increasing gapes being associated with dorsoventral bending.

4.3.2 Models scaled to bite force

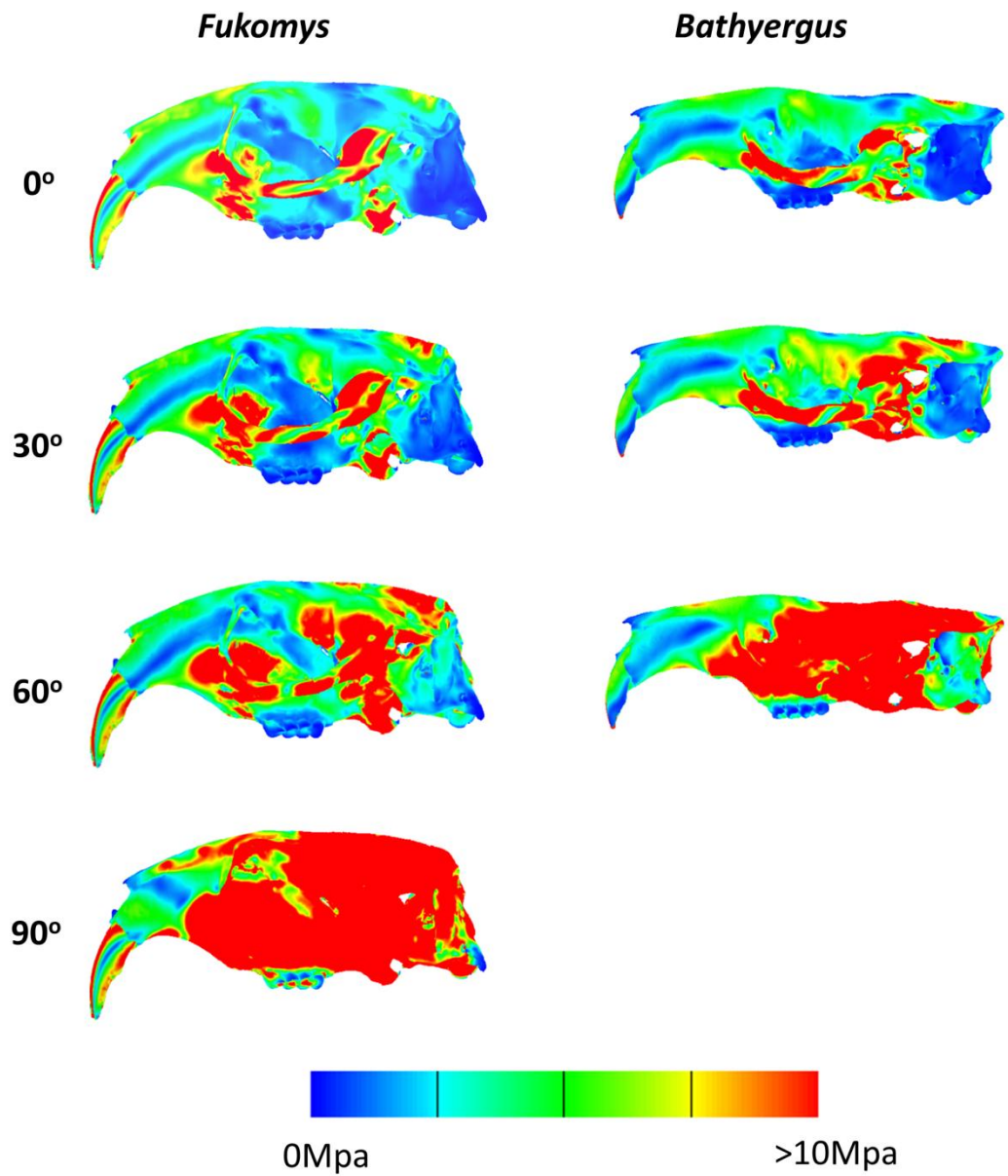


Figure 4.6 Von Mises stress contour maps across models of increasing gape scaled to a bite force of 40N in lateral view.

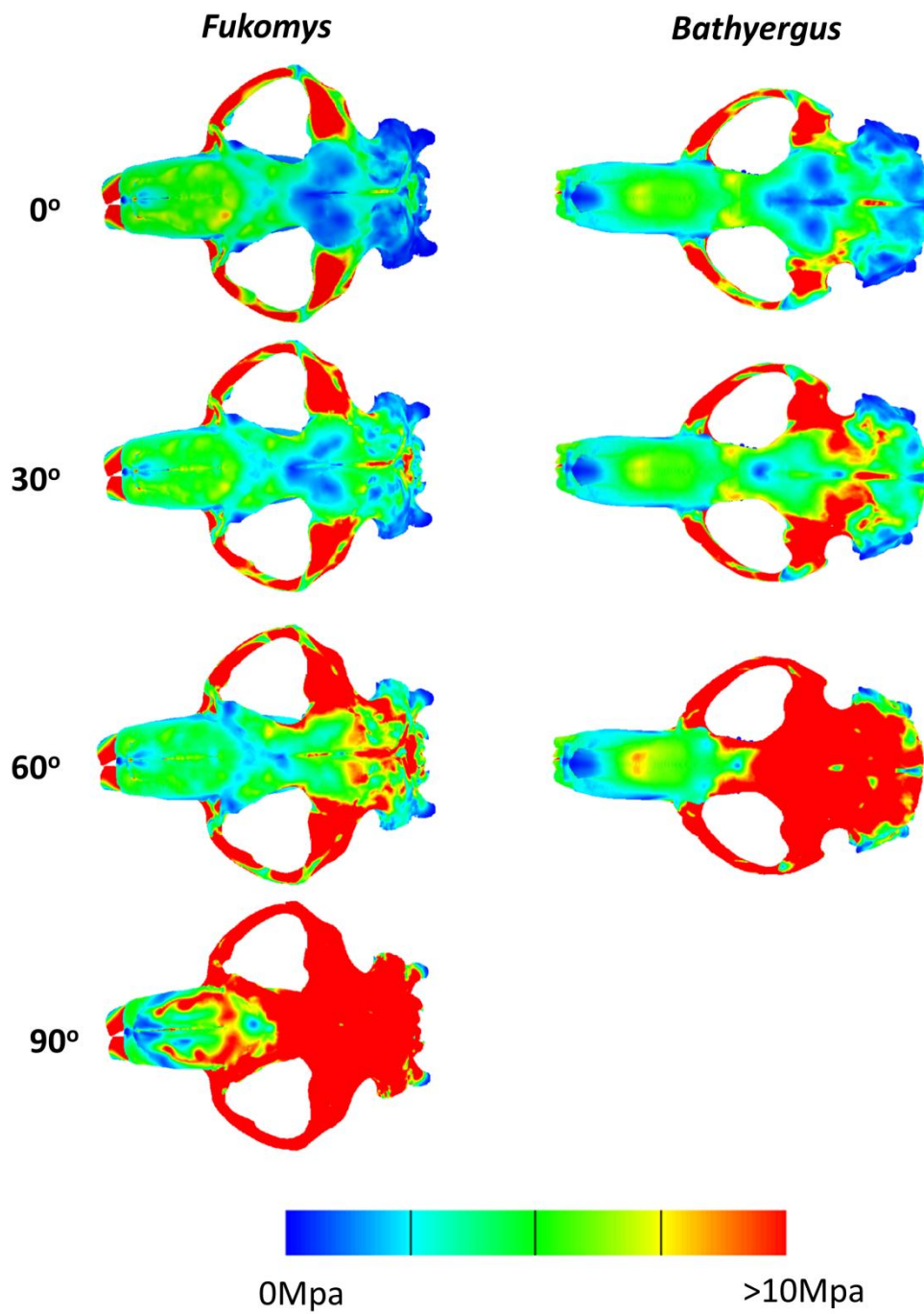


Figure 4.7 Von Mises stress contour maps across models of increasing gape scaled to a bite force of 40N in dorsal view.

Table 4.2. Median von Mises stress of both models scaled to bite force of 40N.

Gape angle (degrees)	Median VM (MPa)	
	<i>Fukomys</i>	<i>Bathyergus</i>
0	2.25	2.33
30	2.72	3.14
60	3.74	6.84
90	12.85	

Figure 4.6 and Figure 4.7 represent VM stress across the crania of the two models (lateral and dorsal, respectively) when scaled to a bite force of 40N from the original bite force output from each model represented in Table 4.1. *Bathyergus* at 90° gape was omitted from this analysis as the bite force from this model was negative, and was therefore considered an unrealistic model loading condition (see below for further explanation). VM stresses in both species have increased compared to VM stresses when the models are scaled to force:area ratio (Table 4.2). Increasing gape also increases VM stress across both species; the reverse of what occurred in the above scaling scenario. From Figure 4.6 and Figure 4.7 it can be seen that *Bathyergus* at 60° gape experiences maximum stresses across the middle and posterior parts of the cranium. A similar pattern is seen in *Fukomys* at 90° gape. The differences between the two species are best represented on the PCA (Figure 4.8). PC1 represents 84.38% variance and PC2 13.06%. PC1 is dominated by the differences between the models at differing angles of gape whilst PC2 shows the difference between the two species. The PCA shows that the crania of *Bathyergus* and *Fukomys* at occlusion have not deformed much from the unloaded model. However, *Bathyergus* deforms more at wider gapes relative to *Fukomys* at the same gapes. Indeed, *Bathyergus* at 60° gape seems to almost deform as much as *Fukomys* at 90° gape. Figure 4.9 shows that large dorsoventral deformations occur when the models are at wide gape.

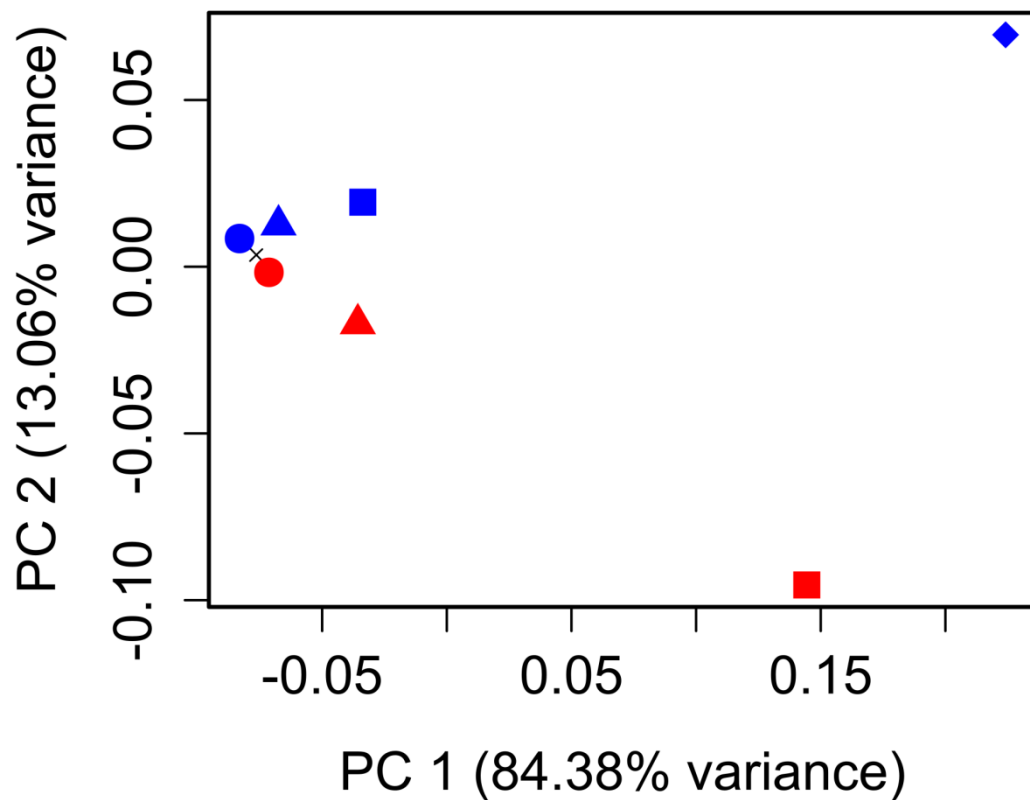


Figure 4.8 PCA plot representing the deformations between the two models scaled to bite force of 40N. Mean unloaded model represented as a black cross. Blue points represent *Fukomys* models and red points represent *Bathyergus* models. Models at occlusion (circles), at 30° gape (triangles), 60° gape (squares) and 90° gape (diamond).

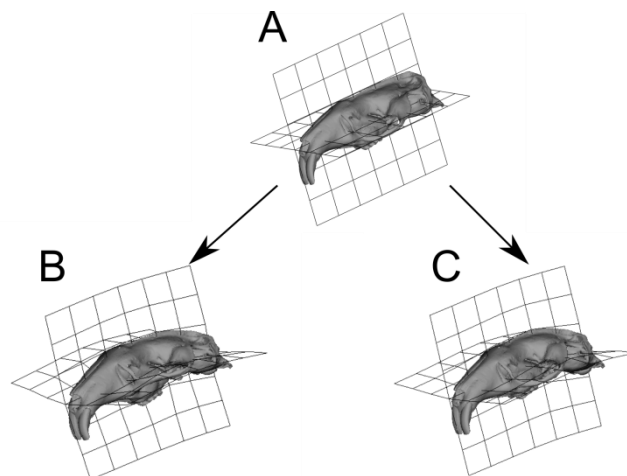


Figure 4.9 Transformation grids and surface warps associated with the PCA plot (Figure 4.8) representing deformation between the two models scaled to bite force. Arrows represent the change in size and shape between mean unloaded model and target. A, mean unloaded model; B, size and shape change from unloaded model to *Fukomys* model at 90° gape; C, size and shape change from unloaded model to *Bathyergus* model at 60° gape.

4.4 Discussion

4.4.1 Models scaled to force:area ratio

Finite element models created and solved in this study have shown that the chisel-tooth digging rodent, *Fukomys*, has a shape that can produce a larger incisor bite force at wider gapes than the scratch digging rodent, *Bathyergus* (Table 4.1). This study agrees with prior research on mammalian masticatory systems that increasing gape decreases bite force (e.g Herring and Herring, 1974; Dumont and Herrel, 2003; Bourke et al., 2008; Williams et al., 2009). The *Fukomys* model also produces the greater bite force, despite having lower muscle input values (Table 4.1). Figure 4.2 and Figure 4.3 represent the VM stress of both models at varying gapes when scaled to force:area ratio, following the method of Dumont et al. (2009). As mentioned previously, comparing the two models in this way allows for the assessment of the effects of shape on performance without the influence of size. From these results, it appears that the shape of the skull of a chisel-tooth digging rodent is optimised to produce a larger bite force at wider gapes. The word optimised is used due to the fact that even though the chisel-tooth digging skull achieved these greater bite forces, it did so at the expense of increased cranial stress- the median stress across the skull was larger at every gape angle tested, relative to the skull of the scratch digging rodent used in this study (see Table 4.1). Under conventional mechanical principles, it can be said that the skull shape of *Bathyergus* is more resistant to ductile fracturing as it experiences lower VM stresses compared to the skull shape of *Fukomys*. This seems to contradict the study's hypothesis that if size is accounted for, *Fukomys* can produce and therefore bear larger forces at the incisors for chisel tooth digging. However, as discussed by Dumont *et al.* (2011) it is unclear if the difference in stress found between the two skull shapes really matters in an evolutionary context, as there is no evidence of an animal skull naturally loading to failure. Indeed, compressive and tensile yield stresses of bone (180 and 130MPa, respectively; Cezayirlioglu et al., 1985) are much higher than the stresses reported in this study (Table 4.1 and Table 4.2). Furthermore, an excellent study by Dumont et al. (2014) showed that bats were adapting their crania in favour of mechanical efficiency (muscle input force to bite force ratio), whereas adaptation to cranial strength (i.e low VM stress) was not as strongly selected for. Although much more work needs to be done in a broader phylogenetic context, their study provides evidence that perhaps the evolution of cranial shape in vertebrates is not about adapting to an optimal shape to resist ductile

fracturing, but evolving a cranium that can function properly without failing under its natural loading.

Results from the geometric morphometric analysis of the force:area ratio scaled models show a rather different pattern seen from the VM stress contour maps. The analysis shows the two models deforming in a symmetrical pattern (Figure 4.4). The main difference between the two models is that as gape increases, *Fukomys* deforms less (plots closer to the unloaded model) and *Bathyergus* deforms more (plots further from the unloaded model). The model that deforms the least from the unloaded model is *Bathyergus* at occlusion (Figure 4.4). When comparing this to *Fukomys* at occlusion, it can be seen that the main difference in deformation occurs at the zygomatic arch, which is more inferiorly deflected in *Fukomys* at occlusion (Figure 4.5B and C). During occlusion, the line of action of the masseter muscles is pulling the zygomatic arch vertically downwards. As the models have been scaled to the same muscle force:surface area ratio, it is unlikely that the greater zygomatic deformation is a product of greater muscle force in *Fukomys*; rather, it is differences in the direction of muscle pull that appear to be leading to this result. It can be seen in Figure 4.1 that the deep masseter of *Bathyergus* has a greater posterior component to its line of action than does that of *Fukomys*. Thus the forces acting on the zygomatic arch of *Fukomys* are likely to produce a greater ventral deflection than is seen in *Bathyergus*.

Figure 4.5D and E represent how both models deform at large gape angles. Both models seem to be deforming by dorsoventral bending of the cranium. As gape increases, the arrangement of the most dominant muscles (Figure 4.1), the temporalis (which attaches to the posterior area of the cranium) and masseters (which attach to the zygoma) will cause dorsoventral bending of the cranium around the TMJ constraints. Less bending will occur at the incisor bite constraint as the muscle vectors rotate with the mandible as gape increases. This results in the muscle vectors directing more force towards the posterior part of the skull, and less force towards the anterior portion (this is also demonstrated by VM stress patterns [Figure 4.2 and Figure 4.3] where cranial stress is concentrated at the posterior areas of the cranium as gape increases). Interestingly, the *Fukomys* model does not experience as much deformation or dorsoventral bending at 90° gape compared to *Bathyergus* (Figure 4.4 and Figure 4.5D&E). This implies that the *Fukomys* cranium is stiffer than the *Bathyergus* cranium, which is to be expected from a cranium that has higher mechanical efficiency (Table 4.1). The stiffer the cranium is

during mastication, the less energy it will waste in deforming, making it more efficient at converting muscle forces into bite forces.

4.4.2 Models scaled to bite force

Scaling both FE models to an ecologically relevant bite force has also given some interesting insight to the performance of the two crania. The model of *Bathyergus* at 90° gape had to be omitted from this analysis as its bite force output was negative and therefore could not be scaled. As gape increases, the muscle vectors rotate closer to the TMJ, therefore reducing their moment magnitude. At wide gape many vectors rotate past the TMJ and at this point work against the other muscles closing the jaw. At these wide gape angles, the shape of the *Bathyergus* cranium is causing more muscles to be working against jaw closing, which is producing a negative bite force. This is clearly an unrealistic scenario that could not happen in nature. Despite there being a complete lack of data on gape angles in *Bathyergus* (along with many other rodents), this result alone shows that the cranial form of *Bathyergus* cannot perform at gapes any higher than 90°. From the VM stress contour maps (Figure 4.6 and Figure 4.7) and the median VM stress of the cranium (Table 4.2) it is clear that the *Fukomys* model performs much better at all gape angles. VM stress across both skulls have increased relative to those scaled by force:area. This is to be expected as none of the force:area scaled models reached an ecologically accurate bite force and thus were scaled “up” to a relevant bite force. This study was not trying to predict absolute bite forces in these species; instead, it was looking at how the cranial morphology copes with having to deal with these ecologically realistic scenarios. From this standpoint, it can be said that *Fukomys* experiences less stress and deforms less compared with *Bathyergus* (Table 4.2 and Figure 4.8) and agrees with the study’s hypotheses that *Fukomys* will perform better at chisel-tooth digging loading scenarios. The results of the VM stress contour plots (Figure 4.6 and Figure 4.7) show that *Fukomys* at 90° gape and *Bathyergus* at 60° gape experience a large increase of stress across the majority of their crania. Combining this result with the GMM analysis of deformation (Figure 4.8), it is seen that these two loading conditions have deformed much further from the unloaded model compared to the other models at smaller gapes. It could be inferred that the cranial morphologies of *Fukomys* and *Bathyergus* cannot achieve sufficient bite forces at these gapes as the skulls waste energy to larger deformations. Indeed, *in vivo* experiments on *Fukomys* have shown that the maximum gape in this genus is 71° (Heindryckx, 2014). The results of this study show that the cranium is a limiting factor in producing a maximal gape

angle of anything over that shown *in vivo*. Despite there not being any gape data for *Bathyergus*, from these results it would seem that *Bathyergus* cannot achieve ecologically relevant bite forces at a gape of more than 60°.

Comparing mechanical efficiency of the models at increasing gape angles adds support to the results above in that the cranial morphology of *Fukomys* is more suited to chisel-tooth digging compared to the cranial morphology of *Bathyergus*. It was found that at occlusion *Fukomys* is 1.2 times more efficient than *Bathyergus* at converting muscle input to bite force output. This increased to 3 times as efficient at 60° (Table 4.1). A higher mechanical efficiency is partly achieved by having masticatory muscles that have increased moment arms around the TMJ. McIntosh and Cox (2016) and Chapter 2 showed that the temporalis muscle of chisel-tooth digging rodents has an increased moment arm compared to *Bathyergus* and therefore could be the muscle driving this improved mechanical efficiency at increased gapes in *Fukomys*. As discussed above, *Fukomys* does not deform as much as *Bathyergus* at higher gapes, and therefore it is unsurprising that *Fukomys* is more efficient at converting input forces into bite force, as it does not lose as much energy in cranial deformation.

4.4.3 Conclusion

This study has shown that the cranial morphology of *Fukomys* is more suited towards a chisel-tooth digging lifestyle because *Fukomys* can operate more efficiently at gapes needed for chisel-tooth digging compared to the cranial morphology of the scratch digging rodent, *Bathyergus*. This result was accomplished by scaling the FE models to evaluate their shape and ecological fitness in the context of performance. The cranial morphology of the chisel-tooth digger in this analysis is clearly able to function well at wide gapes, and, although absolute bite force cannot be predicted with any degree of confidence by our unvalidated models, increasing the efficiency of the masticatory system would necessarily increase bite force. It should be emphasised that the conclusions drawn here relate only to the morphology of the cranium. To understand the biomechanics of digging more thoroughly would require a much more complex model incorporating data on muscle physiology, bone material properties, behaviour, and many other factors, which would be a very fruitful avenue of research. Finite element studies have commonly concentrated on feeding ecology in extant and extinct vertebrates (e.g. Rayfield et al., 2001; Dumont et al., 2005; Cox et al., 2012; Gill et al., 2014; Sharp, 2015, Smith et al., 2015). However, FE studies examining other functions that can affect cranial form such as gape are not as common (Bourke et al., 2008;

Dumont et al., 2011). This is the first study that has examined the effect of digging on the mammalian cranium. It has shown that the use of FEA and GMM is a powerful tool for elucidating cranial digging performance in the absence of *in vivo* data.

Chapter 5: Discussion of thesis

This thesis aimed to show how a specialised group of subterranean rodents have evolved a masticatory system that is suited to their functional requirements. The first study showed that the craniomandibular complex of chisel-tooth digging bathyergids have morphological traits that enhance the functional performance of chisel-tooth digging, when compared to the scratch digging species, *Bathyergus*. Although no evolutionary models were implemented in this study, either through genetic drift or natural selection, it was concluded that chisel-tooth diggers in some way have modified their morphology in order to produce a high bite force whilst maintaining a wide gape. Ordinarily, general mammalian mastication morphologies tend to enhance bite force at the expense of producing a wide gape or *vice versa* due to muscle stretching of the masseter (Herring and Herring, 1974; Paphangkorakit and Osborn, 1997) and morphological changes improving mechanical advantages of masticatory muscles (see Chapters 1 and 2 for discussion). As such, morphological traits that improve bite force, such as shorter jaws and rostra, decrease the capabilities to produce wide gape. However, mammals that require a large bite force at wide gape have ‘solved’ this functional morphological trade-off by improving the performance of the temporalis muscle, such as carnivores (Turnbull, 1970). Experimental data on muscle architecture in carnivores showed that temporalis muscle PCSAs were larger in animals that required a higher bite force at wider gape (Hartstone-Rose et al., 2012). Muscle architecture comparison studies in primates also show that animals that require a high bite force at wide gapes have evolved temporalis muscle PCSAs, fibre lengths and fibre orientations that facilitate this function (Taylor and Vinyard, 2004; Taylor and Vinyard, 2009; Eng et al., 2009).

In most rodents, it is the masseter that dominates the jaw closing masticatory musculature (Turnbull, 1970; Cox and Jeffery, 2011), as their herbivorous diet means large food items are not normally ingested, unlike the carnivores. However, chapter 2 has shown that rodents that are required to have an enhanced bite force at a wide gape have an improved mechanical advantage of the temporalis muscle, which is maintained at higher gapes, compared to a rodent that doesn’t require these functions. This chapter shows that the temporalis muscle is potentially very important in all mammals that require this mechanical trade-off to be solved, and not just important in carnivores.

However, a major problem in this conclusion is that there is no *in vivo* data to validate the results. Bite force data in rodents has only been studied a handful of times (Van Daele et al., 2009; Becerra et al., 2011, 2013, 2014) and only one has studied the effect of gape on bite force (Williams et al., 2009). In order to progress and validate this study, bite force and gape data need to be measured on the rodents studied in Chapter 2. On top of this, the muscle architecture of the temporalis and masseter needs to be studied in these species in order to determine if the bite force and gape performances of these individual muscles correspond to the functional implications of the craniomandibular complex found in Chapter 2 (McIntosh and Cox, 2016). Interestingly, the temporalis muscle of some chisel-tooth digging rodents has been shown to be much larger compared to other rodents (Van Daele et al., 2009; Cox and Faulkes, 2014). This could mean that the temporalis muscle is larger in rodents that require a large bite force and gape.

Chapter 3 expanded the sample size of the first results chapter to include subterranean and terrestrial rodents. The sample included phylogenetically different chisel-tooth diggers and was designed to show if there were morphological convergences in the craniodental form of chisel-tooth digging rodents, when comparing them to the craniodental form of other types of phylogenetically distant rodents, including subterranean and terrestrial genera. Firstly, the chapter found that the incisor radius of curvature in chisel-tooth digging rodents significantly differed from incisor radius of curvature of other rodents. Size was a strong indicator of incisor radius of curvature (see Figure 3.6) in all genera of rodents in the sample. Interestingly, all non-chisel-tooth digging rodents (including both subterranean and terrestrial genera) followed the same size trajectory. I therefore postulated that an increase of incisor radius of curvature seen in chisel-tooth digging rodents was an exclusive character trait of rodents that are required to use their incisors to dig through hard soils, and that possessing a longer incisor is beneficial for force dissipation throughout the skull (see page 79 for discussion). However, an increase of incisor radius of curvature reduces the compression of the dentine covered lingual side and increases the compression on the harder enamel covered side. Additionally, greater amounts of enamel have been found in mole-rats that use their incisors to dig compared to rodents that do not (van der Merwe and Botha, 1998). This could also be an adaptation to reduce stress throughout the incisor, an important property in an incisor which experiences large forces at the tip. Bone is better at resisting compression but is weaker under tension (Currey, 2002) and

similar tests need to be done on rodent incisors to understand all aspects of increasing incisor radius of curvature.

Chapter 3 also found that there is cranial convergence in chisel-tooth digging rodents when phylogenetic methods are not applied, a result that is backed up by Samuels and Van Valkenburgh (2009). However, the sample did have significant phylogenetic signal, and when phylogeny was accounted for, chisel-tooth digging crania were not significantly different from the other rodents in the sample. This highlights the importance of taking into account phylogenetic relationships when studying inter-specific samples. Covariation of incisor and cranial morphology was also strong when phylogenetic correlation was not considered (although the *P* value was close to non-significant). This result shows how incisors with large second moment of areas and radius of curvatures can predict the shape of chisel-tooth digging crania, and could be a factor in cranial shape constraint seen in chisel-tooth digging rodents. This was particularly evident when comparing the non-phylogenetic PCA and PLS results (Figure 3.9 and Figure 3.11), which showed that chisel-tooth digging rodents grouped together in both analyses. However, when phylogeny was accounted for, this relationship was lost. Correcting for phylogeny in a covariation analysis shows how two traits covary through evolutionary time, if a Brownian motion model is assumed (Klingenberg and Marugán-Lobón, 2013). However, covariation between incisors and crania may not have occurred throughout evolution within the rodents, and may have only become necessary at times when rodents were adapting to a subterranean environment. An improvement of this study would be to carry out a separate phylogenetically informed covariation analysis only using chisel-tooth digging rodents, to show if chisel-tooth digging rodents covary in a similar way throughout evolution despite being potentially phylogenetically different. Having said this, selecting taxa based solely on specific characteristics can reduce the effectiveness of phylogenetic analyses (Heath et al., 2008). Comparing how the incisors and crania covary in scratch digging rodents with how the incisors and crania covary in chisel-tooth digging could still be interesting despite potential pitfalls.

Being able to take phylogeny into account in analyses is a powerful tool for biologists interested in the evolution of shape (Monteiro, 2013). However, including phylogeny in a multivariate study such as shape has been difficult to achieve due to cladistic parsimony methods relying on independent, discrete points (such as traditional morphometrics), whereas geometric morphometrics relies on dependent, multivariate

and continuous data (see Adams et al., 2013 for discussion). However, recently a method has been developed to account for phylogeny in multivariate data using a Brownian motion model of evolution (Adams, 2014a,b; Adams and Felice, 2014). Clearly, attempts at combining these two fields are moving in the right direction. However, species evolve through a variety of evolutionary processes and rates (for review see Revell et al., 2008 and Kaliontzopoulou and Adams, 2016). For instance, Brownian motion models can accurately emulate genetic drift in a multivariate sample, as variation of characteristics only increase with phylogenetically distant species. However, in the sample used in this thesis, chisel-tooth digging has evolved in order to dig through hard soils, and therefore has evolved under directionality via an environmental cue. This therefore means that a Brownian motion model of evolution is probably an inappropriate way to model in this particular example, as Brownian motion is a random process. Perhaps a more accurate model would be an Ornstein-Uhlenbeck model (Hansen, 1997; O'Meara et al., 2006), which consistently selects a trait towards an optimum trait value (e.g. chisel-tooth digging). However, as of yet, this model has yet been implemented for multivariate, high dimensional data, but is an area of development that is highly anticipated.

A potential source of error in the first two result chapters may have occurred due to a lack of testing measurement error. This could have potentially led to false positives/negatives. To improve the accuracy of the results in these two chapters an experiment could be set up showing the sensitivity of collecting linear measurements (chapter 2) and geometric morphometric landmarks (chapter 3). For example, measurements could be collected multiple times on one specimen, perhaps on different days. The error variance from this one specimen could then be compared with the variance between two different specimens via an ANOVA to check that the range of error was acceptable.

Finally, Chapter 4 showed that the chisel-tooth digging form of a *Fukomys* cranium had a superior ability to chisel-tooth dig compared with the scratch digging *Bathyergus* cranium. This study combined a novel method of finite element analysis and geometric morphometrics to achieve this conclusion. The main results showed that the *Fukomys* cranium was able to produce a higher bite force at wider gapes, without deforming nearly as much as the *Bathyergus* cranium. This result therefore goes some way to explaining the cranial shape constraint seen in chisel-tooth digging rodents, which may

be functional. However, more FE models of phylogenetically distant chisel-tooth diggers need to be solved to confirm this finding.

The results from Chapter 2 showed that the mechanical advantage of the temporalis was increased in chisel-tooth diggers relative to the scratch digger. To expand on the findings from chapter 4, both FE models could have increased and decreased temporalis muscle strengths and see how this change affects the bite force at different gapes in both models. If performance in both skulls improves in terms of bite force and gape, the importance of temporalis is highlighted. The masseter muscles could also varied to show which muscle is more important in terms of bite force and gape.

A major drawback of this study was that muscle data was not available for the individual specimens, and indeed was not available for the *Bathyergus* species. This therefore meant that the absolute values of the models were inaccurate. I therefore feel that the natural next step in this study would be to gather material properties and muscle PCSA of the mole-rat species before creating finite element models in order to carry out a validation study. With a successful validation, I can be sure that the FE models are reflecting the differences in digging biomechanics in these two species. Despite this lack of validation, these results show that this method is a good indicator in comparing the performance of form between two specimens. In order to be able to validate such models, I feel some aspects of the modelling were oversimplified. For example, muscle wrapping was unaccounted for in my models. The temporalis muscle originates across the entirety of the parietal bone and some of the frontal and squamosal. This therefore means that the muscle wraps around a portion of the skull, which creates tangential and normal loads. Without accounting for muscle wrapping, the loaded forces could be overstressing the skull (Grosse et al., 2007). Also, although the origin of temporalis fans around the skull, the muscle fibres converge on the coronoid process. This convergence was also not accounted for in my models and could affect the stress and deformation patterns across the skull.

Despite these minor issues, the future of finite element analysis and geometric morphometrics in evolutionary biology is bright, especially for rodents. Rodents have some of the most abundant fossil records within all the mammals. Using geometric morphometrics and phylogenetic comparative methods, finite element models can potentially be warped along a phylogeny and fill in the gaps between fossils. The accuracy of these evolutionary warps could also be checked using fossils (Polly, 2001).

Examples of such ancestral reconstructions using geometric morphometrics and finite element analysis showed how carnivores evolved to be efficient bone crackers (Tseng, 2013).

In conclusion, this thesis has shown that chisel-tooth digging constrains the form of the cranium, upper incisors and parts of the mandible that are associated with bite force and gape. Although this thesis focused mainly on African mole-rats, it would be interesting if similar functional constraints were to be found in other subterranean rodents that use their incisors to dig e.g. caviomorphs. This could potentially show just how much digging affects the form of all subterranean rodents.

References

- ADAMS, D. C. 2014a. A generalized K statistic for estimating phylogenetic signal from shape and other high-dimensional multivariate data. *Systematic Biology*, 63, 685-697.
- ADAMS, D. C. 2014b. A method for assessing phylogenetic least squares models for shape and other high-dimensional multivariate data. *Evolution*, 68, 2675-2688.
- ADAMS, D. C. & FELICE, R. N. 2014. Assessing trait covariation and morphological integration on phylogenies using evolutionary covariance matrices. *PLoS One*, 9, e94335.
- ADAMS, D. C. & OTÁROLA-CASTILLO, E. 2013. Geomorph: an R package for the collection and analysis of geometric morphometric shape data. *Methods in Ecology and Evolution*, 4, 393-399.
- ADAMS, D. C. & ROHLF, F. J. 2000. Ecological character displacement in *Plethodon*: Biomechanical differences found from a geometric morphometric study. *Proceedings of the National Academy of Sciences*, 97, 4106-4111.
- ADAMS, D. C., ROHLF, F. J. & SLICE, D. E. 2004. Geometric morphometrics: ten years of progress following the 'revolution'. *Italian Journal of Zoology*, 71, 5-16.
- ADAMS, D. C., ROHLF, F. J. & SLICE, D. E. 2013. A field comes of age: geometric morphometrics in the 21st century. *Hystrix*, 24, 8.
- AGRAWAL, V. 1967. Skull adaptations in fossorial rodents. *Mammalia*, 31, 300-312.
- AGUIRRE, L. F., HERREL, A., VAN DAMME, R. & MATTHYSEN, E. 2003. The implications of food hardness for diet in bats. *Functional Ecology*, 17, 201-212.
- AKERSTEN, W. A. 1981. A graphic method for describing the lateral profile of isolated rodent incisors. *Journal of Vertebrate Paleontology*, 1, 231-234.
- ALLARD, M. W. & HONEYCUTT, R. L. 1992. Nucleotide sequence variation in the mitochondrial 12S rRNA gene and the phylogeny of African mole-rats (Rodentia: Bathyergidae). *Molecular Biology and Evolution*, 9, 27-40.
- ANDERSSON, K., NORMAN, D. & WERDELIN, L. 2011. Sabretoothed carnivores and the killing of large prey. *PLoS One*, 6, e24971.
- ATTARD, M. R. G., CHAMOLI, U., FERRARA, T. L., ROGERS, T. L. & WROE, S. 2011. Skull mechanics and implications for feeding behaviour in a large marsupial carnivore guild: the thylacine, Tasmanian devil and spotted-tailed quoll. *Journal of Zoology*, 285, 292-300.
- BAAB, K. L., PERRY, J. M. G., ROHLF, F. J. & JUNGERS, W. L. 2014. Phylogenetic, ecological, and allometric correlates of cranial shape in Malagasy lemuriforms. *Evolution*, 68, 1450-1468.
- BACIGALUPE, L. D., IRIARTE-DÍAZ, J. & BOZINOVIC, F. 2002. Functional morphology and geographic variation in the digging apparatus of cururos (Octodontidae: *Spalacopus cyanus*). *Journal of Mammalogy*, 83, 145-152.
- BADYAEV, A. V. 2009. Evolutionary significance of phenotypic accommodation in novel environments: an empirical test of the Baldwin effect. *Philosophical Transactions of the Royal Society of London B: Biological Sciences*, 364, 1125-1141.
- BARCIOVA, L., ŠUMBERA, R. & BURDA, H. 2009. Variation in the digging apparatus of the subterranean silvery mole-rat, *Heliophobius argenteocinereus* (Rodentia, Bathyergidae): the role of ecology and geography. *Biological Journal of the Linnean Society*, 97, 822-831.

- BASTIR, M., ROSAS, A. & SHEETS, H. D. 2005. The morphological integration of the Hominoid skull: a partial least squares and PC analysis with implications for European middle Pleistocene mandibular variation. *In*: SLICE, D. (ed.) *Modern Morphometrics in Physical Anthropology*. Springer US.
- BECERRA, F., CASINOS, A. & VASSALLO, A. I. 2013. Biting performance and skull biomechanics of a chisel tooth digging rodent (*Ctenomys tuconax*; Caviomorpha; Octodontoidea). *Journal of Experimental Zoology Part A: Ecological Genetics and Physiology*, 319, 74-85.
- BECERRA, F., ECHEVERRÍA, A., VASSALLO, A. I. & CASINOS, A. 2011. Bite force and jaw biomechanics in the subterranean rodent Talas tuco-tuco (*Ctenomys talarum*) (Caviomorpha: Octodontoidea). *Canadian Journal of Zoology*, 89, 334-342.
- BECERRA, F., ECHEVERRÍA, A. I., CASINOS, A. & VASSALLO, A. I. 2014. Another one bites the dust: bite force and ecology in three caviomorph rodents (Rodentia, Hystricognathi). *Journal of Experimental Zoology Part A: Ecological Genetics and Physiology*, 321, 220-232.
- BECERRA, F., VASSALLO, A. I., ECHEVERRÍA, A. I. & CASINOS, A. 2012. Scaling and adaptations of incisors and cheek teeth in caviomorph rodents (Rodentia, Hystricognathi). *Journal of Morphology*, 273, 1150-1162.
- BECHT, G. 1953. Comparative biologic-anatomical researches on mastication in some mammals. *Konink Nederl Akad Wetensch Ser C*, 56, 508-527.
- BEGALL, S., BURDA, H. & SCHLEICH, C. E. 2007. *Subterranean rodents: news from underground*, Springer. Berlin, Germany.
- BEKELE, A. 1983. The comparative functional morphology of some head muscles of the rodents *Tachyoryctes splendens* and *Rattus rattus*. I. Jaw muscles. *Mammalia*, 47, 395-420
- BENNETT, N. C. & FAULKES, C. G. 2000. *African Mole-Rats: Ecology and Eusociality*, Cambridge University Press, Cambridge, UK
- BIKNEVICIUS, A. & VAN VALKENBURGH, B. 1996. Design for killing: craniodental adaptations of predators. *In*: GITTLEMAN, J. (ed.) *Carnivore behavior, ecology, and evolution, vol 2*. Cornell University Press, Ithaca, New York, USA.
- BINDER, W. J. & VAN VALKENBURGH, B. 2000. Development of bite strength and feeding behaviour in juvenile spotted hyenas (*Crocuta crocuta*). *Journal of Zoology*, 252, 273-283.
- BLANGA-KANFI, S., MIRANDA, H., PENN, O., PUPKO, T., DEBRY, R. & HUCHON, D. 2009. Rodent phylogeny revised: analysis of six nuclear genes from all major rodent clades. *Bmc Evolutionary Biology*, 9, 71.
- BLOMBERG, S. P. & GARLAND, T. 2002. Tempo and mode in evolution: phylogenetic inertia, adaptation and comparative methods. *Journal of Evolutionary Biology*, 15, 899-910.
- BLOMBERG, S. P., GARLAND, T. & IVES, A. R. 2003. Testing for phylogenetic signal in comparative data: behavioral traits are more labile. *Evolution*, 57, 717-745.
- BOOKSTEIN, F. L. 1989. Principal warps: thin-plate splines and the decomposition of deformations. *Pattern Analysis and Machine Intelligence, IEEE Transactions on*, 11, 567-585.
- BOOKSTEIN, F. L. 1991. *Morphometric Tools for Landmark Data: Geometry and Biology*, Cambridge University Press, Cambridge, UK.
- BOOKSTEIN, F. L., GUNZ, P., MITTERÖCKER, P., PROSSINGER, H., SCHÄFER, K. & SEIDLER, H. 2003. Cranial integration in *Homo*: singular warps analysis

- of the midsagittal plane in ontogeny and evolution. *Journal of Human Evolution*, 44, 167-187.
- BOURKE, J., WROE, S., MORENO, K., MCHENRY, C. & CLAUSEN, P. 2008. Effects of gape and tooth position on bite force and skull stress in the dingo (*Canis lupus dingo*) using a 3-dimensional finite element approach. *PLoS One*, 3, e2200.
- BRANDT, J. F. 1855. Beiträge zur nähern Kenntniss der Säugethiere Russlands. *Mémoires de l'Academie Imperiale des Sciences de St Pétersbourg, Sixième Série* 9, 1–375.
- BRIGHT, J. A. & GRÖNING, F. 2011. Strain accommodation in the zygomatic arch of the pig: A validation study using digital speckle pattern interferometry and finite element analysis. *Journal of Morphology*, 272, 1388-1398.
- BRIGHT, J.A. & RAYFIELD, E.J. 2011. Sensitivity and *ex vivo* validation of finite element models of the domestic pig cranium. *Journal of Anatomy*, 219, 456-471.
- BURDA, H., BRUNS, V. and MÜLLER, M. 1990. Sensory adaptations in subterranean mammals. In: NEVO, E. and REIG, O. A. (eds.) *Evolution of Subterranean Mammals at the Organismal and Molecular Levels*, 269-293. Wiley-Liss, New York.
- BURDA, H. & KAWALIKA, M. 1993. Evolution of eusociality in the Bathyergidae. The case of the giant mole rats (*Cryptomys mehowi*). *Naturwissenschaften*, 80, 235-237.
- BUSCH, C., ANTINUCHI, C. D., DEL VALLE, J. C., KITTLEIN, M., MALIZIA, A. I., VASSALLO, A. I. & ZENUTO, R. R. 2000. Population ecology of subterranean rodents. In: EA. LACEY, G. C., AND JL. PATTON (eds.) *Life underground: the biology of subterranean rodent*. University of Chicago Press, Chicago, USA.
- BUTTON, D. J., RAYFIELD, E. J. & BARRETT, P. M. 2014. Cranial biomechanics underpins high sauropod diversity in resource-poor environments. *Proceedings of the Royal Society of London B: Biological Sciences*, 281.
- CAMIN, S., MADOERY, L. & ROIG, V. 1995. The burrowing behavior of *Ctenomys mendocinus* (Rodentia). *Mammalia*, 59, 9-18.
- CARDINI, A. & ELTON, S. 2008. Does the skull carry a phylogenetic signal? Evolution and modularity in the guenons. *Biological Journal of the Linnean Society*, 93, 813-834.
- CEZAYIRLIOGLU, H., BAHNIUK, E., DAVY, D. T. & HEIPLE, K. G. 1985. Anisotropic yield behavior of bone under combined axial force and torque. *Journal of Biomechanics*, 18, 61-69.
- CHEVERUD, J. M. 1982. Phenotypic, genetic, and environmental morphological integration in the cranium. *Evolution*, 36, 499-516.
- CHEVERUD, J. M. 1996. Developmental integration and the evolution of pleiotropy. *American Zoologist*, 36, 44-50.
- CHRISTIANSEN, P. & WROE, S. 2007. Bite forces and evolutionary adaptations to feeding ecology in carnivores. *Ecology*, 88, 347-358.
- CHURAKOV, G., SADASIVUNI, M. K., ROSENBLOOM, K. R., HUCHON, D., BROSIUS, J. & SCHMITZ, J. 2010. Rodent evolution: back to the root. *Molecular Biology and Evolution*, 27, 1315-1326.
- COX, P. G., FAGAN, M. J., RAYFIELD, E. J. & JEFFERY, N. 2011. Finite element modelling of squirrel, guinea pig and rat skulls: using geometric morphometrics to assess sensitivity. *Journal of Anatomy*, 219, 696-709.
- COX, P. G. & FAULKES, C. G. 2014. Digital dissection of the masticatory muscles of the naked mole-rat, *Heterocephalus glaber* (Mammalia, Rodentia). *PeerJ*, 2, e448.

- COX, P. G. & JEFFERY, N. 2011. Reviewing the morphology of the jaw-closing musculature in squirrels, rats, and guinea pigs with contrast-enhanced microCT. *Anatomical Record-Advances in Integrative Anatomy and Evolutionary Biology*, 294, 915-928.
- COX, P. G., KIRKHAM, J. & HERREL, A. 2013. Masticatory biomechanics of the Laotian rock rat, *Laonastes aenigmamus*, and the function of the zygomaticomandibularis muscle. *PeerJ*, 1, e160.
- COX, P. G., RAYFIELD, E. J., FAGAN, M. J., HERREL, A., PATAKY, T. C. & JEFFERY, N. 2012. Functional evolution of the feeding system in rodents. *PLoS One*, 7, e36299
- COX, P. G., RINDERKNECHT, A. & BLANCO, R. E. 2015. Predicting bite force and cranial biomechanics in the largest fossil rodent using finite element analysis. *Journal of Anatomy*, 226, 215-223
- CROFT, D. A., NIEMI, K. & FRANCO, A. 2011. Incisor morphology reflects diet in caviomorph rodents. *Journal of Mammalogy*, 92, 871-879.
- CROMPTON, A. W. & PARKER, P. 1978. Evolution of the mammalian masticatory apparatus: the fossil record shows how mammals evolved both complex chewing mechanisms and an effective middle ear, two structures that distinguish them from reptiles. *American Scientist*, 66, 192-201.
- CURREY, J. D. 2002. *Bones: Structure And Mechanics*, Princeton University Press, New Jersey, USA.
- CURTIS, N., JONES, M. E. H., EVANS, S. E., O'HIGGINS, P. & FAGAN, M. J. 2013. Cranial sutures work collectively to distribute strain throughout the reptile skull. *Journal of The Royal Society Interface*, 10.
- DARWIN, C. 1859. *On the Origin of Species by Means of Natural Selection*, 1st ed. John Murray, London, UK.
- DAVIES, K. C. & JARVIS, J. U. M. 1986. The burrow systems and burrowing dynamics of the mole-rats *Bathyergus suillus* and *Cryptomys hottentotus* in the fynbos of the south-western Cape, South Africa. *Journal of Zoology*, 209, 125-147.
- DECHOW, P. C. & CARLSON, D. S. 1990. Occlusal force and craniofacial biomechanics during growth in rhesus monkeys. *American Journal of Physical Anthropology*, 83, 219-237.
- DEUVE, J. L., BENNETT, N. C., BRITTON-DAVIDIAN, J. & ROBINSON, T. J. 2008. Chromosomal phylogeny and evolution of the African mole-rats (Bathyergidae). *Chromosome Research*, 16, 57-74.
- DOUBE, M., KŁOSOWSKI, M. M., ARGANDA-CARRERAS, I., CORDELIÈRES, F. P., DOUGHERTY, R. P., JACKSON, J. S., SCHMID, B., HUTCHINSON, J. R. & SHEFELBINE, S. J. 2010. BoneJ: Free and extensible bone image analysis in ImageJ. *Bone*, 47, 1076-1079.
- DRUZINSKY, R. E. 2010. Functional Anatomy of incisal biting in *Aplodontia rufa* and sciuriform rodents - part 1: masticatory muscles, skull shape and digging. *Cells Tissues Organs*, 191, 510-522.
- DRUZINSKY, R. E. 2015. The oral apparatus of rodents: variations on the theme of a gnawing machine. In: COX, P. G. & HAUTIER, L. (eds.) *Evolution of the Rodents: Advances in Phylogeny, Functional Morphology and Development*. Cambridge University Press, Cambridge, UK.
- DRYDEN, I. & MARDIA, K. 1998. *Statistical analysis of shape*, Wiley, New York, USA.
- DRYDEN, I. L., HIRST, J. D. & MELVILLE, J. L. 2007. Statistical analysis of unlabeled point sets: comparing molecules in chemoinformatics. *Biometrics*, 63, 237-251.

- DUMONT, E. R., DAVIS, J. L., GROSSE, I. R. & BURROWS, A. M. 2011. Finite element analysis of performance in the skulls of marmosets and tamarins. *Journal of Anatomy*, 218, 151-162.
- DUMONT, E. R., GROSSE, I. R. & SLATER, G. J. 2009. Requirements for comparing the performance of finite element models of biological structures. *Journal of Theoretical Biology*, 256, 96-103.
- DUMONT, E. R. & HERREL, A. 2003. The effects of gape angle and bite point on bite force in bats. *Journal of Experimental Biology*, 206, 2117-2123.
- DUMONT, E. R., PICCIRILLO, J. & GROSSE, I. R. 2005. Finite-element analysis of biting behavior and bone stress in the facial skeletons of bats. *The Anatomical Record Part A: Discoveries in Molecular, Cellular, and Evolutionary Biology*, 283A, 319-330.
- DUMONT, E. R., SAMADEVAM, K., GROSSE, I., WARSI, O. M., BAIRD, B. & DAVALOS, L. M. 2014. Selection for mechanical advantage underlies multiple cranial optima in new world leaf-nosed bats. *Evolution*, 68, 1436-1449.
- ECKART, C. & YOUNG, G. 1936. The approximation of one matrix by another of lower rank. *Psychometrika*, 1, 211-218.
- ELLERMAN, J. 1940. The families and genera of living rodents. British Museum of Natural History, London, UK
- EMERSON, S. B. & RADINSKY, L. 1980. Functional analysis of sabertooth cranial morphology. *Paleobiology*, 6, 295-312.
- ENG, C. M., WARD, S. R., VINYARD, C. J. & TAYLOR, A. B. 2009. The morphology of the masticatory apparatus facilitates muscle force production at wide jaw gapes in tree-gouging common marmosets (*Callithrix jacchus*). *The Journal of Experimental Biology*, 212, 4040-4055.
- EWER, R. F. 1973. *The Carnivores*. Cornell University Press, Itacha, USA.
- FABRE, P.-H., HAUTIER, L., DIMITROV, D. & P DOUZERY, E. 2012. A glimpse on the pattern of rodent diversification: a phylogenetic approach. *Bmc Evolutionary Biology*, 12, 88.
- FAULKES, C. G., ABBOTT, D. H. & JARVIS, J. U. M. 1990. Social suppression of ovarian cyclicity in captive and wild colonies of naked mole-rats, *Heterocephalus glaber*. *Journal of Reproduction and Fertility*, 88, 559-568.
- FAULKES, C. G., BENNETT, N. C., BRUFORD, M. W., OBRIEN, H. P., AGUILAR, G. H. & JARVIS, J. U. M. 1997. Ecological constraints drive social evolution in the African mole-rats. *Proceedings of the Royal Society B-Biological Sciences*, 264, 1619-1627.
- FAULKES, C. G., VERHEYEN, E., VERHEYEN, W., JARVIS, J. U. M. & BENNETT, N. C. 2004. Phylogeographical patterns of genetic divergence and speciation in African mole-rats (Family : Bathyergidae). *Molecular Ecology*, 13, 613-629.
- FELSENSTEIN, J. 1985. Phylogenies and the comparative method. *The American Naturalist*, 125, 1-15.
- FERNANDEZ, M.E., VASSALLO, A.I. & ZARATE, M. 2000. Functional morphology and palaeobiology of the pliocene rodent *Actenomys* (Caviomorpha: Octodontidae): the evolution to a subterranean mode of life. *Biological Journal of the Linnean Society*, 71, 71-90.
- FIGUEIRIDO, B., TSENG, Z. J. & MARTÍN-SERRA, A. 2013. Skull shape evolution in durophagous carnivorans. *Evolution*, 67, 1975-1993.
- FILIPPUCCI, M. G., KAWALIKA, M., MACHOLAN, M., SCHARFF, A. & BURDA, H. 1997. Allozyme differentiation and systematic relationship of Zambian giant mole-rats, *Cryptomys mechowii* (Bathyergidae, Rodentia). *Zeitschrift Fur Säugetierkunde-International Journal of Mammalian Biology*, 62, 172-178.

- FITTON, L. C., PRÔA, M., ROWLAND, C., TORO-IBACACHE, V. & O'HIGGINS, P. 2015. The impact of simplifications on the performance of a finite element model of a *Macaca fascicularis* cranium. *The Anatomical Record*, 298, 107-121.
- FITTON, L. C., SHI, J. F., FAGAN, M. J. & O'HIGGINS, P. 2012. Masticatory loadings and cranial deformation in *Macaca fascicularis*: a finite element analysis sensitivity study. *Journal of Anatomy*, 221, 55-68.
- FREEMAN, P. W. & LEMEN, C. A. 2008. A simple morphological predictor of bite force in rodents. *Journal of Zoology*, 275, 418-422.
- GAMBARYAN, P. P. & GASC, J. P. 1993. Adaptive properties of the musculoskeletal system in the mole-rat *Myospalax myospalax* (Mammalia, Rodentia), cinefluorographical, anatomical, and biomechanical analyses of burrowing. *Zool. Jb. Anat.*, 123, 363-401.
- GANS, C. 1961. The feeding mechanism of snakes and its possible evolution. *American Zoologist*, 1, 217-227.
- GANS, C. 1982. Fiber architecture and muscle function. *Exercise and sport sciences reviews*, 10, 160-207.
- GANS, C. & DE VREE, F. 1987. Functional bases of fiber length and angulation in muscle. *Journal of Morphology*, 192, 63-85.
- GARLAND, T., BENNETT, A. F. & REZENDE, E. L. 2005. Phylogenetic approaches in comparative physiology. *Journal of Experimental Biology*, 208, 3015-3035.
- GARLAND, T., JR. & IVES, A. R. 2000. Using the past to predict the present: confidence intervals for regression equations in phylogenetic comparative methods. *The American Naturalist*, 155, 346-364.
- GERALDES, D. M. & PHILLIPS, A. T. M. 2014. A comparative study of orthotropic and isotropic bone adaptation in the femur. *International Journal for Numerical Methods in Biomedical Engineering*, 30, 873-889.
- GILL, P. G., PURNELL, M. A., CRUMPTON, N., BROWN, K. R., GOSTLING, N. J., STAMPANONI, M. & RAYFIELD, E. J. 2014. Dietary specializations and diversity in feeding ecology of the earliest stem mammals. *Nature*, 512, 303-305.
- GOMES RODRIGUES, H., ŠUMBERA, R. & HAUTIER, L. *in press*. Life in burrows channelled the morphological evolution of the skull in rodents: the case of African mole-rats (Bathyergidae, Rodentia). *Journal of Mammalian Evolution*. DOI 10.1007/s10914-015-9305-x
- GOSWAMI, A. 2006. Morphological integration in the carnivoran skull. *Evolution*, 60, 169-183.
- GOSWAMI, A., MILNE, N. & WROE, S. 2011. Biting through constraints: cranial morphology, disparity and convergence across living and fossil carnivorous mammals. *Proceedings of the Royal Society of London B: Biological Sciences*, 278, 1831-1839.
- GOSWAMI, A., SMAERS, J. B., SOLIGO, C. & POLLY, P. D. 2014. The macroevolutionary consequences of phenotypic integration: from development to deep time. *Philosophical Transactions of the Royal Society of London B: Biological Sciences*, 369.
- GRAFEN, A. 1989. The phylogenetic regression. *Philosophical Transactions of the Royal Society of London. B, Biological Sciences*, 326, 119-157.
- GRÖNING, F., FAGAN, M. J. & O'HIGGINS, P. 2011. The effects of the periodontal ligament on mandibular stiffness: a study combining finite element analysis and geometric morphometrics. *Journal of Biomechanics*, 44, 1304-1312.
- GROSSE, I. R., DUMONT, E. R., COLETTA, C. & TOLLESON, A. 2007. techniques for modeling muscle-induced forces in finite element models of skeletal

- structures. *The Anatomical Record: Advances in Integrative Anatomy and Evolutionary Biology*, 290, 1069-1088.
- HALLGRÍMSSON, B., JAMNICZKY, H., YOUNG, N. M., ROLIAN, C., PARSONS, T. E., BOUGHNER, J. C. & MARCUCIO, R. S. 2009. Deciphering the palimpsest: studying the relationship between morphological integration and phenotypic covariation. *Evolutionary Biology*, 36, 355-376.
- HALLGRÍMSSON, B., LIEBERMAN, D. E., YOUNG, N. M., PARSONS, T. & WAT, S. 2007. Evolution of covariance in the mammalian skull. *Novartis Foundation Symposium*. John Wiley, New York, USA.
- HAMMER, Ø., HARPER, D. & RYAN, P. 2001. PAST: Paleontological statistics software package for education and data analysis. *Palaeontologia Electronica* 4. 9
- HAMPTON, P. M. & MOON, B. R. 2013. Gape size, its morphological basis, and the validity of gape indices in western diamond-backed rattlesnakes (*Crotalus atrox*). *Journal of Morphology*, 274, 194-202.
- HAMRICK, M. W. 1996. Articular size and curvature as determinants of carpal joint mobility and stability in strepsirrhine primates. *Journal of Morphology*, 230, 113-127.
- HANSEN, T. F. 1997. Stabilizing selection and the comparative analysis of adaptation. *Evolution*, 51, 1341-1351.
- HARTSTONE-ROSE, A., PERRY, J. M. G. & MORROW, C. J. 2012. Bite force estimation and the fiber architecture of felid masticatory muscles. *The Anatomical Record: Advances in Integrative Anatomy and Evolutionary Biology*, 295, 1336-1351.
- HAUTIER, L. & COX, P. G. 2015. Rodentia: a model order? In: COX, P. G. & HAUTIER, L. (eds.) *Evolution of the Rodents: Advances in Phylogeny, Functional Morphology and Development*. Cambridge University Press, Cambridge, UK.
- HAUTIER, L., COX, P. G. & LEBRUN, R. 2015. Grades and clades among rodents: the promise of geometric morphometrics. In: COX, P. G. & HAUTIER, L. (eds.) *Evolution of the Rodents*. Cambridge University Press, Cambridge, UK.
- HAUTIER, L., LEBRUN, R. & COX, P. G. 2012. Patterns of covariation in the masticatory apparatus of hystricognathous rodents: Implications for evolution and diversification. *Journal of Morphology*, 273, 1319-1337.
- HAUTIER, L., LEBRUN, R., SAKSIRI, S., MICHAUX, J., VIANEY-LIAUD, M. & MARIVAUX, L. 2011. Hystricognathy vs Sciurognathy in the rodent jaw: a new morphometric assessment of hystricognathy applied to the living fossil *Laonastes* (Diatomyidae). *Plos One*, 6, e18698.
- HEATH, T. A., HEDTKE, S. M. & HILLIS, D. M. 2008. Taxon sampling and the accuracy of phylogenetic analyses. *Journal of Systematics and Evolution*, 46, 239-257.
- HEINDRYCKX, S. 2014. Kinetics of chisel-tooth digging by African mole-rats (*Fukomys*, Bathyergidae, Rodentia). Masters dissertation. University of Ghent, Belgium.
- HERREL, A., DAMME, R. V., VANHOOYDONCK, B. & VREE, F. D. 2001. The implications of bite performance for diet in two species of lacertid lizards. *Canadian Journal of Zoology*, 79, 662-670.
- HERREL, A., DE SMET, A., AGUIRRE, L. F. & AERTS, P. 2008. Morphological and mechanical determinants of bite force in bats: do muscles matter? *Journal of Experimental Biology*, 211, 86-91.
- HERREL, A., O'REILLY, J. C. & RICHMOND, A. M. 2002. Evolution of bite performance in turtles. *Journal of Evolutionary Biology*, 15, 1083-1094.

- HERREL, A., VAN DAMME, R. & DE VREE, F. 1996. Sexual dimorphism of head size in *Podarcis hispanica atrata*: testing the dietary divergence hypothesis by bite force analysis. *Netherlands Journal of Zoology*, 46, 253-262.
- HERRING, S. 1975. Adaptations for gape in the hippopotamus and its relatives. *Forma et functio*, 8, 85-100.
- HERRING, S. W. 1972. The role of canine morphology in the evolutionary divergence of pigs and peccaries. *Journal of Mammalogy*, 53, 500-512.
- HERRING, S. W. 1993. Functional morphology of mammalian mastication. *American Zoologist*, 33, 289-299.
- HERRING, S. W. 2007. Masticatory muscles and the skull: A comparative perspective. *Archives of Oral Biology*, 52, 296-299.
- HERRING, S. W. & HERRING, S. E. 1974. The superficial masseter and gape in mammals. *The American Naturalist*, 108, 561-576.
- HERRING, S. W. & TENG, S. 2000. Strain in the braincase and its sutures during function. *American Journal of Physical Anthropology*, 112, 575-593.
- HERZBERG, F. & SCHOUR, I. 1941. The pattern of appositional growth in the incisor of the rat. *The Anatomical Record*, 80, 497-506.
- HIEMAE, K. & KAY, R. F. 1972. Trends in the evolution of primate mastication. *Nature*, 240, 486-487.
- HILDEBRAND, M. 1985. Digging of quadrupeds. In: HILDEBRAND, M., BRAMBLE, D.M., LIEM, K.F. and WAKE, D.B. (eds.) *Functional Vertebrate Morphology*, 89-109. The Belknap Press, London, England.
- HOLLIGER, C. D. 1916. *Anatomical Adaptations in the Thoracic Limb of the California Pocket Gopher and Other Rodents*. University of California publications in Zoology, 13:447-494.
- HOOGLAND, J. L. 1981. The evolution of coloniality in white-tailed and black-tailed prairie dogs (Sciuridae: *Cynomys Leucurus* and *Cynomys ludovicianus*). *Ecology*, 62, 252-272.
- HUISKES, R. & CHAO, E.Y. 1983 A survey of finite element analysis in orthopedic biomechanics: the first decade. *Journal of Biomechanics*, 16, 385-409.
- HYLANDER, W. L. 2013. Functional links between canine height and jaw gape in catarrhines with special reference to early hominins. *American Journal of Physical Anthropology*, 150, 247-259.
- HYLANDER, W. L., JOHNSON, K. R. & CROMPTON, A. W. 1987. Loading patterns and jaw movements during mastication in *Macaca fascicularis*: A bone-strain, electromyographic, and cineradiographic analysis. *American Journal of Physical Anthropology*, 72, 287-314.
- INGRAM, C. M., BURDA, H. & HONEYCUTT, R. L. 2004. Molecular phylogenetics and taxonomy of the African mole-rats, genus *Cryptomys* and the new genus *Coetomys* Gray, 1864. *Molecular Phylogenetics and Evolution*, 31, 997-1014.
- JAMES, C. T., OHAZAMA, A., TUCKER, A. S. & SHARPE, P. T. 2002. Tooth development is independent of a Hox patterning programme. *Developmental Dynamics*, 225, 332-335.
- JANECEK, L. L., HONEYCUTT, R. L., RAUTENBACH, I. L., ERASMUS, B. H., REIG, S. & SCHLITTER, D. A. 1992. Allozyme variation and systematics of african mole-rats (Rodentia, Bathyergidae). *Biochemical Systematics and Ecology*, 20, 401-416.
- JARVIS, J. & BENNETT, N. 1991. Ecology and behavior of the family Bathyergidae. In: SHERMAN, P. W., JARVIS, J. U. M. & ALEXANDER, R. D. (eds.) *The biology of the naked mole-rat*. Princeton University Press, New Jersey, USA.
- JARVIS, J. U. & SHERMAN, P. W. 2002. *Heterocephalus glaber*. *Mammalian Species*, 706, 1-9.

- JARVIS, J. U. M. 1981. Eusociality in a mammal: cooperative breeding in naked mole-rat colonies. *Science*, 212, 571-573.
- JARVIS, J. U. M. & BENNETT, N. C. 1990. The evolutionary history, population biology and social-structure of African mole-rats (Family: Bathyergidae). In: NEVO, E. & REIG, O. A. (eds.) *Evolution of Subterranean Mammals at the Organismal and Molecular Levels*. Wiley-Liss, New York.
- JARVIS, J. U. M., O'RIAIN, M. J., BENNETT, N. C. & SHERMAN, P. W. 1994. Mammalian eusociality: a family affair. *Trends in Ecology & Evolution*, 9, 47-51.
- JARVIS, J. U. M. & SALE, J. B. 1971. Burrowing and burrow patterns of East African mole-rats *Tachyoryctes*, *Heliophobius* and *Heterocephalus*. *Journal of Zoology*, 163, 451-479.
- KALIONTZOPOULOU, A. & ADAMS, D. C. 2016. Phylogenies, the comparative method, and the conflation of tempo and mode. *Systematic Biology*, 65, 1-15.
- KENAGY, G. J. 1973. Daily and seasonal patterns of activity and energetics in a heteromyid rodent community. *Ecology*, 54, 1201-1219.
- KENDALL, D. G. 1984. Shape manifolds, procrustean metrics, and complex projective spaces. *Bulletin of the London Mathematical Society*, 16, 81-121.
- KILTIE, R. A. 1982. Bite force as a basis for niche differentiation between rain forest peccaries (*Tayassu tajacu* and *T. pecari*). *Biotropica*, 14, 188-195.
- KLINGENBERG, C. P. 2008. Morphological integration and developmental modularity. *Annual review of ecology, evolution, and systematics*, 39, 115-132.
- KLINGENBERG, C. P. 2009. Morphometric integration and modularity in configurations of landmarks: tools for evaluating a priori hypotheses. *Evolution & Development*, 11, 405-421.
- KLINGENBERG, C. P. 2013. Cranial integration and modularity: insights into evolution and development from morphometric data. *Hystrix, the Italian Journal of Mammalogy*, 24, 43-58.
- KLINGENBERG, C. P. 2014. Studying morphological integration and modularity at multiple levels: concepts and analysis. *Philosophical Transactions of the Royal Society of London B: Biological Sciences*, 369.
- KLINGENBERG, C. P. & MARUGÁN-LOBÓN, J. 2013. Evolutionary covariation in geometric morphometric data: analyzing integration, modularity, and allometry in a phylogenetic context. *Systematic Biology*, 62, 591-610.
- KOCK, D., INGRAM, C. M., FRABOTTA, L. J., HONEYCUTT, R. L. & BURDA, H. 2006. On the nomenclature of Bathyergidae and *Fukomys* n. gen. (Mammalia : Rodentia). *Zootaxa*, 51-55.
- KORTH, W. W. & RYBCZYNSKI, N. 2003. A new, unusual castorid (Rodentia) from the earliest Miocene of Nebraska. *Journal of Vertebrate Paleontology*, 23, 667-675.
- KOUAME, K., LEONARD, C. J. & NYATIA, E. 2006. Comparative mandibular anatomy of two mole rat species *Bathyergus suillus* and *Georychus capensis*. *African Journal of Animal and Biomedical Sciences*, 1, 30-40.
- KRATOCHWIL, K., DULL, M., FARINAS, I., GALCERAN, J. & GROSSCHEDL, R. 1996. Lef1 expression is activated by BMP-4 and regulates inductive tissue interactions in tooth and hair development. *Genes & development*, 10, 1382-1394.
- KUPCZIK, K., DOBSON, C. A., FAGAN, M. J., CROMPTON, R. H., OXNARD, C. E. & O'HIGGINS, P. 2007. Assessing mechanical function of the zygomatic region in macaques: validation and sensitivity testing of finite element models. *Journal of Anatomy*, 210, 41-53.

- LANDRY, S. O., JR. 1957a. Factors affecting the procumbency of rodent upper incisors. *Journal of Mammalogy*, 38, 223-234.
- LANDRY, S. O., JR. 1957b. *The Interrelationships of the New and Old World Hystricomorph Rodents*. University of California Publications in Zoology, 56, 1-118.
- LAVOCAT, R. 1973. Les rongeurs du Miocène de l'Afrique Orientale. I. Miocène Inférieur. *Mémoires et Travaux de l'Institut de l'Ecole Pratique des Hautes Etudes, Montpellier*, 1, 1-284.
- LESSA, E. P. 1990. Morphological evolution of subterranean mammals -integrating structural, functional, and ecological perspectives. In: NEVO, E. & REIG, O. A. (eds.) *Evolution of Subterranean Mammals at the Organismal and Molecular Levels*. Wiley-Liss, New York, USA.
- LESSA, E. P. & PATTON, J. L. 1989. Structural constraints, recurrent shapes, and allometry in pocket gophers (genus *Thomomys*). *Biological Journal of the Linnean Society*, 36, 349-363.
- LESSA, E. P. & STEIN, B. R. 1992. Morphological constraints in the digging apparatus of pocket gophers (Mammalia: Geomyidae). *Biological Journal of the Linnean Society*, 47, 439-453.
- LESSA, E. P. & THAELER, C. S., JR. 1989. A reassessment of morphological specializations for digging in pocket gophers. *Journal of Mammalogy*, 70, 689-700.
- LESSA, E. P., VASSALLO, A. I., VERZI, D. H. & MORA, M. S. 2008. Evolution of morphological adaptations for digging in living and extinct ctenomyid and octodontid rodents. *Biological Journal of the Linnean Society*, 95, 267-283.
- LEVY, S. 1953. Structural analysis and influence coefficients for delta wings. *Journal of the Aeronautical Sciences*, 20, 449-454.
- LIN, G., XIE, J., CI, H., TANG, L., SU, J. & ZHANG, T. 2010. Morphological adaptations of incisors in the subterranean Gansu zokor, *Myospalax cansus* (Rodentia, Spalacidae). *Folia Zoologica*, 59, 295-300.
- LIU, J., SHI, J., FITTON, L., PHILLIPS, R., O'HIGGINS, P. & FAGAN, M. 2012. The application of muscle wrapping to voxel-based finite element models of skeletal structures. *Biomechanics and Modeling in Mechanobiology*, 11, 35-47.
- LOVEGROVE, B. & JARVIS, J. U. 1986. Coevolution between mole-rats (Bathyergidae) and a geophyte, *Micranthus* (Iridaceae). *Cimbebasia*, 8, 80-85.
- LUO, Z.-X. & WIBLE, J. R. 2005. A late Jurassic digging mammal and early mammalian diversification. *Science*, 308, 103-107.
- MACE, G. M., HARVEY, P. H. & CLUTTON-BROCK, T. H. 1981. Brain size and ecology in small mammals. *Journal of Zoology*, 193, 333-354.
- MAIER, W. & SCHRENK, F. 1987. The hystricomorphy of the Bathyergidae, as determined from ontogenetic evidence. *Zeitschrift Fur Säugetierkunde-International Journal of Mammalian Biology*, 52, 156-164.
- MARTINS, E. P. & HANSEN, T. F. 1997. Phylogenies and the comparative method: a general approach to incorporating phylogenetic information into the analysis of interspecific data. *The American Naturalist*, 149, 646-667.
- MARUGÁN-LOBÓN, J. & BUSCALIONI, Á. D. 2006. Avian skull morphological evolution: exploring exo- and endocranial covariation with two-block partial least squares. *Zoology*, 109, 217-230.
- MAYNARD SMITH, J. & SAVAGE, R. 1959. The mechanics of mammalian jaws. *School Science Review*, 141, 289-301.
- MCCOLLUM, M. & SHARPE, P. T. 2001. Evolution and development of teeth. *Journal of Anatomy*, 199, 153-159.

- MCHENRY, C. R., CLAUSEN, P. D., DANIEL, W. J. T., MEERS, M. B. & PENDHARKAR, A. 2006. Biomechanics of the rostrum in crocodylians: a comparative analysis using finite-element modeling. *The Anatomical Record Part A: Discoveries in Molecular, Cellular, and Evolutionary Biology*, 288A, 827-849.
- MCINTOSH, A. F. & COX, P. G. 2016. Functional implications of craniomandibular morphology in African mole-rats (Rodentia: Bathyergidae). *Biological Journal of the Linnean Society*, 117, 447-462.
- METZGER, K. A. & HERREL, A. 2005. Correlations between lizard cranial shape and diet: a quantitative, phylogenetically informed analysis. *Biological Journal of the Linnean Society*, 86, 433-466.
- MILNE, N. & O'HIGGINS, P. 2012. Scaling of form and function in the xenarthran femur: a 100-fold increase in body mass is mitigated by repositioning of the third trochanter. *Proceedings of the Royal Society of London B: Biological Sciences*, 279, 3449-3456.
- MITTEROECKER, P., GUNZ, P., BERNHARD, M., SCHAEFER, K. & BOOKSTEIN, F. L. 2004. Comparison of cranial ontogenetic trajectories among great apes and humans. *Journal of Human Evolution*, 46, 679-698.
- MITTEROECKER, P., GUNZ, P., NEUBAUER, S. & MÜLLER, G. 2012. How to explore morphological integration in human evolution and development? *Evolutionary Biology*, 39, 536-553.
- MONTEIRO, L. R. 2013. Morphometrics and the comparative method: studying the evolution of biological shape. *2013*, 24, 8.
- MORA, M., OLIVARES, A. I. & VASSALLO, A. I. 2003. Size, shape and structural versatility of the skull of the subterranean rodent *Ctenomys* (Rodentia, Caviomorpha): functional and morphological analysis. *Biological Journal of the Linnean Society*, 78, 85-96.
- MORGAN, C. C. & VERZI, D. H. 2011. Carpal-metacarpal specializations for burrowing in South American octodontoid rodents. *Journal of Anatomy*, 219, 167-175.
- MORLOK, W. F. 1983. Vergleichend- und funktionell-anatomische Untersuchungen an Kopf, Hals und Vorderextremität subterranean Nagetiere (Mammalia, Rodentia). *Courier Forschungsinstitut Senckenberg* 64:1-237
- MÜLLER, A. 1933. Die Kaumuskulatur des *Hydrochoerus capybara* und ihre Bedeutung für die Formgestaltung des Schädels. *Morphologisches Jahrbuch*, 72, 1-59.
- NEDBAL, M. A., ALLARD, M. W. & HONEYCUTT, R. L. 1994. Molecular systematics of hystricognath rodents - evidence from the mitochondrial-12S ribosomal-rna gene. *Molecular Phylogenetics and Evolution*, 3, 206-220.
- NEUBÜSER, A., PETERS, H., BALLING, R. & MARTIN, G. R. 1997. Antagonistic interactions between fgf and bmp signaling pathways: a mechanism for positioning the sites of tooth formation. *Cell*, 90, 247-255.
- NEVO, E. 1969. Mole rat *Spalax ehrenbergi*: Mating behavior and its evolutionary significance. *Science*, 163, 484-486.
- NEVO, E. 1979. Adaptive convergence and divergence of subterranean mammals. *Annual Review of Ecology and Systematics*, 10, 269-308.
- NEVO, E. 1999. *Mosaic Evolution of Subterranean Mammals: Regression, Progression, and Global Convergence*, Oxford University Press, Oxford, UK.
- NEVO, E., BENSILOMO, R., BEILES, A., JARVIS, J. U. M. & HICKMAN, G. C. 1987. Allozyme differentiation and systematics of the endemic subterranean mole rats of South-Africa. *Biochemical Systematics and Ecology*, 15, 489-502.

- NEVO, E. & REIG, O. 1990. *Evolution of subterranean mammals at the organismal and molecular levels: proceedings of the fifth International Theriological Congress held in Rome, Italy, August 22-29, 1989*, Wiley-Liss, New York, USA.
- NOWAK, R. M. 1999. *Walker's Mammals of the World*, Johns Hopkins University Press, Baltimore, USA.
- O'HIGGINS, P. 2000. The study of morphological variation in the hominid fossil record: biology, landmarks and geometry. *Journal of Anatomy*, 197, 103-120.
- O'HIGGINS, P. & MILNE, N. 2013. Applying geometric morphometrics to compare changes in size and shape arising from finite elements analyses. *Hystrix, the Italian Journal of Mammalogy* 24, 126-132.
- O'HIGGINS, P., COBB, S. N., FITTON, L. C., GRÖNING, F., PHILLIPS, R., LIU, J. & FAGAN, M. J. 2011. Combining geometric morphometrics and functional simulation: an emerging toolkit for virtual functional analyses. *Journal of Anatomy*, 218, 3-15.
- O'HIGGINS, P., FITTON, L., PHILLIPS, R., SHI, J., LIU, J., GRÖNING, F., COBB, S. & FAGAN, M. 2012. Virtual functional morphology: novel approaches to the study of craniofacial form and function. *Evolutionary Biology*, 39, 521-535.
- O'MEARA, B. C. 2012. Evolutionary inferences from phylogenies: a review of methods. *Annual review of ecology, evolution, and systematics*, 43, 267-285.
- O'MEARA, B. C., ANÉ, C., SANDERSON, M. J. & WAINWRIGHT, P. C. 2006. Testing for different rates of continuous trait evolution using likelihood. *Evolution*, 60, 922-933.
- OFFERMANS, M. & DE VREE, F. 1990. Mastication in springhares, *Pedetes capensis*: A cineradiographic study. *Journal of Morphology*, 205, 353-367.
- OGNEV, S. I. 1962. *Mammals of the U.S.S.R. and Adjacent Countries*. National Science Foundation, Washington, D.C, USA.
- OLSON, E. C. & MILLER, R. L. 1958. *Morphological integration*. University of Chicago Press, Chicago, USA.
- OSBORN, J. 1969. Dentine hardness and incisor wear in the beaver. *Acta anatomica*, 72, 123.
- OXNARD, C. & O'HIGGINS, P. 2009. Biology clearly needs morphometrics. Does morphometrics need biology? *Biological Theory*, 4, 84-97.
- PAGEL, M. 1999. Inferring the historical patterns of biological evolution. *Nature*, 401, 877-884.
- PAPHANGKORAKIT, J. & OSBORN, J. W. 1997. Effect of jaw opening on the direction and magnitude of human incisal bite forces. *Journal of Dental Research*, 76, 561-567.
- PARADIS, E., CLAUDE, J. & STRIMMER, K. 2004. APE: analyses of phylogenetics and evolution in R language. *Bioinformatics*, 20, 289-290.
- PATTERSON, B. D. & UPHAM, N. S. 2014. A newly recognized family from the Horn of Africa, the Heterocephalidae (Rodentia: Ctenohystrica). *Zoological Journal of the Linnean Society*, 172, 942-963.
- PEREZ, S. I., KLACZKO, J., ROCATTI, G. & DOS REIS, S. F. 2011. Patterns of cranial shape diversification during the phylogenetic branching process of New World monkeys (Primates: Platyrrhini). *Journal of Evolutionary Biology*, 24, 1826-1835.
- PERRY, J. M. G. & WALL, C. E. 2008. Scaling of the chewing muscles in prosimians. In: VINYARD, C., RAVOSA, M. J. & WALL, C. (eds.) *Primate Craniofacial Function and Biology*. Springer, Boston, USA.
- PINHEIRO, J. BATES, D., DEBROY, S., SARKAR, D and R Core Team (2016). *nlme: Linear and Nonlinear Mixed Effects Models*.

- POLLY, P. D. 2001. Paleontology and the comparative method: ancestral node reconstructions versus observed node values. *The American Naturalist*, 157, 596-609.
- POLLY, P. D., LAWING, A. M., FABRE, A.-C. & GOSWAMI, A. 2013. Phylogenetic principal components analysis and geometric morphometrics. *Hystrix, the Italian Journal of Mammalogy*, 24, 33-41.
- PORRO, L. B., METZGER, K. A., IRIARTE-DIAZ, J. & ROSS, C. F. 2013. In vivo bone strain and finite element modeling of the mandible of Alligator mississippiensis. *Journal of Anatomy*, 223, 195-227.
- POUGH, F. H. & GROVES, J. D. 1983. Specializations of the body form and food habits of snakes. *American Zoologist*, 23, 443-454.
- POWELL, P. L., ROY, R. R., KANIM, P., BELLO, M. A. & EDGERTON, V. R. 1984. Predictability of skeletal muscle tension from architectural determinations in guinea pig hindlimbs. *Journal of Applied Physiology*. 57. 1715-1721
- R Core Team. 2016. R: a language and environment for statistical computing. R Foundation for Statistical Computing, Vienna, Austria.
- RADINSKY, L. B. 1985. Approaches in evolutionary morphology: a search for patterns. *Annual Review of Ecology and Systematics*, 16, 1-14.
- RAYFIELD, E. J. 2007. Finite element analysis and understanding the biomechanics and evolution of living and fossil organisms. *Annual Review of Earth and Planetary Sciences*, 35, 541-576.
- RAYFIELD, E. J. 2011. Strain in the ostrich mandible during simulated pecking and validation of specimen-specific finite element models. *Journal of Anatomy*, 218, 47-58.
- RAYFIELD, E. J., NORMAN, D. B., HORNER, C. C., HORNER, J. R., SMITH, P. M., THOMASON, J. J. & UPCHURCH, P. 2001. Cranial design and function in a large theropod dinosaur. *Nature*, 409, 1033-1037.
- REICHMAN, O. & SMITH, S. C. 1990. Burrows and burrowing behavior by mammals. *Current mammalogy*, 2, 197-244.
- REICHMAN, O. J., WICKLOW, D. T. & REBAR, C. 1985. Ecological and mycological characteristics of caches in the mounds of dipodomys spectabilis. *Journal of Mammalogy*, 66, 643-651.
- RENCHER, A. C. & SCHAALJE, G. B. 2008. *Linear models in statistics*, John Wiley & Sons. New Jersey, USA.
- REVELL, L. J. 2009. Size-correction and principal components for interspecific comparative studies. *Evolution*, 63, 3258-3268.
- REVELL, L. J. 2010. Phylogenetic signal and linear regression on species data. *Methods in Ecology and Evolution*, 1, 319-329.
- REVELL, L. J. 2012. phytools: an R package for phylogenetic comparative biology (and other things). *Methods in Ecology and Evolution*, 3, 217-223.
- REVELL, L. J., HARMON, L. J. & COLLAR, D. C. 2008. Phylogenetic signal, evolutionary process, and rate. *Systematic Biology*, 57, 591-601.
- RICHMOND, B. G., WRIGHT, B. W., GROSSE, I., DECHOW, P. C., ROSS, C. F., SPENCER, M. A. & STRAIT, D. S. 2005. Finite element analysis in functional morphology. *The Anatomical Record Part A: Discoveries in Molecular, Cellular, and Evolutionary Biology*, 283A, 259-274.
- ROBB, G. N., WOODBORNE, S. & BENNETT, N. C. 2012. Subterranean sympatry: an investigation into diet using stable isotope analysis. *PLoS One*, 7, e48572.
- ROBERTS, A. 1951. The mammals of South Africa. The Mammals of South Africa book fund. Johannesburg, South Africa.
- ROHLF, F. J. 1999. Shape statistics: procrustes superimpositions and tangent spaces. *Journal of Classification*, 16, 197-223.

- ROHLF, F. J. 2000. On the use of shape spaces to compare morphometric methods. *Hystrix, the Italian Journal of Mammalogy*, 11, 9-25
- ROHLF, F. J. 2001. Comparative methods for the analysis of continuous variables: geometric interpretations. *Evolution*, 55, 2143-2160.
- ROHLF, F. J. & CORTI, M. 2000. Use of two-block partial least-squares to study covariation in shape. *Systematic Biology*, 49, 740-753.
- ROHLF, F. J. & SLICE, D. 1990. Extensions of the procrustes method for the optimal superimposition of landmarks. *Systematic Zoology*, 39, 40-59.
- ROSS, C. F., PATEL, B. A., SLICE, D. E., STRAIT, D. S., DECHOW, P. C., RICHMOND, B. G. & SPENCER, M. A. 2005. Modeling masticatory muscle force in finite element analysis: sensitivity analysis using principal coordinates analysis. *The Anatomical Record Part A: Discoveries in Molecular, Cellular, and Evolutionary Biology*, 283A, 288-299.
- RÜBER, L. & ADAMS, D. C. 2001. Evolutionary convergence of body shape and trophic morphology in cichlids from Lake Tanganyika. *Journal of Evolutionary Biology*, 14, 325-332.
- RUFF, C. 1988. Hindlimb articular surface allometry in hominoidea and *Macaca*, with comparisons to diaphyseal scaling. *Journal of Human Evolution*, 17, 687-714.
- RUXTON, G. D. 2006. The unequal variance t-test is an underused alternative to Student's t-test and the Mann–Whitney U test. *Behavioral Ecology*, 17, 688-690.
- SAMUELS, J. X. 2009. Cranial morphology and dietary habits of rodents. *Zoological Journal of the Linnean Society*, 156, 864-888.
- SAMUELS, J. X. & VAN VALKENBURGH, B. 2009. Craniodental adaptations for digging in extinct burrowing beavers. *Journal of Vertebrate Paleontology*, 29, 254-268.
- SANTANA, S.E. 2014. The muscles behind the bite force: bat muscles in 3D, photograph, viewed 15th March 2016. <http://faculty.washington.edu/ssantana/wordpress/the-muscles-behind-the-bite-force-bat-muscles-in-3d/>
- SANTANA, S. E. 2015. Quantifying the effect of gape and morphology on bite force: biomechanical modelling and in vivo measurements in bats. *Functional Ecology*. DOI: 10.1111/1365-2435.12522
- SANTANA, S. E., DUMONT, E. R. & DAVIS, J. L. 2010. Mechanics of bite force production and its relationship to diet in bats. *Functional Ecology*, 24, 776-784.
- SATOH, K. 1998. Balancing function of the masticatory muscles during incisal biting in two murid rodents, *Apodemus speciosus* and *Clethrionomys rufocanus*. *Journal of Morphology*, 236, 49-56.
- SCHLUTER, D. 2000. *The Ecology of Adaptive Radiation*, Oxford University Press, Oxford, UK.
- SCHNEIDER, C. A., RASBAND, W. S. & ELICEIRI, K. W. 2012. NIH Image to ImageJ: 25 years of image analysis. *Nat Meth*, 9, 671-675.
- SEBASTIÃO, H. & MARROIG, G. 2013. Size and shape in cranial evolution of 2 marsupial genera: *Didelphis* and *Philander* (Didelphimorphia, Didelphidae). *Journal of Mammalogy*, 94, 1424-1437.
- SENEY, M. L., KELLY, D. A., GOLDMAN, B. D., ŠUMBERA, R. & FORGER, N. G. 2009. Social structure predicts genital morphology in African mole-rats. *PLoS One*, 4, e7477.
- SHARP, A. C. 2015. Comparative finite element analysis of the cranial performance of four herbivorous marsupials. *Journal of Morphology*, 276, 1230-1243.
- SHERMAN, P. W., JARVIS, J. U. M. & ALEXANDER, R. D. 1991. *The Biology of the Naked Mole-Rat*, Princeton University Press, New Jersey, USA.

- SIMPSON, G. G. 1945. The principles of classification and a classification of mammals. *Bulletin of the American Museum of Natural History*, 85, 1-307.
- SLICE, D. E. 2007. Geometric morphometrics. *Annual Review of Anthropology*, 36, 261-281.
- SMITH, A. L., BENAZZI, S., LEDOGAR, J. A., TAMVADA, K., PRYOR SMITH, L. C., WEBER, G. W., SPENCER, M. A., LUCAS, P. W., MICHAEL, S., SHEKEBAN, A., AL-FADHALAH, K., ALMUSALLAM, A. S., DECHOW, P. C., GROSSE, I. R., ROSS, C. F., MADDEN, R. H., RICHMOND, B. G., WRIGHT, B. W., WANG, Q., BYRON, C., SLICE, D. E., WOOD, S., DZIALO, C., BERTHAUME, M. A., VAN CASTEREN, A. & STRAIT, D. S. 2015. The feeding biomechanics and dietary ecology of *Paranthropus boisei*. *The Anatomical Record*, 298, 145-167.
- SMITH, C. C. 1970. The coevolution of pine squirrels (*Tamiasciurus*) and conifers. *Ecological Monographs*, 40, 349-371.
- SMITH, R. 1984. Comparative functional morphology of maximum mandibular opening (gape) in primates. In: CHIVERS, D., WOOD, B. & BILSBOROUGH, A. (eds.) *Food Acquisition and Processing in Primates*. Springer, Boston, USA.
- STEIN, B. R. 2000. Morphology of subterranean rodents. In: LACEY, E. A., PATTON, J. L. & CAMERON, G. N. (eds.) *Life Underground: The Biology of Subterranean Rodents*. University of Chicago Press, Chicago, USA.
- STRAIT, D. S., WANG, Q., DECHOW, P. C., ROSS, C. F., RICHMOND, B. G., SPENCER, M. A. & PATEL, B. A. 2005. Modeling elastic properties in finite-element analysis: how much precision is needed to produce an accurate model? *The Anatomical Record Part A: Discoveries in Molecular, Cellular, and Evolutionary Biology*, 283A, 275-287.
- SWARTZ, S. M. 1989. The functional morphology of weight bearing: limb joint surface area allometry in anthropoid primates. *Journal of Zoology*, 218, 441-460.
- TAYLOR, A. B., ENG, C. M., ANAPOL, F. C. & VINYARD, C. J. 2009. The functional correlates of jaw-muscle fiber architecture in tree-gouging and nongouging callitrichid monkeys. *American Journal of Physical Anthropology*, 139, 353-367.
- TAYLOR, A. B. & VINYARD, C. J. 2004. Comparative analysis of masseter fiber architecture in tree-gouging (*Callithrix jacchus*) and nongouging (*Saguinus oedipus*) callitrichids. *Journal of Morphology*, 261, 276-285.
- TAYLOR, A. B. & VINYARD, C. J. 2009. Jaw-muscle fiber architecture in tufted capuchins favors generating relatively large muscle forces without compromising jaw gape. *Journal of Human Evolution*, 57, 710-720.
- TERHUNE, C. E., HYLANDER, W. L., VINYARD, C. J. & TAYLOR, A. B. 2015. Jaw-muscle architecture and mandibular morphology influence relative maximum jaw gapes in the sexually dimorphic *Macaca fascicularis*. *Journal of Human Evolution*, 82, 145-158.
- TIPHAINE, C., YAOWALAK, C., CYRIL, C., HELDER, G.-R., JACQUES, M., PAUL, T., MONIQUE, V.-L., LAURENT, V. & VINCENT, L. 2013. Correlated changes in occlusal pattern and diet in stem Murinae during the onset of the radiation of old world rats and mice. *Evolution*, 67, 3323-3338.
- TORO-IBACACHE, V., FITTON, L. C., FAGAN, M. J. & O'HIGGINS, P. 2016. Validity and sensitivity of a human cranial finite element model: implications for comparative studies of biting performance. *Journal of Anatomy*, 228, 70-84.
- TSENG, Z. J. 2013. Testing adaptive hypotheses of convergence with functional landscapes: a case study of bone-cracking hypercarnivores. *PLoS One*, 8, e65305.

- TSENG, Z. J. & WANG, X. 2010. Cranial functional morphology of fossil dogs and adaptation for durophagy in *Borophagus* and *Epicyon* (Carnivora, Mammalia). *Journal of Morphology*, 271, 1386-1398.
- TULLBERG, T. 1899. Über das System der Nagethiere: eine phylogenetische Studie. *Nova Acta Regiae Societatis Scientiarum Upsaliensis Series*, 3, 18: 1-514
- TURNBULL, W. D. 1970. Mammalian masticatory apparatus. *Fieldiana (Geology)*, 18, 147-356.
- UYEDA, J. C., CAETANO, D. S. & PENNELL, M. W. 2015. Comparative analysis of principal components can be misleading. *Systematic Biology*, 64, 4:677-689
- VAN DAELE, P., DAMMANN, P., MEIER, J. L., KAWALIKA, M., VAN DE WOESTIJNE, C. & BURDA, H. 2004. Chromosomal diversity in mole-rats of the genus *Cryptomys* (Rodentia : Bathyergidae) from the Zambezi region: with descriptions of new karyotypes. *Journal of Zoology*, 264, 317-326.
- VAN DAELE, P., VERHEYEN, E., BRUNAIN, M. & ADRIAENS, D. 2007a. Cytochrome b sequence analysis reveals differential molecular evolution in African mole-rats of the chromosomally hyperdiverse genus *Fukomys* (Bathyergidae, Rodentia) from the Zambezi region. *Molecular Phylogenetics and Evolution*, 45, 142-157.
- VAN DAELE, P., FAULKES, C. G., VERHEYEN, E. & ADRIAENS, D. 2007b. African mole-rats (Bathyergidae): A complex radiation in tropical soils. In: BEGALL, S., BURDA, H. & SCHLEICH, C. E. (eds.) *Subterranean Rodents: News from Underground*. Springer Berlin Heidelberg, Germany.
- VAN DAELE, P., HERREL, A. & ADRIAENS, D. 2009. Biting performance in teething African mole-rats (*Fukomys*, Bathyergidae, Rodentia). *Physiological and Biochemical Zoology*, 82, 40-50.
- VAN DAELE, P. A., BLONDE, P., STJERNSTEDT, R. & ADRIAENS, D. 2013. A new species of African mole-rat (*Fukomys*, Bathyergidae, Rodentia) from the Zaire-Zambezi Watershed. *Zootaxa*, 3636, 171-189.
- VAN DER MERWE, M. & BOTHA, A. J. 1998. Incisors as digging tools in mole-rats (Bathyergidae). *South African Journal of Zoology*, 33, 230-235.
- VAN EIJDEN, T. M. G. J., KORFAGE, J. A. M. & BRUGMAN, P. 1997. Architecture of the human jaw-closing and jaw-opening muscles. *The Anatomical Record*, 248, 464-474.
- VAN GENDEREN, C., OKAMURA, R. M., FARINAS, I., QUO, R.-G., PARSLOW, T. G., BRUHN, L. & GROSSCHEDL, R. 1994. Development of several organs that require inductive epithelial-mesenchymal interactions is impaired in LEF-1-deficient mice. *Genes & development*, 8, 2691-2703.
- VAN SPRONSEN, P. H., WEIJS, W. A., VALK, J., PRAHL-ANDERSEN, B. & VAN GINKEL, F. C. 1989. Comparison of jaw-muscle bite-force cross-sections obtained by means of magnetic resonance imaging and high-resolution CT scanning. *Journal of Dental Research*, 68, 1765-1770.
- VAN VALKENBURGH, B. 2007. Déjà vu: the evolution of feeding morphologies in the Carnivora. *Integrative and Comparative Biology*, 47, 147-163.
- VASSALLO, A. I. 1998. Functional morphology, comparative behaviour, and adaptation in two sympatric subterranean rodents genus *Ctenomys* (Caviomorpha: Octodontidae). *Journal of Zoology*, 244, 415-427.
- VASSALLO, A. I., BECERRA, F., ECHEVERRÍA, A. I. & CASINOS, A. 2016. Ontogenetic integration between force production and force reception: a case study in *Ctenomys* (Rodentia: Caviomorpha). *Acta Zoologica*, 97, 2: 232-240
- VASSALLO, A. I. & ECHEVERRÍA, A. I. 2009. Evolution of brain size in a highly diversifying lineage of subterranean rodent genus *Ctenomys* (Caviomorpha: Ctenomyidae). *Brain, Behavior and Evolution*, 73, 138-149.

- VERZI, D. H., ALVAREZ, A., ITATI OLIVARES, A., MORGAN, C. C. & VASSALLO, A. I. 2010. Ontogenetic trajectories of key morphofunctional cranial traits in South American subterranean ctenomyid rodents. *Journal of Mammalogy*, 91, 1508-1516.
- VERZI, D. H. & OLIVARES, A. I. 2006. Craniomandibular joint in South American burrowing rodents (Ctenomyidae): adaptations and constraints related to a specialized mandibular position in digging. *Journal of Zoology*, 270, 488-501.
- VINYARD, C. J. & PAYSEUR, B. A. 2008. Of “mice” and mammals: utilizing classical inbred mice to study the genetic architecture of function and performance in mammals. *Integrative and Comparative Biology*, 48, 324-337.
- VINYARD, C. J., WALL, C. E., WILLIAMS, S. H. & HYLANDER, W. L. 2003. Comparative functional analysis of skull morphology of tree-gouging primates. *American Journal of Physical Anthropology*, 120, 153-170.
- VINYARD, C. J., WALL, C. E., WILLIAMS, S. H. & HYLANDER, W. L. 2008. Patterns of variation across primates in jaw-muscle electromyography during mastication. *Integrative and Comparative Biology*, 48, 294-311.
- VLECK, D. 1979. The energy cost of burrowing by the pocket gopher *Thomomys bottae*. *Physiological Zoology*, 52, 122-136.
- WALLACE, E. D. & BENNETT, N. C. 1998. The colony structure and social organization of the giant Zambian mole-rat, *Cryptomys mechowi*. *Journal of Zoology*, 244, 51-61.
- WALMSLEY, C. W., MCCURRY, M. R., CLAUSEN, P. D. & MCHENRY, C. R. 2013. Beware the black box: investigating the sensitivity of FEA simulations to modelling factors in comparative biomechanics. *PeerJ*, 1, e204.
- WALTON, A. H., NEDBAL, M. A. & HONEYCUTT, R. L. 2000. Evidence from intron 1 of the nuclear transthyretin (prealbumin) gene for the phylogeny of African mole-rats (Bathyergidae). *Molecular Phylogenetics and Evolution*, 16, 467-474.
- WANG, X., TEDFORD, R. H. & TAYLOR, B. E. 1999. Phylogenetic systematics of the Borophaginae (Carnivora, Canidae). *Bulletin of the American Museum of Natural History*, 221:1-207
- WATSON, P. J., GRÖNING, F., CURTIS, N., FITTON, L. C., HERREL, A., MCCORMACK, S. W. & FAGAN, M. J. 2014. Masticatory biomechanics in the rabbit: a multi-body dynamics analysis. *Journal of The Royal Society Interface*, 11: 20140564
- WATT, J. M. & BREYER-BRANDWIJK, M. G. 1962. *The medicinal and poisonous plants of southern and eastern Africa: being an account of their medicinal and other uses, chemical composition, pharmacological effects and toxicology in man and animal*. E. & S. Livingstone, USA.
- WEBER, G. W., BOOKSTEIN, F. L. & STRAIT, D. S. 2011. Virtual anthropology meets biomechanics. *Journal of Biomechanics*, 44, 1429-1432.
- WEIJS, W. & HILLEN, B. 1985. Cross-sectional areas and estimated intrinsic strength of the human jaw muscles. *Acta morphologica neerlando-scandinavica*, 23, 267-274.
- WEIJS, W. A. 1980. Biomechanical models and the analysis of form: a study of the mammalian masticatory apparatus. *American Zoologist*, 20, 707-719.
- WERDELIN, L. 1989. Constraint and adaptation in the bone-cracking canid *Osteoborus* (Mammalia: Canidae). *Paleobiology*, 15, 387-401.
- WERDELIN, L. & SOLOUNIAS, N. 1991. The Hyaenidae: taxonomy, systematics and evolution. *Fossils and strata*, 30, 1-104.
- WEST-EBERHARD, M. J. 2003. *Developmental Plasticity and Evolution*. OUP, USA.

- WHEELWRIGHT, N. T. 1985. Fruit-Size, Gape Width, and the Diets of Fruit-Eating Birds. *Ecology*, 66, 808-818.
- WILKINS, K. T. 1988. Prediction of direction of chewing from cranial and dental characters in *Thomomys* pocket gophers. *Journal of Mammalogy*, 69, 46-56.
- WILKINS, K. T. & WOODS, C. A. 1983. Modes of mastication in pocket gophers. *Journal of Mammalogy*, 64, 636-641.
- WILLIAMS, K. R. & EDMUNDSON, J. T. 1984. Orthodontic tooth movement analysed by the finite element method. *Biomaterials*, 5, 347-351.
- WILLIAMS, P. E. & GOLDSPIK, G. 1978. Changes in sarcomere length and physiological properties in immobilized muscle. *Journal of Anatomy*, 127, 459-468.
- WILLIAMS, S. H., PEIFFER, E. & FORD, S. 2009. Gape and bite force in the rodents *Onychomys leucogaster* and *Peromyscus maniculatus*: does jaw-muscle anatomy predict performance? *Journal of Morphology*, 270, 1338-1347.
- WILSON, D. E. & REEDER, D. A. M. 2005. *Mammal Species of the World: A Taxonomic and Geographic Reference*, Johns Hopkins University Press, USA.
- WILSON, L. A. B. & SÁNCHEZ-VILLAGRA, M. R. 2010. Diversity trends and their ontogenetic basis: an exploration of allometric disparity in rodents. *Proceedings of the Royal Society of London B: Biological Sciences*, 277, 1227-1234.
- WOOD, A. E. 1965. Grades and clades among rodents. *Evolution*, 19, 115-130.
- WOOD, S. A., STRAIT, D. S., DUMONT, E. R., ROSS, C. F. & GROSSE, I. R. 2011. The effects of modeling simplifications on craniofacial finite element models: The alveoli (tooth sockets) and periodontal ligaments. *Journal of Biomechanics*, 44, 1831-1838.
- WROE, S., MCHENRY, C. & THOMASON, J. 2005. Bite club: comparative bite force in big biting mammals and the prediction of predatory behaviour in fossil taxa. *Proceedings of the Royal Society of London B: Biological Sciences*, 272, 619-625.
- WROE, S. & MILNE, N. 2007. Convergence and remarkably consistent constraint in the evolution of carnivore skull shape. *Evolution*, 61, 1251-1260.
- WROE, S., MORENO, K., CLAUSEN, P., MCHENRY, C. & CURNOE, D. 2007. High-resolution three-dimensional computer simulation of hominid cranial mechanics. *The Anatomical Record: Advances in Integrative Anatomy and Evolutionary Biology*, 290, 1248-1255.
- YANG, Z., KUMAR, S. & NEI, M. 1995. A new method of inference of ancestral nucleotide and amino acid sequences. *Genetics*, 141, 1641-1650.
- ZELOVA, J., SUMBERA, R., OKROUHLIK, J., SKLIBA, J., LOVY, M. & BURDA, H. 2011. A seasonal difference of daily energy expenditure in a free-living subterranean rodent, the silvery mole-rat (*Heliophobius argenteocinereus*; Bathyergidae). *Comparative Biochemistry and Physiology a-Molecular & Integrative Physiology*, 158, 17-21.

Appendix A (for chapter 2)

Table A.1 Number of individual specimens included in each T-test analysis

Analysis	<i>Bathyergus</i>	<i>Cryptomys</i>	<i>Fukomys</i>	<i>Georchus</i>	<i>Heliophobius</i>	<i>Heterocephalus</i>
Condyle height	10	3	10	3	10	5
Condyle length	10	3	10	3	10	5
Cranial width	10	4	10	2	9	5
Head height	10	4	10	3	10	5
Jaw length	10	3	10	3	10	5
MA of deep masseter	11	3	7	3	8	4
MA of superficial masseter	11	3	7	3	8	4
MA of temporalis	11	3	7	3	8	4
Rostral length	10	4	10	3	10	5
Upper incisor procumbency	11	6	10	5	10	5

Appendix B (McIntosh and Cox, 2016)